MOLECULAR LEVEL DESIGN OF ENGINEERED COATINGS

FOR ANTIMICROBIAL AND ANTIBIOFILM SURFACES

by

Buket ALKAN TAŞ

Submitted to the Graduate School of Engineering and Natural Sciences

in partial fulfillment of the requirements for the degree of

Doctor of Philosophy

Department of Material Science and Engineering Program

Thesis Advisor: Asst. Prof. Hayriye ÜNAL

SABANCI UNIVERSITY

20 JULY 2022

Buket ALKAN TAŞ, a Ph.D. student of Sabancı University Faculty of Engineering and Natural Sciences student ID 21987, successfully defended the dissertation entitled "Molecular level design of engineered coatings for antimicrobial and antibiofilm surfaces", which she prepared after fulfilling the requirements specified in the associated legislations, before the jury whose signatures are below.

APPROVED BY:

Thesis Advisor: **Asst. Prof. Hayriye ÜNAL**   ....
Sabancı University

Jury Members: **Asst. Prof. Serkan ÜNAL**   ....
Sabancı University

    Prof. Bahattin KOÇ   ....
Sabancı University

    Prof. Metin Hayri ACAR   ....
Istanbul Technical University

    Prof. İlknur Dağ   ....
Eskişehir Osmangazi University

Date of Approval   **: 20 July 2022**

ABSTRACT

MOLECULAR LEVEL DESIGN OF ENGINEERED COATINGS

FOR ANTIMICROBIAL AND ANTIBIOFILM SURFACES

Buket ALKAN TAŞ

Doctor of Philosophy, 2022

Material Science and Engineering

Thesis Advisor: Asst. Prof. Hayriye ÜNAL

Keywords: Antimicrobial Food Packaging, Halloysite Nanotubes, Carvacrol, Thin Film Coatings, Methicillin-Resistant *Staphylococcus aureus* (MRSA), Antibacterial/Antibiofilm Coatings, Lysostaphin, Polydopamine, Waterborne Polyurethane, Photothermal Therapy, NIR Light

Microorganisms that adhere to and colonize materials surfaces do not only create health risks due to infections, but they also adversely affect their functions by deteriorating material properties. There is a substantial need for antimicrobial coatings that can prevent microbial

adhesions or kill adhered microorganisms on surfaces in many different industries from food to health. In this thesis, the design of different antibacterial and antibiofilm coatings, that are engineered based on antibacterial agent release, light-activation and contact-killing has been proposed. Antibacterial agent release-based coatings have been designed for use in food packaging by encapsulation of carvacrol in halloysite nanotubes, followed by their incorporation onto polyethylene packaging films by the Layer-by-Layer thin film coating technique. Antibacterial coatings composed of safe ingredients have been produced for food packaging films, which will contribute to food safety and extend the shelf life of foods by showing activity against both foodborne pathogens and biofilms. Secondly, light-activated antibacterial coatings were designed by hybrid coatings prepared from polydopamine-coated waterborne polyurethane particles. The photothermally activated coatings developed in this study offer an effective approach for light-activated sterilization of material surfaces. Thirdly, safe, and non-toxic waterborne polyurethane-based nanocomposite coatings comprising lysostaphin enzyme immobilized on polydopamine-functionalized surfaces were designed to establish contact-killing coatings. The lysostaphin-based contact-killing hybrid coatings developed in this study offer an effective approach to prevent nosocomial infections caused by *Staphylococcus aureus* as being applicable to the surfaces in healthcare facilities and medical devices.

ÖZET

ANTİMİKROBİYAL VE ANTİBİYOFİLM ÖZELİKLİ KAPLAMALARIN

MOLEKÜLER SEVİYEDE TASARIMI

Buket ALKAN TAŞ

Doktora Tezi, 2022

Malzeme Bilimi ve Mühendisliği

Tez Danışmanı: Dr. Öğr. Üyesi Hayriye ÜNAL

Anahtar Kelimeler: Antimikrobiyal Gıda Ambalajları, Haloysit Nanotüpler, Karvakrol, İnce Film Kaplama, Metisiline Dayanıklı *Staphylococcus aureus* (MRSA), Antibakteriyel/Antibiyofilm Kaplama, Lizostafin, Polidopamin, Su Bazlı Poliüretan, Fototermal Terapi, NIR Işık

Malzeme yüzeylerine yapışan ve kolonize olan mikroorganizmalar, enfeksiyonlar nedeniyle sadece sağlık riskleri oluşturmakla kalmaz, aynı zamanda malzeme özelliklerini bozarak fonksiyonlarını da olumsuz etkiler. Gıdadan sağlığa pek çok farklı endüstride, mikrobiyal yapışmaları önleyebilen veya yüzeylere yapışan mikroorganizmaları öldürebilen

antimikrobiyal kaplamalara önemli bir ihtiyaç vardır. Bu tezde, antibakteriyel madde salınımı, ışık aktivasyonu ve temasla öldürmeye dayalı olarak tasarlanmış farklı antibakteriyel ve antibiyofilm kaplamaların tasarımı önerilmiştir.

Antibakteriyel ajanların salınımına dayalı öldürme mekanizmasına sahip yüzey kaplamalar, halloysit nanotüplerde karvakrolün kapsüllenmesi ve ardından katman-katman ince film kaplama tekniği ile polietilen ambalaj malzemesine dahil edilmesiyle gıda ambalajında kullanılmak üzere tasarlanmıştır. Böylece, hem gıda kaynaklı patojenlere hem de biyofilmlere karşı aktivite göstererek gıda güvenliğine katkı sağlayacak ve hem de gıdaların raf ömrünü uzatacak, güvenli içeriklerden oluşan antimikrobiyal gıda ambalaj malzemeleri elde edilmiştir. İkinci olarak, polidopamin kaplı su bazlı poliüretan partiküllerden oluşan hibrit kaplamalar ile ışıkla aktive olan antibakteriyel kaplamalar tasarlanmıştır. Bu çalışmada geliştirilen fototermal özellikli yüzey kaplamaları, yüzeylerin ışık yardımıyla sterilize edilmesi için etkili bir yaklaşım sunmaktadır. Üçüncüsü, polidopamin ile işlevselleştirilmiş yüzeyler üzerinde hareketsizleştirilmiş lizostafin enzimini içeren güvenli ve toksik olmayan su bazlı poliüretan nanokompozit kaplamalar, temasla öldürmeye dayalı kaplamalar oluşturmak için tasarlanmıştır. Bu çalışmada geliştirilen lizostafin bazlı temasla öldürmeye dayalı hibrit kaplamalar, sağlık tesislerinde ve tıbbi cihazlarda yüzeylere uygulanarak *Staphylococcus aureus*'un neden olduğu hastane enfeksiyonlarının önlenmesinde etkili bir yaklaşım sunmaktadır.

To the hero of my sleepless nights

ACKNOWLEDGEMENTS

I would like to express my deep regards and thanks to my advisor, Asst. Prof. Hayriye Ünal, for her sincere supervision, intellectual deepness, tolerance and advice during my PhD education. She has inspired me not only on how to be a successful scientist but also on how to be a successful and strong woman. Thanks to her supportive character, I always felt her wind behind me as I sailed into unfamiliar waters, and this always gave me courage. She guided me to open my mind to research to look for different views. It was a great pleasure for me to work with her.

I would like to express my gratitude to Asst. Prof. Serkan Ünal for contributing to my scientific development by encouraging me to think with his questions and allowing me to see the finest details in my work by looking with questioning eyes. From the very beginning to the end, he provided many contributions to my PhD adventure with both his intellectual knowledge and support in every subject.

I would like to express my sincere gratitude to Prof. Dr. Metin Hayri Acar for not only being my dissertation jury member but also for touching my life, both scientifically and morally, throughout my academic career. The sentence that he says, "the person lives with his preferences," rings in my ears at every decision stage in my life, enabling me to own my decisions. He supported me in every aspect of my life, guided me to know myself and find my truth, and will always have a special place in my life.

July 2022

Buket ALKAN TAŞ

TABLE OF CONTENT

ABBREVIATIONS

AEAS   : Sodium 2-[(2-aminoethyl) amino] ethane sulphonate

AMPs   : Antimicrobial Peptides

CHI   : Chitosan

DAIs   : Device-associated Infections

DCAMA   : Dipicolyl aminoethyl methacrylate

DLS   : Dynamic Light Scattering

DMF   : Dimethylformamide

DMOAP   : Dimethyl octadecyl [3-(trimethoxy silyl) propyl] ammonium chloride

ECM   : Extracellular Matrix

EDA   : Ethylenediamine

EOs   : Essential Oils

EPTMAC   : 2,3-epoxypropyl trimethylammonium chloride

EVOH   : Ethylene-vinyl alcohol

FTIR   : Fourier Transform Infrared

GPC   : Gel Permeation Chromatography

HACC   : (hydroxypropyltrimethyl ammonium chloride chitosan

HAIs	**:**	Healthcare-associated Infections
HDI	**:**	Hexamethylene diisocyanate
HNT	**:**	Halloysite Nanotubes
LbL	**:**	Layer-by-Layer
LSCM	**:**	Laser Scanning Confocal Microscope
LYS	**:**	Lysostaphin
MDR	**:**	Multi Drug Resistant
MIC	**:**	Minimum Inhibitory Concentration
MRSA	**:**	Methicillin-Resistant *Staphylococcus aureus*
NIR	**:**	Near-Infrared
NO	**:**	Nitric Oxide
PDA	**:**	Polydopamine
PDI	**:**	Polydispersity Index
PDMS	**:**	Poly (dimethylsiloxane)
PE	**:**	Polyethylene
PEG	**:**	Polyethylene glycol
PMAA	**:**	Poly (methacrylic acid)
PSS	**:**	Poly (sodium-4-styrene sulfonate)
PTT	**:**	Photothermal Therapy

QACs : Quaternary Ammonium Compounds

ROS : Reactive Oxygen Species

SI-ATRP : Surface-initiated Atom Transfer Radical Polymerization

SI-RAFT : Surface-initiated Reversible Addition-Fragmentation Chain Transfer

TGA : Thermogravimetric Analysis

TPGDDA : Tripropylene glycol diacrylate

TRIS : Tris(hydroxymethyl)aminomethane

TSB : Tryptic soy broth

WPU : Waterborne Polyurethane

UTM : Universal Testing Machine

SYMBOLS

μm	: Micrometer
nm	: Nanometer
mm	: Millimeter
cm	: Centimeter
g	: Gram
mg	: Milligram
μg	: Microgram
°C	: Degree Celsius
°K	: Degree Kelvin
N	: Newton
s	: Second
min	: Minute
h	: Hour
mbar	: Millibar
rpm	: Revolutions per Minute
mL	: Milliliter

L	: Liter
μL	: Microliter
M	: Molar
mM	: Millimolar
W	: Watt
kDa	: Kilodalton
Da	: Dalton
MPa	: Megapascal
CFU	: Colony Forming Unit

LIST OF TABLES

LIST OF FIGURES

CHAPTER 1: General Introduction

1.1. Dissertation overview and objectives

Bacterial attachment to surfaces is a major health concern in food packaging applications, healthcare environments, and any frequently encountered surface such as door handles and keyboards. In addition, biofilms are formed as a result of the attachment of bacteria to either biotic or abiotic surfaces and their subsequent colonization on these surfaces. Because biofilms naturally have an extracellular polymer matrix that acts as a shield to protect them against antibacterial agents and harsh environmental stresses, biofilm-associated infections are much more difficult to combat [1]. Bacterial colonization in food packaging materials both shortens the shelf life of foods, thus causing food waste and economic losses, and seriously threatens human health due to contact with contaminated food [2]. Besides, considering nosocomial infections caused by methicillin-resistant bacteria in healthcare settings, it is an undeniable fact that these infections increase the rate of mortality and morbidity, prolong hospital stay and increase the burden on the economy [3-4]. Designing antimicrobial and anti-biofilm coatings that can prevent and eradicate bacterial colonization in food-contact materials, healthcare settings, medical devices, and surfaces that are essential to be disinfected can contribute to community health and prevent industrial-economic losses arising from bacterial contamination.

Pathogenic bacteria on the surfaces can be killed chemically by an antibacterial agent incorporated into the surface, targeting the bacteria, and destroying the cell components. Releasing the antibacterial agent [5] is the prominent approach in antibacterial surface coatings using chemical agents. In this thesis, as a first approach, antibacterial food packaging materials were designed by the coating of packaging films with an antibacterial essential oil-release system. In the literature, there are studies on the incorporation of antibacterial agents directly into the coating material; however, the direct incorporation of the antibacterial agent may have disadvantages such as decreased stability, reduced antibacterial activity, and unsatisfactory shelf life [6-8]. To overcome these problems, carvacrol, the essential oil, was incorporated into packaging material as a thin film coating via Layer-by-Layer (LbL) coating following the encapsulation of carvacrol into halloysite nanotube; thus, the sustained release of the antibacterial agent was ensured, enabling the food packaging to show antibacterial activity for a long time. The coatings composed of natural and non-toxic components developed in this study provided an effective approach to obtain food packaging materials that contribute to food safety by inhibiting food contamination.

The physical destruction of the attached and accumulated pathogenic bacteria on the surface with an external stimulus is a much more promising method. With the integration of photothermal agents that convert light into heat to the coating material, hyperthermia effect is created thanks to the external stimulus of light, and the cell wall of bacteria can be physically destroyed irreversibly without the need for any chemicals [9]. There are many studies in the literature in which various nanoparticles such as graphene [10], carbon nanotubes [11], noble-metal nanoparticles [12] etc. are used as antibacterial photothermal agents. However, they have some disadvantages such as potential toxicity, poor photostability under long-term

light irradiation, unstable nature in large-scale application, and high cost. Therefore, conjugated polymers, which are non-toxic, can be coated on almost any surface, are easily processed and cheap, come to the fore as promising photothermal agents [13-14]. With this motivation, as a second approach, a hybrid polymer system was fabricated by coating of waterborne polyurethane solid particles with photothermal polydopamine by a one-pot reaction. This hybrid polymer system can be used as a coating material for any surface and moreover, bulk materials can be obtained. Thanks to the conjugated structure of polydopamine, these produced materials create destructive effects on bacteria when irradiated with NIR light and can be used as an effective antibacterial coating that enables light-activated physical sterilization.

The desired surface can be adapted with a contact-active agent through immobilization techniques such as non-covalent adsorption [15], ionic interaction [16], encapsulation [17], and covalent bonding [18-20] to target the cell components of the pathogenic bacteria. Thus, the bacteria can be irreversibly destroyed by the antimicrobial agent. Enzymes, with proven antibacterial activity against bacteria, are in the class of antibacterial agents that target the cell wall of bacteria and kill them by contact [21]. In this thesis, antibacterial surfaces with the ability to kill by contact were produced by utilization of lysostaphin, which is the most effective enzyme against methicillin-resistant *S. aureus* (MRSA), to combat healthcare-associated infections (HAIs) caused by methicillin-resistant bacteria. While designing an antibacterial coating with the help of enzyme, the suitability of the method to be chosen for the incorporation of enzymes into the coating material is important in terms of maintaining the enzyme stability and enzymatic activity. Since the non-covalent immobilization of enzymes to the coating material can lead to problems such as decreased enzyme stability and

leaching of enzyme from the coating surface, lysostaphin was covalently immobilized onto polydopamine-functionalized-halloysite nanotube and then incorporated into the coating material. Thus, safe, non-toxic antibacterial coatings that can be applied to operating rooms, medical devices, and similar surfaces in healthcare-settings has been developed with the purpose of prevention of HAIs caused by MRSA.

Knowledge from the lysostaphin-based killing study and the study of hybrid polymer system composed of waterborne polyurethane and polydopamine was used to present a new material design. In this study, the hybrid polydopamine-polyurethane polymer system was coated as a thin film on the substrate and lysostaphin was covalently immobilized onto the coating due to the reaction between the functional groups of polydopamine and lysostaphin. The destructive effect of lysostaphin on *S. aureus* biofilms has been proven by various studies in the literature [22]. In the light of this information, the main goal of this study was to kill not only the planktonic cells attached to the surface, but also to effectively destroy biofilms on the surface. Coatings that are able to kill bacteria by contact due to the lysostaphin enzyme have important advantages such as being environmentally friendly, volatile organic compound free, nanoparticle free, easily applicable to large surface areas and having effective antibiofilm properties.

1.2. Review on the main approaches towards the design of antimicrobial coatings

Pathogenic microorganisms tend to attach to any solid surface and subsequently colonize to form biofilms and these pathogenic strains can be transferred from surfaces to humans causing microbial infections. Microbial contamination is a major concern for many industries such as healthcare, marine, and food industries. While application of chemical disinfectants such as chlorine, hydrogen peroxide, ethanol and UV light sterilization are typical approaches for surface cleaning, and therefore stopping infections, these solutions are mostly not sufficient and not well-established, mainly because they need to be applied periodically to the surface and bacteria can gain resistance to these chemicals [23]. Moreover, these cleaning methods may not completely clean the surfaces from bacteria, and even if the bacterial population on the surface decreases, the presence of bacteria remaining on the surface causes the risk for transmission of bacteria to continue [24].

Hospital environments and surfaces of medical devices are important sources for bacterial contamination and the spreading of bacteria from contaminated surfaces causes infections that threaten human life. Healthcare-associated infections (HAIs), especially originating from multiple drug-resistance (MDR) pathogens, cause an increase in death rates and high financial losses every year [25-26]. Therefore, surface modification of biomedical devices is necessary to combat pathogenic bacteria. In addition, modification of high-contact surfaces in hospital settings such as door handles, keyboards, switches, air conditioners, etc., which are effective in the spread of bacteria, with antibacterial agents is important for the control of the microbial population [27].

Apart from some traditional food preservation techniques such as drying, freezing, heating, fermentation, salting etc. [28], innovative methods that protect food from bacterial

contamination are increasing in demand. With the use of antibacterial food packaging materials, the shelf life of foods can be extended, and also their freshness and safety can be protected, and therefore food-borne microbial outbreaks and food waste can be prevented. In this context, antibacterial food packaging that is designed by the incorporation of an antibacterial agent into packaging material or coating the surface of the packaging film with an antibacterial agent plays an important role in the control of microorganisms, that cause spoilage of food [29].

The two strategies for designing an antimicrobial surface are that the surface (i) has the ability to kill microorganisms, or (ii) prevents the attachment of pathogenic microorganisms. In both strategies, the surface should have high antibacterial activity on both sessile and planktonic bacteria. The durability of the surface, the absence of harmful components for humans and the environment, and cost-effectiveness are also important parameters. Although strategies that prevent bacteria from adhering to the surface are effective for short-term use, bacteria tend to adhere to surfaces over time, as they do not show a destructive effect on bacteria, which triggers the formation of biofilm on the surface. For this reason, active surfaces that chemically damage the cell components of bacteria either by the release of an antibacterial agent or by direct contact (contact-killing) of the bacteria are more reliable methods of combating bacteria [30-31]. In addition to the chemical destruction of bacteria by a biocidal agent, antibacterial photothermal therapy, which allows eradication of bacteria by damaging the bacterial cell wall via hyperthermic effect, has attracted a lot of attention in recent years [32]. In this method, bacteria are irreversibly destroyed physically without the need for any chemical agent.
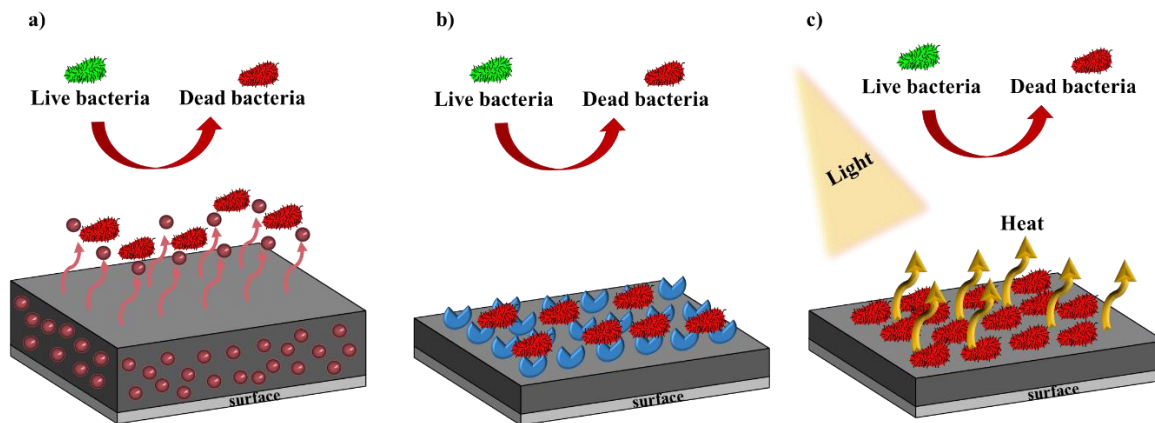
Figure 1. A schematic illustration of antibacterial surface coatings designed to deactivate bacteria by release-killing (a), contact-killing (b), photothermal-killing (c).

In this thesis, antibacterial/antibiofilm surface coatings have been developed that have the potential to be used in food packaging, surfaces in healthcare settings, and many other high-contact surfaces, showing high activity on bacteria and biofilms by release of antibacterial agents, contact-killing, and photothermal effect (Figure 1).

1.2.1 Release-based antibacterial coatings

Release-killing surface coatings deactivate bacteria through the release of an antibacterial agent, which was incorporated into the coating either alone or via a carrier. When the antibacterial agent is incorporated into the coating without any carrier, it can be released in an uncontrolled manner due to the non-covalent binding interactions between the antibacterial agent and the coating causing a fast release. Thus, the concentration of the antibacterial agent may decrease, and the coating material may lose its antibacterial activity when the concentration of the antibacterial agents remains below the minimum inhibitory concentration (MIC) that will kill the pathogenic bacteria over time. From this perspective, the incorporation of an antibacterial agent-loaded nanocarrier into the coating material

following encapsulation of the antibacterial agent into a nanocarrier such as graphene, montmorillonite, halloysite nanotubes, etc. can be a good strategy for controlled and sustained release.

Antibiotics, metal nanoparticles, nitric oxide (NO), and essential oils are some examples of antibacterial agents used in release-based antibacterial coatings.

i)   Antibiotics

Device-associated infections (DAIs) caused by bacterial attachment and colonization on an indwelling device placed inside the body, such as an implant, both cause negative effects on the patient's quality of life due to prolonged hospital stay and an economic burden. Moreover, DAIs can lead to increased mortality and morbidity rates. The incorporation of antibiotics into medical devices plays an important role in the fight against DAIs as the controlled release of antibiotics ensures that the local concentration of antibiotics necessary to kill pathogenic microorganisms is maintained [33]. Many studies on release-based antibacterial surface coatings designed by loading antibiotics on medical devices were reported and some of these studies were summarized in Table 1.

Although antibiotics are the oldest and most commonly used antibacterial agents to fight pathogenic microorganisms, they have some limitations. During the release, the concentration of the antibiotic below the MIC provokes the pathogenic microorganisms to become resistant to the drug, and therefore the antibacterial activity against the bacteria is lost [34]. In addition, biofilms formed as a result of colonization of surface attached bacteria have an extracellular polymer matrix that provides a physical barrier against extreme environmental conditions and antibiofilm therapies [35]. Even if antibiotics are

8

effective on planktonic cells, antibiotics cannot completely eradicate biofilms because they do not have the ability to penetrate this barrier.

Table 1. Examples of antibiotics used in release-based antibacterial surfaces, the delivery system used, targeted microorganisms, and application fields or substrates used.

Antibiotics	Delivery system	Microorganism	Application field/substrate	Ref.
Gentamicin sulfate Triclosan	PDMS	*S. aureus*	Bio-optical materials	36
Cationic antibiotics	LbL multilayer assembly	*S. epidermidis*	Si wafers	37
Gentamicin Polymyxin B	PMAA hydrogel	*S. aureus* *E. coli*	Responsive coatings	38
Triclosan	LbL multilayer assembly	*S. aureus* *E. coli*	Self-defensive coating	39
Gentamicin sulfate Ciprofloxacin	Hydroxyapatite nanoparticle	*P. aeruginosa*	Titanium substrate	40
Vancomycin	Silk Fibroin Nanofibers	*S. aureus*	Titania nanotubes	41
Vancomycin	PEG-based hydrogel	*S. aureus*	Ti implants	42
Rifampicin	Multi-walled carbon nanotube	*S. epidermidis*	Titanium alloy	43
Moxifloxacin	Organic-inorganic sol-gel	*S. aureus* *E. coli* *S. epidermidis*	Ti implants	44

ii)   Metal nanoparticles

Metal nanoparticles such as silver, copper, etc. demonstrate bactericidal activity via oligodynamic effect by the release of positively charged ions that attach to cellular proteins of bacteria and cause deactivation and precipitation of proteins [45]. Contrary to antibiotics, the risk of bacteria gaining resistance to metal nanoparticles is lower; therefore, they can be used as antibacterial agents to be an alternative to antibiotics.

Different forms of silver such as metallic and ions are widely implemented in the biomedical field through incorporation into the coating material. In silver-based coatings, the bacterial cell wall is damaged via effects such as interfering with DNA replication, impairing the permeability of the cell membrane, inactivating the protein, and interrupting the respiratory chain, thereby disrupting the cell integrity [46]. Broad-spectrum activity against both gram-negative and gram-positive bacterial strains was exhibited by silver-containing coatings applied to implants and medical devices, demonstrating that silver-containing coatings are effective in combating DAIs [47-51].

Copper and its compounds are also widely utilized in antimicrobial coatings due to their broad spectrum of activity against pathogens. Copper and its derivatives cause reactive-oxygen species (ROS) production, and penetration to the cell wall of bacteria, thereby creating stress on bacteria [45, 52-53]. Li et al. demonstrated the strong killing activity of copper nanoparticles against both gram-negative and gram-positive bacteria by designing copper-containing coatings on flat surfaces [54]. Furthermore, Phan et al. indicated that different types of copper species such as copper (II) sulfate, copper hydroxide, copper oxide, and copper nanoparticles (Cu NPs) which were incorporated into nanofiber and nanowires showed significant antibacterial activity against *E. coli* and *B. subtilis* [53].

Although coatings based on the release of metal nanoparticles prevent biofilm formation following the bacterial attachment, the cytotoxic effect that may occur on mammalian cells because of the accumulation of metal ions limits their use.

iii)   Nitric oxide (NO)

The reaction between NO and other reactive oxygen species induce the oxidation of lipids, nitration of the cell wall components, and interaction with DNA causing a lethal effect on bacteria [55-56]. In order to ensure the controlled release of NO in coating systems, it is necessary to use donor molecules such as organic nitrates, nitrites, metal-NO complexes, nitrosamines, *N*-diazeniumdiolates (NONOates) and *S*-nitrosothiols (RSNOs) that spontaneously decompose to liberate NO continuously [57]. Sadrearhami et al. have fabricated antibacterial coatings that were both antifouling and highly effective against gram-negative and gram-positive bacteria with a combination of NO precursors and PEG by taking advantage of polydopamine chemistry [58]. Ho et al. have developed solvent-free coatings that release NO continuously and prevent the attachment of pathogenic bacteria and even biofilm formation [59].

iv)   Essential oils (EOs)

EOs, which are natural products of aromatic plants, pass through the cell membrane of microorganisms and cause a lethal effect on them through interaction with lipophilic parts of the cell, thanks to their oily, volatile structure, and thus, they show a high antibacterial effect against a wide variety of pathogenic microorganisms [60-61]. EOs are considered safe because of their natural structure, and they do not cause cytotoxicity in mammalian cells. For this reason, they are frequently used in the food industry both in food preservation strategies and in the prevention of foodborne diseases [62-63]. The incorporation of EOs into

the food packaging materials instead of their direct addition into food prevents disadvantages such as changing the smell of the food, thus packaging materials containing EOs can extend the shelf life of the food by protecting it from the pathogenic bacteria. However, EOs are volatile compounds, so the direct incorporation of EOs into bulk packaging material has some limitations such as a decrease in the effective concentration of EOs due to methods that require heat treatment during packaging film production such as film blowing, extrusion, etc. Besides, EOs are susceptible to oxidative degradation, so they may lose their stability in photothermal applications. Encapsulation of EOs and subsequently incorporating encapsulated EOs either directly into a food packaging film or incorporating them as coatings are important strategies to avoid these disadvantages, as well as allow for the controlled release of the EOs [64]. Makvana et al developed antibacterial glass surfaces against *E. coli* and *B. cereus* that can be used for the packaging of liquid foods by coating glass surfaces with cinnamaldehyde encapsulated in liposomes [65]. Moreover, *Thymus capitatus* and *Origanum vulgare* EOs encapsulated in polymeric poly(ε-caprolactone) (PCL) nanocapsules through nanoprecipitation method have demonstrated high antimicrobial activity against foodborne pathogens in a controlled-release manner [66]. Also, clay nanotubes are good candidates for the encapsulation of EOs due to their porous nature and due to the fact that they can act as reservoirs for controlled-release systems [67].

1.2.2   Contact-killing antibacterial coatings

Contact-killing coatings show antibacterial activity only on direct contact of the antimicrobial agent, that is immobilized on the coating without any leakage, with the pathogenic bacteria [68]. The non-leaching features of the contact-active coatings provide long-

term antimicrobial activity, inhibition of toxicity caused by excessive accumulation in the environment, and improvement in selectivity [69]. Quaternary ammonium compounds (QACs), antimicrobial peptides (AMPs), and enzymes are the most commonly used contact active antibacterial agents incorporated into coatings.

i)   Quarternary ammonium compounds (QACs)

QACs are composed of a positively charged central nitrogen atom and nonpolar alkyl or aryl groups bound to the nitrogen atom (R_4N^+). The antimicrobial action of QACs originates from the disruption of bacterial cell integrity and the dispersal of the cell's cytoplasmic components due to the affinity between the positively charged nitrogen of the QACs and the negatively charged bacterial cell wall [70]. Many studies on the antibacterial surfaces designed by the incorporation of QACs onto coating materials were reported and some of these studies were listed in Table 2.

Table 2. Examples of QACs used in antibacterial contact-killing coatings, the applied surfaces, immobilization techniques, and target microorganisms.

QAC	Applied surface	Immobilization technique	Microorganism	Ref.
PDMAEMA⁺	Glass, PDMS, and silicon wafer	SI-RAFT	*S. aureus* *E. coli*	[71]
Octyl-ammonium functional QAC	PDMS catheter	SI-ATRP	*S. aureus*	[72]
TPGDA	Bone cements	Michael addition reaction	*S. aureus* *E. coli* *P. aeruginosa*	[73]
HACC	Titanium implant surface	Covalently bonded by the silanisation	*S. epidermidis*	[74]
DCAMA	Dental implants	Spin coating	*S. aureus*	[75]
EPTMAC	Microfibril cellulose	Grafted-onto cellulose by nucleophilic addition	*B. subtilis* *S. aureus* *E. coli*	[76]
DMOAP	PVDF membranes EVOH membranes	Grafted to membranes	*E. coli*	[77]
Mixture of QACs	Anodized aluminum	Impregnation into nanoholes	*E. faecalis* *S. aureus* *E. coli* *P. aeruginosa*	[78]

ii)   Antimicrobial peptides (AMPs)

Antimicrobial peptides (AMPs) are part of the innate immune system produced by almost all living species and show antimicrobial activity on many pathogenic microorganisms such as bacteria, viruses, fungi etc. [79]. They are composed of amino acid chains containing lysine or arginine residues, which provide a positive net charge to AMPs. The cationic nature of AMPs is the key feature to their antimicrobial efficacy, since positively charged AMPs interact electrostatically with the negatively charged microbial membrane, causing AMPs to accumulate on the cell membrane. Subsequently, AMPs penetrate the cell and interact with the vital components of the cell such as cytoplasm, nucleic acids, etc. [80-81]. AMPs are potential candidates for being alternatives to antibiotics, due to their broad-spectrum antibacterial activity, high efficacy even at low concentrations, target specificity, and low drug resistance [82]. Many studies have been reported in which AMPs have been used on medical device surfaces such as implants [83], catheters [84-86], titanium surfaces [87-88] to combat pathogenic bacteria by utilizing the antibacterial activity of AMP. Furthermore, Cao et al. stated that stainless steel exhibited an effective antibiofilm property as a result of the dopamine-mediated incorporation of two types of peptides into the steel surface [89].

iii)   Enzymes

Enzymes, the defense mechanism of living organisms from bacterial attack, are the most promising contact-killing agents due to the concern about drug-resistance in bacteria. Antibacterial action of enzymes mostly is target-dependent causing disruption of cell integrity of bacteria through aiming at specific components of cell. Since the degradation in the bacterial cell is irreversible, the bacteria often cannot gain resistance to enzymes.

In addition, enzymes are highly effective on biofilms by easily passing through the extracellular matrix (ECM), which is a natural defense mechanism of the biofilm against environmental stress and antibacterial agents.

Enzymes can be immobilized onto surfaces or carriers via adsorption, covalent bonding, entrapment and cross-linking to obtain effective enzyme stability, multiple and long-term usage; thus, the surfaces that fight against pathogenic microorganism can be designed in many industries, especially healthcare industry [90-92]. Enzymes immobilized on various substrates used in antimicrobial applications, reported in literature, were listed in Table 3.

Table 3. Enzymes immobilized on various substrates and their applications.

Enzyme	Applied surface	Immobilization technique	Ref.
	Chitosan nanofiber	Cross-linking	[93]
	Cellulose nanofiber	Adsorption	[94]
Lysozyme	Agarose WB200	Covalent bonding	[95]
	Wool fiber	Covalent bonding	[20]
	Cellulose acetate nanofibers	İonic interaction	[96]
Heparin	Chitosan-grafted polyurethane	Covalent bonding	[97]
Nisin and lysozyme	Nanocrystalline cellulose	Covalent bonding	[98]
	PDA-coated surfaces	Covalent bonding	[99]
	Cellulose fibers	Covalent bonding	[100]
Lysostaphin	TiO$_2$ nanoparticle	Cross-linking	[101]
	Polylactide nanoparticles	Adsorption	[102]
	Carbon nanotube	Covalent bonding	[103]
Lysostaphin, serrapeptase and DNase	Mesoporous silica nanoparticles	Covalent bonding	[104]

1.2.3   Light-activated antibacterial coatings

Antibacterial photothermal therapy is a physical sterilization method, in which the antimicrobial action relies on creating a hyperthermia effect on pathogenic bacteria by means of photothermal agents, resulting in irreversible destruction of the cell wall [105-106]. In general, photothermal agents convert absorbed light energy to thermal energy when irradiated by the proper light source, causing an increase in local temperature. Light-activated photothermal

therapy, in contrast to chemical-based killing techniques, shows a more effective antibacterial activity in short treatment time, and drug resistance of bacteria is prevented as well [107-108]. Surfaces killing bacteria photothermally can be produced by immobilization of photothermal agents onto surfaces via physical methods such as hydrophobic interaction, electrostatic interaction, or hydrogen bonding, or chemical methods such as covalent bonding. Noble-metal nanoparticles, carbon-based nanomaterials and polymer-based materials are mostly used as photothermal agents [14, 109].

i)   Noble-metal nanoparticles

Local surface plasmon resonance (LSPR), the attractive characteristic of noble metals such as Au, Ag, and Pt, provides free electrons oscillating at the surface following the absorption of a specific wavelength of light, resulting in heat generation on the surface [110]. The heat-generating capacity of metal nanoparticles can also be adjusted by changing their shape, size and morphology, making metal nanoparticles advantageous photothermal agents [111]. Representative examples of noble-metal nanoparticles used as photothermal agents in photothermal antimicrobial surfaces were listed in Table 4.

Table 4. Photothermal antibacterial surfaces designed by using noble-metal nanoparticles.

PTAs	Substrate	Immobilization technique	Microorganism	Ref.
Gold nanoparticle	Silicone rubber	Physical deposition	*S. aureus*	[112]
	Titanium	Physical deposition	*S. aureus, E. coli*	[113]
	Nanocellulose paper	Physical deposition	*B. subtilis, S. aureus, E. coli, P. aeruginosa*	[114]
Gold nanorod	Glass	Physical deposition	*E. coli*	[115]
	Titanium	Electrostatic self-assembly	*S. epidermis, S. aureus, E. coli, P. aeruginosa*	[116]
Gold nanostar	Glass	Covalent bonding	*S. aureus, E. coli*	[117]
Gold nanoshell	PDMS	Covalent bonding	*E. faecalis*	[118]
	TiO$_2$	Acid-catalyzed sol–gel technique	*S. aureus, E. coli, P. aeruginosa*	[119]
Silver	Titanium plates	Electrostatic adsorption	*S. aureus, E. coli*	[120]
	Biocompatible polysaccharide	Embedment	*S. aureus, E. coli*	[121]
Platinum	Gold nanorod	Wet chemical reduction method	*S. aureus, P. aeruginosa*	[122]

ii)   Carbon-based nanomaterials

Carbon-based nanomaterials, such as graphene-based nanomaterials (GBNs), carbon nanotubes (CNTs) and carbon dots (CDs) attract a lot of attention as photothermal agents due to their high surface area, low toxicity, and high thermal conductivity [10, 123-124]. Additionally, the high light absorption capacity of black carbon materials provides superior photo-absorption properties, resulting in effective light-to-heat conversion under

proper light irradiation. Many studies using carbon-based nanomaterials in antimicrobial photothermal therapy have been reported and some of these studies are listed in the Table 5. Despite their superior light-to-heat conversion capacities, carbon-based nanomaterials have some disadvantages such as high production costs, the difficulty of producing the same quality in high quantities and dispersion problems within the coating material.

Table 5. Carbon-based nanomaterials used in antimicrobial photothermal therapy.

PTAs	Substrate	Irradiation condition	Microorganism	Ref.
Graphene oxide	Polyether sulfone	LbL	*S. aureus, E. coli*	[125]
	Glass	LbL	*E. coli*	[126]
	Iron oxide	Hydrothermal method	*S. aureus, E. coli*	[127]
	Nanocellulose paper	Physical deposition	*B. subtilis, S. aureus, E. coli, P. aeruginosa*	[114]
Reduced graphene oxide	Bacterial nanocellulose	Blending	*E. coli*	[128]
	Au nanostar	Seed-mediated growth	MRSA	[129]
Graphene	Glass	Laser induced forward transfer	*E. coli*	[130]
Carbon nanotubes	Hydrogel	Oxidative coupling	*S. aureus, E. coli*	[131]
Multi-walled carbon nanotubes	Waterborne polyurethane	Embedment	*P. aeruginosa*	[11]
Single-walled carbon nanotubes	Melt-blown polypropylene surgical mask	Single-step spray-coating	*E. coli*	[132]

iii)   Polymer-based materials

Conjugated polymers (CPs) have an excellent light-harvesting ability due to the free entanglement of delocalized electrons in their π-conjugated backbones [133]. CPs are remarkable photothermal agents that can be used in PTT due to their high photothermal conversion efficiency, photostability, biocompatibility, simple manufacturing processes, applicability to almost any surface, and low cost [14, 134]. PANI, one of the conjugated polymers, absorbs light strongly in the visible and NIR regions and converts most of the absorbed light into heat due to its low luminescence, which makes PANI an excellent photothermal material [135]. Another conjugated polymer, polypyrrole (PPy), is demanded in many photothermal applications thanks to its excellent stability and biocompatibility as well as high light-to-heat conversion ability [14]. Poly(3,4 ethylenedioxythiophene) (PEDOT), which is frequently used in photothermal therapy, draws attention with its excellent photostability and high photothermal conversion efficiency, as well as its low production cost and resistance to oxidation [14, 136]. Furthermore, besides versatile adhesive properties, polydopamine (PDA) has arisen as a candidate that can be used in PTT due to its high photothermal conversion efficiency, biocompatibility, hydrophilic character, and being not cytotoxic [137-139]. PDA exhibits photothermal properties due to the non-radiative relaxation as a result of the return of the delocalized electrons from the upper energy level to the ground energy level after being stimulated under external stimuli such as light. Some examples on photothermally active antimicrobial surfaces designing by conjugated polymers were summarized in Table 6.

Table 6. Summary of photothermal antimicrobial surfaces based on the polymer-based photothermal agents.

CPs	Substrate	Irradiation conditions	Microorganism	Ref.
PANI	Persistent luminescence nanoparticles	808 nm, 1.5 W cm^{-2}	*S. aureus, E. coli*	[140]
	Silicon, polystyrene, polypropylene, PET	808 nm, 2 W cm^{-2}	*S. aureus, E. coli*	[141]
PPy	Glass fiber membranes	4.5 sun solar light	*E. coli*	[142]
	Carbon nanotubes	808 nm, 1 W cm^{-2}	*P. aeruginosa*	[143]
	Carbon nanoparticles	808 nm, 1 W cm^{-2}	*P. aeruginosa*	[144]
PEDOT	Magnetic iron oxide nanoparticles	808 nm, 2 W cm^{-2}	*S. aureus, E. coli*	[145]
	Glass substrate, 3D cotton structure	808 nm, 2 W cm^{-2}	*S. aureus, E. coli*	[146]
PDA	Titanium	808 nm, 1 W cm^{-2}	*S. aureus* biofilm	[138]
	Glass, silicon wafer, PVC, SR tubes	808 nm, 0.9 W cm^{-2}	*E. coli, S. aureus, C. albicans*	[147]
	Titanium	808 nm, 1 W cm^{-2}	*S. aureus*	[148]
	HNT	808 nm, 0.8 W cm^{-2}	*S. aureus*	[149]

1.3. Dissertation structure

This thesis consists of a total of six chapters, including a general introduction and conclusion. The thesis includes four published journal articles. All references are combined in the "references" section.

A summary of each chapter is as follows:

Chapter 1: The dissertation overview, the aims of the studies and a literature review for the approaches mentioned in the thesis were included.

Chapter 2: The study on antibacterial food packaging films fabricated by the coating of packaging material with an essential oil that is encapsulated in halloysite nanotubes was presented. The antibacterial activity of the coating materials against *Aeromonas hydrophila*, which is usually transmitted by food products that cause gastroenteritis, was investigated both on the coated packaging material and on chicken meat samples wrapped with coated packaging material.

Chapter 3: The study of waterborne polyurethane-polydopamine coatings that destroy bacteria physically without any antibacterial agent due to the light-to-heat conversion was presented. The solid particles in the waterborne polyurethane dispersion were coated with polydopamine with a one-pot reaction, followed by casting films from the hybrid polymer dispersions. The NIR-induced temperature elevations of films were investigated. Furthermore, the antibacterial/antibiofilm properties of the films, which were associated with the death of the attached and/or accumulated bacteria on the surface as a result of the increase in temperature with NIR stimulus, were investigated.

Chapter 4: The fabrication of coating materials that can be used in the fight against *S. aureus*, which causes healthcare-associated infections, was presented. The coating material was designed by the incorporation of hybrid nanoparticles obtained by covalent immobilization of lysostaphin onto polydopamine coated halloysite nanotubes into polyurethane. The antibacterial and antibiofilm activities of the obtained coating materials, which have the capacity to kill bacteria by contact due to the lysostaphin, were investigated.

Chapter 5: The study on antibacterial/antibiofilm coatings fabricated by immobilization of lysostaphin onto thin-film coatings of hybrid polymer system composed of waterborne polyurethane and polydopamine was presented. The antibacterial and antibiofilm properties, as well as the stabilities of the coating materials, were investigated.

Chapter 6: The overall conclusion results for all chapters were included.

CHAPTER 2: Carvacrol loaded halloysite coatings for antimicrobial food packaging applications

2. 1.   Abstract

Antimicrobial thin film coatings that can be utilized in food packaging provide an effective approach to enhance food quality and safety. Here, the coating of polyethylene films with an antimicrobial thin film through a Layer-by-Layer (LbL) assembly is demonstrated. Halloysite nanotubes (HNTs) which are tubular clay nanoparticles were utilized for the encapsulation and sustained release of carvacrol, the active component of essential thyme oil. Antimicrobial thin film coatings of 225 nm thickness were prepared by the deposition of ten bilayers of chitosan (CHI) and carvacrol loaded HNTs onto the polyethylene surface by spray LbL. Coated films reduced the viability of a food pathogen, *Aeromonas hydrophila* by 85% and the aerobic count on chicken meat surfaces by 48%. Furthermore, coated film surfaces demonstrated lower bacterial attachment compared to control polyethylene films indicating their antibiofilm character. Composed of natural and safe components, antimicrobial coatings developed in this study provide a novel and effective approach to obtain antimicrobial food packaging materials that can greatly contribute to food safety.

2. 2.   Introduction

Food packaging materials that can prevent microbial spoilage of food samples provide an efficient solution to shelf life extension. Antimicrobial films can inhibit and/or mitigate the growth of microorganisms through the release of antimicrobial agents from the film surface to the food or the packaging headspace [150]. When an ideally designed sustained release system is utilized, the antimicrobial agent can be retained in the packaging headspace over a longer period; thereby extend the shelf life of packaged food over a reasonable amount of time. The traditional approach to obtain antimicrobial food packaging films is to incorporate antimicrobial agents into synthetic polymers. Polyolefins such as polyethylene and polypropylene are the most commonly utilized polymeric film materials for food packaging applications due to their low cost, good mechanical strength, transparency and suitability for heat sealing and printing [151]. Organic acids, enzymes, bacteriocins, fungicides, inherently antimicrobial polymers, natural extracts and essential oils have been incorporated into polyethylene or polypropylene matrices resulting in films with moderate antimicrobial activity [150, 152].

The main problem associated with the bulk incorporation of antimicrobial agents into polymer matrices is the fact that high temperature processing conditions during melt compounding and film manufacturing processes are expected to decrease the effective concentrations of mostly volatile or temperature sensitive antimicrobial agents. On the other hand, the coating of the inner surface of packaging materials with antimicrobial agents under ambient conditions provides an opportunity for the utilization of these agents in packaging applications more effectively. Several examples exist where antibacterial agents have been coated onto polymeric film surfaces by embedding within polymeric resins [153-159] or directly by

noncovalent [65, 160-161] or covalent [162-164] surface immobilization. While all these coating methods result in food packaging films that are somehow effective against pathogenic microorganisms, they do not provide a great control mechanism for the a function of the nanoscale coating thickness. One effective approach that enables such nanoscale control is the coating of film surfaces by LbL assembly containing active agents. Using this aqueous solution based technique, durable, multilayer coatings with nanoscale thicknesses can be obtained through sequential assembly of oppositely charged electrolytes taking advantage of electrostatic interactions on a charged surface [165-166]. Due to its environmentally friendliness, cost effectiveness and versatility, LbL technique has been widely utilized to functionalize surfaces in a variety of application areas [167-169] while its implementation to prepare antimicrobial food packaging materials has been limited [170-171].

HNTs are naturally formed aluminum silicate nanoparticles presenting a hollow tubular structure. They are widely utilized as multifunctional nanoparticles for drug delivery and controlled release studies [172-175]. We and others have previously demonstrated that loading of HNTs with antibacterial essential oils results in natural and safe antibacterial nanoparticles with sustained release behaviour, which can be incorporated into polymeric matrices to prepare films and coatings with antimicrobial and antibiofilm properties [176-178]. Although these studies show the effectiveness of loaded HNTs in bulk films, to the best of our knowledge, deposition of active agent loaded HNTs onto a material surface as a precisely controlled thin film coating with a sustained release behaviour has not been reported previously.

In this study, we report the use of HNTs loaded with carvacrol, the active component of essential thyme oil as a sustained release system and demonstrate the nanoscale coating of

polyethylene (PE) surfaces with carvacrol loaded HNTs using LbL assembly technique to obtain food packaging films active against food pathogens.

2. 3.   Materials and Methods

2.3.1. Materials

Carvacrol was supplied by Tokyo Chemical Industry Co. (Japan). HNTs were provided by Eczacıbaşı Esan (Turkey). Commercially available corona treated low density PE films with a thickness of 65 μm were used as substrates for the LbL coating application. Poly (sodium-4- styrene sulfonate), MW 70 000 g/mol (PSS), low molecular weight CHI and glacial acetic acid (> 99.8%) were purchased from Sigma Aldrich. *A. hydrophila*, ATCC 35654) was purchased from Medimark (France) and Tryptic soy broth (TSB) was purchased from Biolife (Italy). Deionized water was used in all experiments.

2.3.2. Preparation of carvacrol loaded HNTs (crv-HNTs)

HNTs were mixed with carvacrol at a ratio of 0.1 g HNT/mL. HNTcarvacrol mixture was subjected to ultrasonication with a microprobe (Q700, QSONICA, CT, USA) for 30 min in an ice bath (pulse on 2 s, pulse off 5 s). HNT-carvacrol mixture was then transferred into a vacuum jar connected to a vacuum pump. 1 mbar pressure was applied for 30 min to remove air inside HNTs followed by application of atmospheric pressure for 10 min to allow carvacrol molecules enter evacuated HNTs. The cycle was repeated twice to increase loading efficiency. The solid phase in the resulting suspension comprising crv-HNTs was separated by centrifugation at 5000 rpm for 5 min, and the excess carvacrol was removed. Crv-HNTs were washed with ethanol once by centrifugation to remove surface adsorbed carvacrol molecules

and they were dried overnight at room temperature in an open container. Dry crv-HNTs were kept in a closed container at room temperature.

2.3.3. LbL assembly of CHI/crv-HNT:PSS thin films

CHI solution as the polycationic bath was prepared with a concentration of 1 g/L using 0.1M of glacial acetic acid. An aqueous solution of PSS and crv-HNTs as the anionic bath containing 2 g/L PSS and 1 g/L crv-HNTs was prepared using deionized water and stirred at 1000 rpm for 1 h to obtain a stable negatively charged solution. The pH values of the cationic and anionic polyelectrolytes were determined to be 3.4 and 5.5, respectively. Thin film coatings were directly deposited from these solutions without further pH adjustment.

Spray LbL assembly was performed with a home-built programmable robotic spraying system. A robotic arm equipped with a set of airbrush with nozzle size of 0.35mm was used to coat 100×100mm substrate surface. Working distance of the spray tip was kept at 50mm from the substrate. The robotic arm was programmed to vertically spray solutions along the y-axis of 100mm and move on the x-axis by a step size of 10mm without spraying and then y-axis spraying was repeated until the whole surface was uniformly coated. Airbrushes were calibrated to spray polyelectrolyte solutions at 5 μL/s. Polyelectrolyte solutions were sprayed for 3 s and the rinse water was sprayed for 20 s. Based on the travel time and distance, amount of sprayed solutions was calculated to be 0.15 μL/mm for polyelectrolytes and 1 μL/mm for the rinse water.

The deposition cycle was repeated until desired number of bilayer architecture was reached. To investigate the formation of the LbL architecture, glass substrates were first coated with CHI/crv-HNT:PSS thin films. Glass slides (75 x 25 mm, Corning Inc.) were used after a cleaning protocol. Briefly, glass slides were sonicated for 15 min in the micro-90 diluted

cleaning solution (Sigma-Aldrich) and washed with distilled water twice under sonication for 15 min, followed by plasma cleaning for one minute (Harrick Plasma PDC-002 (230 V)), which also introduces negative charges on substrate surfaces. Glass slide surfaces were then coated by following the spray LbL protocol described above to deposit CHI/crv-HNT:PSS coatings with number bilayers from two to ten. Thicknesses of coated films on glass substrates with two to ten bilayers were determined by KLA-Tencor P6 Surface Profilometer. Approximately 1mm of Z range on the surface was scanned by applying 1 mg force with 50 μm/s velocity. For the assembly of CHI/crv-HNT:PSS thin films on PE surfaces, PE substrates (15×15 cm) were washed with deionized water for purification and dried with nitrogen airgun followed by the spray LbL protocol described above. Antibacterial studies were performed on PE films coated with 10 bilayers of CHI/crv-HNT: PSS, designated as PE/(CHI/crv-HNT: PSS)$_{10}$. As control films without crv-HNTs, PE substrates were coated with 10 bilayers of CHI/PSS, designated as PE/(CHI/PSS)$_{10}$.

For the investigation of the surface morphology of thin films obtained by spray LbL, samples were coated with Au-Pd and visualized by LEO Supra 35 V P Scanning Electron Microscopy.

2.3.4. Bacterial viability

A. hydrophila were grown in 3 mL TSB overnight at 30 °C. Cells were harvested by centrifugation, washed twice in sterile Phosphate Buffered Saline (PBS) and re-suspended in PBS at a concentration of 10^9 CFU/mL. 1 cm×1 cm pieces of PE/(CHI/crv-HNT:PSS)$_{10}$ films were incubated in *A. hydrophila* suspensions of 10^8 CFU/mL in PBS at 30 °C in a shaker incubator. As controls, neat PE films and PE/(CHI/PSS)$_{10}$ films of the same size were also incubated with cells along with a "cells only" sample without a film. Films were removed after 48 h and aliquots of suspensions were serially diluted. 100 μL of each dilution was plated

on TSB agar plates. Bacterial colonies were counted after overnight incubation at 30 °C. The bacterial viability test was repeated three times for each sample. Viability values were calculated by comparing the number of colonies in samples incubated with films to the number of colonies in "cells only" sample and reported as the mean value with standard error calculated from three separate tests.

2.3.5. Bacterial growth on chicken surfaces wrapped with crv-HNT/PE films

Fresh chicken meat samples were cut in 3 cm×3 cm pieces, weighing 8 g each, wrapped with PE, PE/(CHI/crv-HNT:PSS)$_{10}$, PE/(CHI/PSS)$_{10}$ films and incubated at 4 °C. Following a 24 h incubation, bacteria on the chicken meat surface were transferred into TSB by using a sterile swab. Aliquots of suspensions were serially diluted. 100 µL of each dilution was plated on TSB agar plates. Bacterial colonies were counted after overnight incubation at 30 °C. Each sample was tested three times.

2.3.6. Bacterial attachment on crv-HNT/PE surfaces

1 cm×1 cm pieces of films were incubated with *A. hydrophila* in wells of a 12-well plate. Each well contained 10^8 CFU/mL *A. hydrophila* in TSB. After incubation for 48 h at 30 °C, bacterial suspensions were removed from wells and films were rinsed with sterile PBS twice. Films were stained with BacLight Live/Dead stain (L-7012, Invitrogen, USA) for 30 min in dark at room temperature followed by rinsing with PBS. Films were then mounted onto coverslips and imaged with a Carl-Zeiss LSM 710 Laser Scanning Confocal Microscope equipped with a Plan-Apochromat 63x/1.40 oil objective. Reported images are 3-D renderings of Z-stacks created by using Zen 2010 software.

2. 4. Results and Discussion

2.4.1 Coating of PE film surfaces with CHI/crv-HNT:PSS

The use of crv-HNT nanoparticles as antimicrobial agents has been previously reported by Hendessi et al. [176]. The ultrasonic treatment of HNTs in the presence of excess carvacrol followed by vacuum application to replace water and air within HNTs with carvacrol molecules resulted in approximately 15 wt. % loading of carvacrol (Figure 2a). Encapsulated carvacrol was shown to be released in a sustained manner over a period of one week at room temperature (Figure 2b). Crv-HNT nanoparticles were demonstrated to be active against a panel of foodborne pathogens including *Pseudomonas putida, Aeromonas hydrophila, Listeria monocytogenes, and Staphylococcus aureus* as shown by agar diffusion assays.
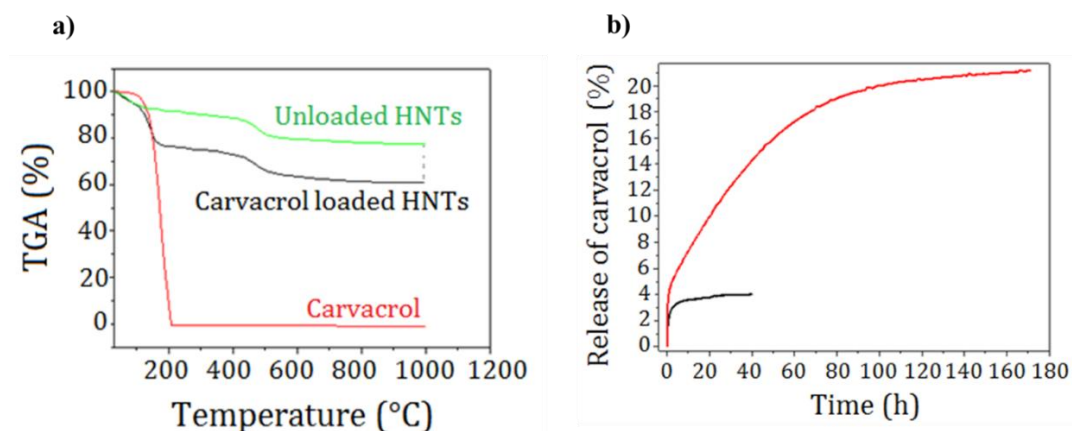
Figure 2. (a) Temperature dependent weight loss curves for unloaded HNTs (green), carvacrol loaded HNTs (black), and carvacrol (red) obtained by TGA; (b) carvacrol release curves represented by time dependent percent weight loss of carvacrol loaded HNTs (red) and unloaded HNTs (black) as calculated by isothermal TGA at 30 °C [176].

In this study, the thin film coating of PE film surface with crv-HNTs was performed by LbL assembly of alternating positively charged CHI and negatively charged crv-HNT:PSS layers

on the plasma treated film surface as schematically shown in Figure 3. HNTs, which inherently carry a negative charge due to their silicon dioxide outer surfaces were mixed with PSS polymer in a ratio of 1:2 to provide sufficient anionic charge density and form a stable aqueous dispersion that would allow a homogeneous distribution on the surface. The positively charged layer of the coating architecture was formed by CHI, a linear polysaccharide based biopolymer, which was also expected to contribute to the antimicrobialactivity of the coating due to its known effectiveness against pathogenic microorganisms.

An automated spray-LBL technique was utilized for the LbL thin film assembly of CHI and crv-HNTs layers on the PE surface. The automated spray LbL process allows a faster deposition of electrolyte layers onto large area surfaces, which renders this coating method suitable for larger scale applications [179-180]. In this work, we aimed to demonstrate the applicability of the spray LbL technique to coat PE film surfaces with crv-HNTs in a short time, as a feasible, nanoscale coating method for food packaging applications.

Firstly, the formation of CHI/crv-HNT:PSS thin film coatings via the spray LbL technique was investigated by evaluating the deposited film thickness as a function of deposited number of bilayers on a glass substrate. The film thickness growth curve obtained by profilometry measurements as a function of the number of deposited bilayers is shown in Figure 4. The film thickness increased almost linearly as a function of the number of deposited bilayers, resulting in approximately 225 nm film thickness when ten bilayers were deposited. Larger variations were observed in film thicknesses as the number of bilayers increased, which can be explained by the potentially higher surface roughness as more HNTs were incorporated onto the surface.
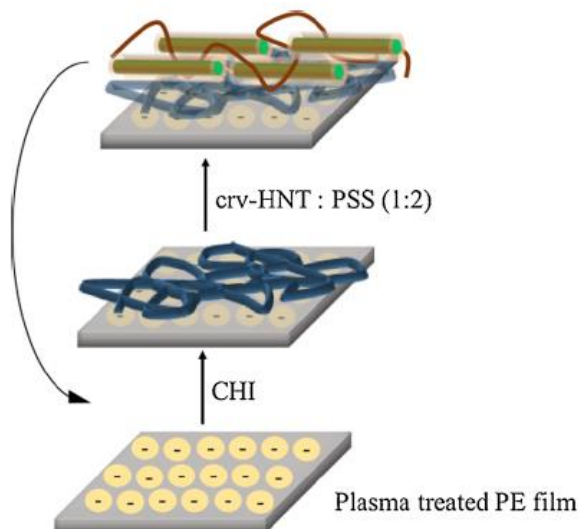
Figure 3. Schematic representation of the LbL assembly of CHI and crv-HNTs on PE film surface.

Next, PE film surfaces coated with carvacrol loaded HNTs were investigated to evaluate the distribution of HNTs on the PE surface. Figure 5 shows representative scanning electron microscopy (SEM) images of PE surfaces coated with ten bilayers of CHI/crv-HNT:PSS by the spray LbL technique. SEM images clearly show that crv-HNTs were successfully deposited on the film surface presenting a homogeneous distribution of HNTs as tubular nanoparticles with varying widths of 10–150 nm and lengths of 0.1–1 μm. The homogeneous distribution of crv-HNTs is desirable for a uniform antibacterial activity throughout the film surfaces.
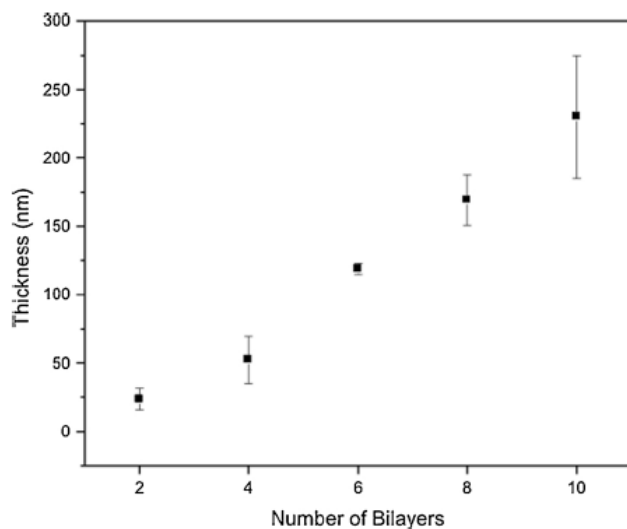
Figure 4. Growth curves of spray LbL assembled CHI/crv-HNT:PSS thin films.

It should be noted that the deposition of a ten-bilayer thin film coating of homogeneously distributed HNTs via the custom designed spray LbL approach was ten times faster than the deposition of the same coating via the conventional LbL system by the dipping process. This unparalleled coating speed along with a highly homogenous distribution of antimicrobial agent loaded HNTs makes the spray LbL approach a promising method for the preparation of thin film coatings on PE surfaces for food packaging applications.
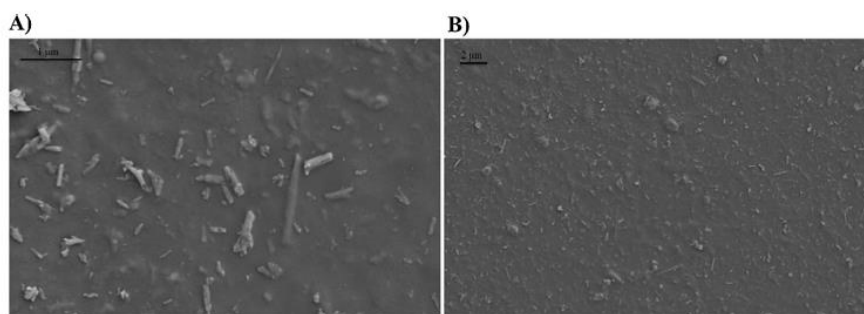
Figure 5. Representative SEM images of PE film surfaces coated with crv-HNTs through spray LbL technique. The scale bar represents 1 μm in (A) and 2 μm in (B).

2.4.2 Antimicrobial properties of crv-HNT coated PE surfaces

As the LbL assembly allows the preparation of crv-HNT thin films of any thickness by varying the number of bilayers, the amount of HNTs releasing carvacrol from the surface and thus the antimicrobial activity of the film can be controlled as desired. Antimicrobial properties of spray LbL coated film surfaces were demonstrated with PE films having ten bilayers of crv-HNT:PSS and CHI, as ten bilayer-coatings provide a good balance between practical coating preparation times and effective carvacrol concentrations within the coating.

The antimicrobial activity of crv-HNT coated PE films was evaluated against the food pathogen *A. hydrophila*, as a representative species, by using the viable-cell counting method. *A. hydrophila* are aquatic gram negative pathogens causing gastroenteritis, which are usually transmitted by food products [181]. Furthermore, their accumulation makes material surfaces susceptible to the biofilm formation, which is a great challenge for several industries causing both financial losses and infection related health problems [182]. Aqueous suspensions of *A. hydrophila* were incubated with LbL coated PE films of equal surface areas for 24 h followed by plating serially diluted suspensions and viable-cell counting. Viability values were calculated in comparison to viable cell counts in suspensions that were not incubated with any films. As demonstrated in Figure 6, neat PE films that were not coated did not show any antimicrobial activity. PE films coated with CHI/crv-HNT:PSS, on the other hand, resulted in 85% decrease in the viability of cells, demonstrating a strong bactericidal effect against *A. hydrophila*. Considering the known antimicrobial activity of CHI, in order to better understand its contribution in the film co-deposited with crv-HNT, the antimicrobial effect of CHI/PSS coated PE/(CHI/PSS)$_{10}$ film was also determined. Incubation of cells with this control film, lacking crv-HNTs on the surface led to significantly higher viability than PE/(CHI/crv-

HNT:PSS)$_{10}$ films, demonstrating that the antibacterial effect was significantly arising from crv-HNTs on the CHI/crv-HNT:PSS coated PE surface. Apparently, carvacrol molecules that were released from HNTs over the 24 h of incubation presented a killing effect on *A. hydrophila* cells.
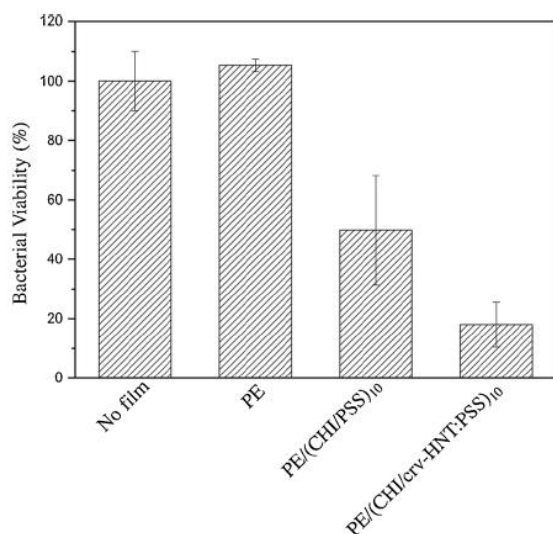
Figure 6. Viability of A. hydrophila incubated in the presence of films of equal sizes for 24h.

The effectiveness of crv-HNT coated PE films as active food packaging materials with antimicrobial activity was evaluated on actual chicken meat samples. Pieces of chicken meat samples cut to the same size were wrapped with neat PE, PE/(CHI/crv-HNT:PSS)$_{10}$ and PE/(CHI/PSS)$_{10}$ films. The total number of viable bacteria on chicken meat surfaces was determined for each package by the aerobic plate count following a 24 h incubation at 4 °C as a way to compare their background microbiological status. Differences in aerobic plate count results for chicken meat samples wrapped with two control films, neat PE and CHI coated PE, and crv-HNT coated PE films are shown in Figure 7. While the PE/(CHI/PSS)$_{10}$ presented only 0.4 log difference, PE/(CHI/crv- HNT: PSS)$_{10}$ films presented 1.4 log difference compared to neat PE films. The growth of microorganisms on the chicken surface in contact

with crv-HNT thin film coating was inhibited due to the sustained release of carvacrol. These results clearly demonstrate that the microbiological quality of chicken meat samples packaged with PE films coated with crv-HNTs through the LbL assembly was significantly improved relative to chicken meat samples packaged with neat PE films. This improvement on the microbiological quality would be reflected as a longer shelf-life for food products packaged with crv-HNT coated films as bacteria-related spoilage would be postponed.
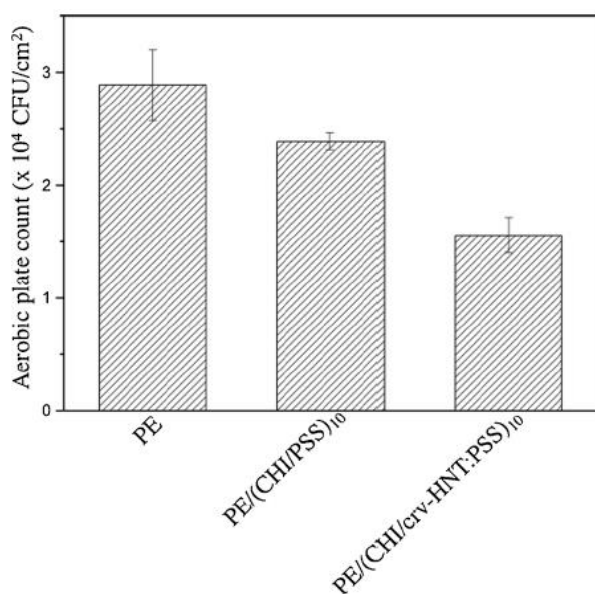
Figure 7. Aerobic plate count of chicken meat surfaces wrapped with neat PE films and thin film coated PE films following a 24 h incubation at 4 °C.

The effectiveness of crv-HNT coated PE films against bacterial surface attachment was also investigated to evaluate their antibiofilm properties. PE/(CHI/crv-HNT:PSS)$_{10}$ films along with control films including neat PE films and PE films coated only with CHI and PSS were incubated with *A. hydrophila* cells in growth medium for 48 h. Following the incubation, films were washed to remove unadhered cells and stained with live-dead indicator fluorophores. Figure 8 shows representative laser scanning confocal microscopy images of stained films.

The neat PE film surface was highly colonized with live bacteria as shown by the green staining of cells. On the other hand, surfaces of films coated with only CHI:PSS and both CHI and crv-HNTs:PSS were significantly less colonized by bacteria due to the antimicrobial activity of thin film coatings. Interestingly, while cells colonized on PE/(CHI/PSS)$_{10}$ were mostly alive, cells colonized on PE/(CHI/crv-HNT:PSS)$_{10}$ films were dead to a much greater extent. These results clearly demonstrate that the nanoscale crv-HNT coating imparts antibiofilm character to the PE surface by both mitigating bacterial attachment and killing the surface attached bacteria.
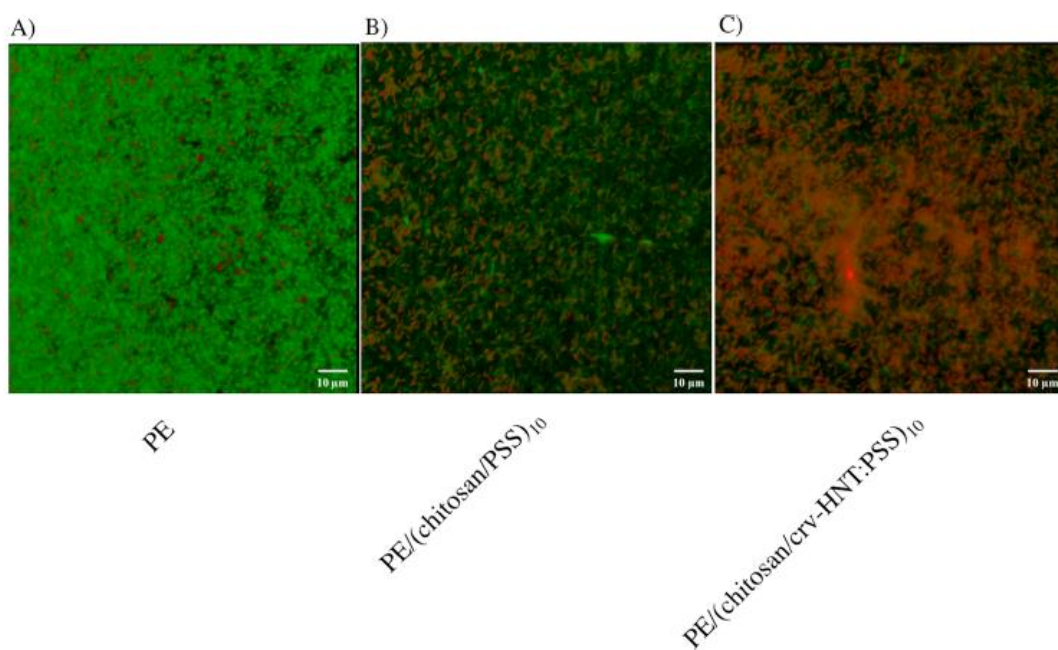
Figure 8. Representative laser scanning confocal microscopy images of surfaces of neat PE film (A), PE film coated with bilayers of CHI and PSS (B), and PE films coated with bilayers of CHI and crv-HNTs dispersed in PSS (C) following a 24 h incubation with A. hydrophila and staining with live-dead cell stain.

While an extensive evaluation of antimicrobial activity of prepared films against a panel of food pathogens is required before defining their actual shelf-life extending capabilities,

antimicrobial and antibiofilm properties of films reported in this study poses a great potential for use as food packaging materials that keep food safe for longer.

The coating design presented in this work provides a modular system, where clay nanoparticles act as encapsulating agents that allow the sustained release of any antimicrobial agent from a nano-sized thin film coating. While the antimicrobial activity of prepared coatings on food packaging film surfaces was demonstrated with carvacrol molecules as a natural antimicrobial agent, various other types of antimicrobial agents can be utilized based on the microbiological requirements for food products to be packaged and kept fresh.

2. 5.   Conclusions

A thin film coating of carvacrol loaded HNTs that can serve as antimicrobial active layer for food packaging applications was assembled on food packaging films by spray LbL deposition technique.

While the custom spray LbL approach provided an unparalleled coating speed and highly homogenous distribution of high aspect ratio nanostructures, the sustained release of carvacrol from homogeneously distributed and immobilized HNTs through the fabricated thin film coating on the polyethylene surface imparted antimicrobial and antibiofilm properties against food pathogens. The contribution of prepared packaging films to the microbiological quality of food products would potentially slow down the bacteria-related spoilage and extend their shelf-life. Composed of natural and safe components, films demonstrated in this study have a great potential for utilization as food packaging materials that are effective against foodborne infections and financial losses caused by food spoilage.

CHAPTER 3: NIR-responsive waterborne polyurethane-polydopamine coatings for light-driven disinfection of surfaces

3. 1.   Abstract

Apart from conventional chemical-based methods, alternative disinfection methods that can physically destroy bacteria are needed. Here, biocompatible, non-toxic, environmentally friendly hybrid coatings prepared from dispersions of polydopamine-coated waterborne polyurethane particles (WPU-PDA) that offer effective light-to-heat conversion were designed to eradicate pathogenic bacteria and biofilms using photothermal therapy. The resulting WPU-PDA hybrid coatings demonstrated an effective photothermal activity by reaching 155 °C under 4 min NIR-laser irradiation and staying stable upon multiple irradiation cycles. WPU-PDA coatings induced hyperthermia on *S. aureus* resulting in a 3.5 log reduction of viable cells with a killing activity that is stable for at least 20 contamination/disinfection cycles. Furthermore, the prepared coatings were shown to have antibiofilm properties resulting in a 3 min NIR-light activated 3.9 log reduction in the viability through physical disruption of biofilm bacteria. Light-activated

antibacterial/antibiofilm coatings demonstrated here provide a strong potential for NIR-light activated disinfection of surfaces.

3. 2.   Introduction

Bacteria have the ability to adhere to almost any material surface and subsequently form biofilms [183-184]. Pathogenic bacteria accumulated on material surfaces can result in deterioration of surface properties, as well as threaten public health by causing infections [185-186]. Therefore, disinfection of different material surfaces, from biomedical devices such as implants to environmental surfaces such as hospital walls, filtration systems or food packaging, is essential for reducing biological contamination and improving the efficacy of the materials. Chemical decontamination via the incorporation of antibacterial agents into surfaces is the conventional method that is frequently used today [187-188]. Antimicrobial peptides [189-190], antimicrobial enzymes [191-192], nanoparticles[193], quaternary ammonium compounds [18, 194] and antibiotics [195-196] are examples of antibacterial agents used for the fabrication of chemically-active antibacterial surfaces that can inhibit the attachment of bacteria to the surfaces and/or kill already attached bacteria. However, these antibacterial agents used in surface decontamination have some disadvantages such as low resistance to environmental conditions, reduced performance in long-term or multiple-use, high cost and bacteria gaining resistance to the antibacterial agents [197]. Alternatively, external stimuli-triggered physical disinfection of surfaces based on disruption of bacterial cells strongly overcomes the disadvantages of chemical disinfection.

Photothermal therapy (PTT) based on light-to-heat conversion causing temperature elevations under near infrared (NIR) light irradiation, provides an important physical

sterilization method for direct in-situ decontamination of materials [198-199]. Antibacterial PTT ensures efficient elimination of bacteria through various hyperthermia effects such as cell membrane rupture, protein/enzyme denaturation and degradation of nucleic acids [32]. While antibacterial PTT is advantageous in terms of short treatment times and the fact that bacteria can not gain resistance, it also provides broad-spectrum disinfection with higher antibacterial efficacy compared to conventional disinfection methods in which antibacterial agents are used [109, 200]. NIR light-activated PTT is also superior to other photosensitive antibacterial disinfection systems based on ultraviolet (UV) radiation, such as direct UV disinfection or photodynamic therapy due to the high penetrability and nontoxicity of the NIR light, which allows deep disinfection without being harmful [201]. The fact that photothermal disinfection of surfaces provides heat-based killing that can inactivate other pathogens such as viruses as well makes this method a promising tool for a broad range of antimicrobial applications including the development of reusable personal protective equipment which has become vital during COVID-19 pandemic [202-203].

Noble-metal nanoparticles such as Au, Ag and Pt [122, 204-206]; carbon-based nanomaterials such as graphene, carbon nanotubes and carbon dots [11, 126, 128, 207]; metal sulfide/oxide nanomaterials [208-209] and small molecule-based nanomaterials such as cyanine-based dyes and Prussian blue [210-211] are the most used photothermal agents due to their strong NIR light-absorbing capability and excellent photothermal conversion features. Nevertheless, polymer-based photothermal materials such as conjugated polymers are promising candidates since they do not have the limitations shown by most photothermal nanoparticles such as toxicity, poor photostability under long-term light irradiation, difficulty in large-scale application and high cost [212-215]. Most conjugated polymers composed of alternating π and σ-bonds present

light-to-heat conversion capability as they strongly absorb light in the near-infrared (NIR) window and are preferred in PTT due to their high photothermal conversion efficiency, biodegradability, cost effectiveness, good photostability and easy production [14, 134].

Polydopamine, a mussel-inspired polymer, can be synthesized by oxidation polymerization of the dopamine monomer under alkaline conditions [216]. The catechol groups of polydopamine allow easy adhesion on both organic and inorganic materials; thus, any surface can be coated with polydopamine to take advantage of its non-cytotoxicity, good biocompatibility and durability [217-219]. Furthermore, polydopamine can convert NIR light to heat effectively due to its conjugated structure and thereby introduces photothermal features to the material that is coated [220]. The produced light-activated heat can be utilized for the inactivation of pathogenic bacteria and biofilms deposited on material surfaces with the incorporation of polydopamine into the nanoparticles [221-223], hydrogels [224-226], hybrid nanofibrous scaffolds [227] and surface coatings [138, 147, 228]. However, the large-scale application of polydopamine coatings is one of the drawbacks of such applications and limits the practical use of these materials. Besides, polydopamine-coated nanoparticles produced for PTT may not be homogeneously distributed in the coating matrix, thus, the inability to dissipate the temperature equally on the coating material surface leads to antibacterial PTT not to be used effectively. Recently, coating of waterborne polyurethane (WPU) solid particles with polydopamine in aqueous dispersion was demonstrated to result in a photothermal polymer matrix that exhibits the light-to-heat conversion properties of polydopamine in its entirety [229].

In this study, we have designed antibacterial coatings from a photothermal polymer matrix consisting of polydopamine coated WPU particles specifically for use in light-activated

disinfection of surfaces. The NIR-induced temperature elevations in the waterborne polyurethane/polydopamine matrix allows significant bacterial killing activity resulting in efficient light-activated disinfection. The design approach adopted here synergistically combines the advantages of WPU and polydopamine in a single polymer matrix, allowing for biocompatible, non-toxic, environmentally friendly antibacterial coatings that can be effectively disinfected by NIR-light and easily applied on a large scale.

3. 3.   Materials and Methods

3.3.1   Chemicals

Dopamine (3-hydroxytyramine hydrochloride) was purchased from Acros Organics Inc. Ultrapure Tris base (Tris(hydroxymethyl)aminomethane) was purchased from MP Biomedicals, LLC. Sodium hydroxide pellets, hydrochloric acid (ACS reagent, 37%), ethylenediamine (EDA) and acetone (99.5%) were purchased from Sigma-Aldrich Inc. Hexamethylene diisocyanate (HDI) and a linear polyester formed from adipic acid, butane-1,4-diol, ethylene glycol, diethylene glycol (Desmophen 1652, Mn=2000 g/mol) were purchased from Covestro AG. Sodium 2-[(2-aminoethyl) amino] ethane sulphonate (AEAS, 50 wt% in water) was kindly donated by Evonik Industries. The polyester polyol was dried at 80 °C under vacuum (~2 mbar) for 15 min prior to use. Tryptic soy broth (TSB) and agar powder were purchased from Medimark (Italy). Deionized (DI) water was used in all experiments. All chemicals were used without any further purification unless stated otherwise.

3.3.2　Synthesis of WPU

The WPU was synthesized using the acetone method [191, 230]. NCO-terminated polyurethane prepolymer was synthesized by charging a four-necked, 1-L glass round-bottomed-flask equipped with a heating mantle, stirrer, condenser and a thermocouple with 170.8 g of polyester polyol and 29.0 g of HDI, allowing the mixture to polymerize at 80 °C until reaching the theoretical NCO content, which was determined by the standard di-butyl amine back titration method (ASTM D2572-97). Once the theoretical NCO value was achieved, the reaction temperature was dropped to 50 °C while dissolving the prepolymer in acetone to obtain 40 wt. % solid content. Upon the complete dissolution of the prepolymer in acetone, the chain extension step was carried out by adding the mixture of 13.3 g AEAS (50 wt. % in water) and 1.9 g EDA dropwise into the solution at 50 °C. FTIR spectroscopy was employed to ensure the sharp NCO peak detected around 2267 cm^{-1} arising from the prepolymer's NCO end-groups completely disappeared at the end of the chain extension reaction as expected. Afterwards, the prepared polyurethane polymer was dispersed in water by slowly adding 110.00 g of distilled water into the flask while cooling the mixture to 40 °C. Finally, acetone was removed from the reaction mixture by vacuum distillation and complete removal of acetone was ensured at 45 °C, 50 mbar. WPU with approximately 35 wt. % solid content with the pH value of 7.0 was obtained by filtering the final dispersion through a 50-micron filter.

3.3.3　Preparation and characterization of WPU-PDA

WPU-PDA was prepared as reported earlier [229], but with modifications in pH and solid content of the reaction mixture. 0.56 g of dopamine (6 mg/mL) was dissolved in 10 mL of distilled water. Dopamine solution was added to WPU dispersion dropwise with the help of

a dropping funnel and the final solid content of WPU was adjusted to 6 % by adding an extra 84 mL of water. The pH value of the reaction was adjusted to 8.5 by using ultrapure Tris base. The reaction mixture was kept at 40 °C for 24 h with stirring at 200 rpm. Dark brown dispersions were obtained at the end of the reaction.

The hydrodynamic diameter of WPU and WPU-PDA solid particles was determined by using a Dynamic Light Scattering (DLS) instrument (Zetasizer Nano - ZS, Malvern Instruments Ltd., UK) equipped with laser diffraction and polarized light detectors at three wavelengths. Measurements were performed by preparing dispersions of an adequate concentration in the cell at room temperature.

The WPU-PDA dispersion was cast into a Teflon mold (15 cm × 5 cm) at room temperature and dried under ambient conditions for three days. Following the drying process, films were washed with excess amount of distilled water to remove any potential chemical residues from the surface. Finally, prepared films were kept in an oven at 80 °C for two h and stored in a desiccator under dark. The final film thicknesses were measured to be approximately 0.2 ± 0.05 mm by using a digimatic micrometer (Mitutoyo Quicmike, no. 99MAB041M). WPU films that were used as control samples were prepared by performing the same procedure using a WPU dispersion with a solid content of 6 %.

The absorbance spectra of WPU and WPU-PDA films were recorded using Agilent Carry 5000 UV-VIS-NIR Spectrophotometer in the spectral range from 400 to 1200 nm.

Static contact angle measurements of WPU and WPU-PDA hybrid film was performed by the sessile-drop method using a Theta Lite Contact Angle Measurement System with an optical tensiometer. Approximately, 10 µl distilled water was dropped on the surface at room temperature and contact angle values were recorded by the optical tensiometer equipped with

a high-resolution digital camera. At least three measurements were taken for each sample and average contact angle values were reported.

To determine the thermal conductivity of films, the Hot Disk Thermal Constant Analyser (TPS2500 S) was performed.

The mechanical properties of films were tested by a universal testing machine Zwick Roell Z100 UTM with a load cell of 200 N and a crosshead speed of 25 mm/min according to the testing method determined by ASTM D1708-10. An average of at least four replicates of each sample was reported.

3.3.4 Photothermal performance of WPU-PDA films

WPU and WPU-PDA hybrid films (10 mm × 10 mm) were exposed to NIR laser at 808 nm (STEMINC, SMM22808E1200) (Doral, FL USA) with a laser power of 0.8 W/cm^2 for 4 min, followed by cooling down to room temperature by switching off the laser. The temperature was recorded every 2 s with an infrared thermal camera (FLIR E6XT 2.1L).

The photothermal stability of films was evaluated by three cycles of laser on–off treatment. In each cycle, the samples were irradiated for 4 min with the laser on, followed by cooling to room temperature with the laser off. Meanwhile, the temperature was recorded every 10 s. All measurements were repeated three times and average values were reported. After each cycle samples were dissolved in dimethylformamide (DMF) and analyzed by gel permeation chromatography (GPC) (Triple detection Viscotek GPCmaxVE-2001). HPLC grade DMF at 55 °C was used during measurements and the eluent flow rate was set to 1 mL/min. A mixed-D column system (D5000-D3000-D1000-DGuard or D5000 D3000-DGuard) was utilized with refractive index (RI), multiple angle laser light scattering (MALLS) and viscometer

detectors. The weight average molecular weight of the samples was calculated from a conventional calibration made with 12 narrow PMMA standards in the range of 0.6–300 kDa.

3.3.5 Evaluation of NIR-driven antibacterial activity of WPU-PDA films

S. aureus ATCC 29213 (3 mL) grown in TSB overnight at 37 °C in a shaker incubator (200 rpm) were centrifuged, rinsed twice in sterile Tris buffer (pH=7.5) and resuspended in Tris at a concentration of 10^7 CFU/mL. WPU and WPU-PDA samples (10 mm × 10 mm) were placed into a sterile 12-well plate and 30 μL of bacterial suspension was put onto each sample. Then, samples were subjected to a continuous 808 nm laser irradiation for 1 min and 3 min. The samples that were not irradiated were used as controls. To collect bacteria from the sample surfaces, 1 mL of Tris buffer was added into each well and shaken in a rotational shaker at 200 rpm for 15 min. Bacterial suspensions were then serially diluted and plated onto TSB agar. Following the incubation of agar plates at 37 °C for 18 h, colonies grown on plates were counted and the number of bacteria was calculated as log CFU/cm^2. Each sample was tested three times.

Multiple on-off cycles of NIR light exposure were performed on bacteria-treated samples to assess the reusability of WPU-PDA hybrid films. For this purpose, 30 μL of bacterial suspension (10^6 CFU/mL) was placed onto WPU-PDA films (10 mm x 10 mm) followed by continuous 808 nm laser irradiation for 3 min. Then, the films were washed with Tris buffer and the bacteria on the film surface were transferred to the buffer. The films were then dried under nitrogen gas flow and 30 μL of bacterial suspension was placed onto dried film samples for the second round of irradiation. Treatments of films was repeated for 20 cycles. After each cycle, the number of bacteria was determined by serial dilution, plating and colony counting. Each sample was tested three times.

3.3.6   Evaluation of NIR-driven antibiofilm properties of WPU-PDA films

WPU and WPU-PDA hybrid films (10 mm x 10 mm) were incubated with 2 mL of *S. aureus* suspension containing 10^8 CFU/mL in a 12-well plate overnight at 37 °C under static conditions. Following the incubation, the films were removed and gently washed twice with sterile Tris. The films were stained by LIVE/DEAD BacLight kit and incubated for 10 min in the dark at room temperature. The excess staining solution was rinsed with PBS. The films were mounted onto coverslips and visualized with a Carl Zeiss LSM 710 laser scanning confocal microscope equipped with a Plan-Apochromat 63×/1.40 oil objective before and after exposure to NIR laser light for 10 min. Reported images are 3-D renderings of Z-stacks created by using the Zen 2010 software.

To determine the effect of laser exposure on biofilms quantitatively, after eliminating unattached bacteria by gently immersing of films into the Tris buffer, films were put into 1 mL of Tris buffer and then agitated in an ultrasound bath for 20 min followed by vortexing for 30 s. The viable cell counting method was performed on the Tris buffer solution containing bacteria released from biofilms. Each sample was tested three times.

The morphology of bacteria before and after laser exposure was investigated by using LEO Supra 35 V P scanning electron microscopy (SEM). Samples were fixed in 2.5% glutaraldehyde in sterile PBS for 2 h at room temperature. After fixation, samples were rinsed twice with sterile PBS followed by dehydration through a series of increasing ethanol concentrations. Dried samples were coated with Au/Pd for SEM visualization.

3. 4.   Results and Discussions

Catechol chemistry of polydopamine (PDA) presents a material-independent surface coating technology that allows PDA to be deposited on any surface due to its mussel-inspired character [231]. Here, WPU solid particles were coated with PDA to impart photothermal features to the WPU [229]. The schematic illustration of the synthesis of PDA coated WPU (WPU-PDA) particles is shown in Figure 9a.
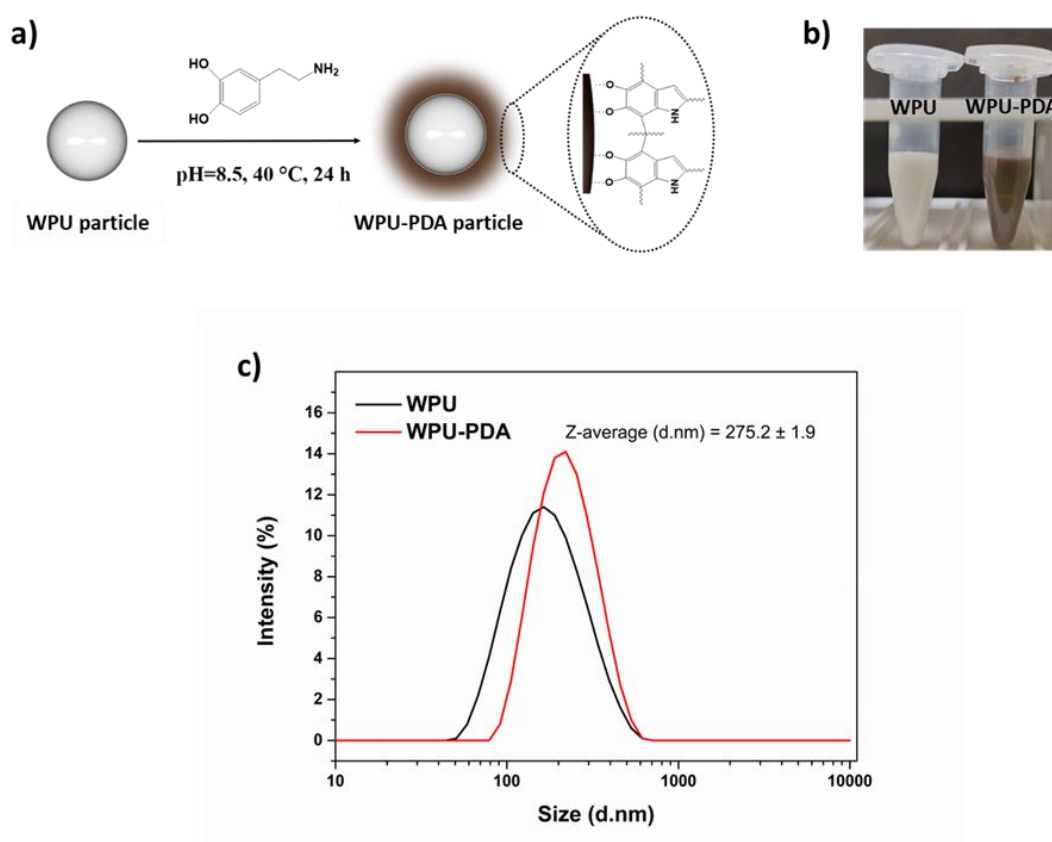
Figure 9. Schematic illustration of WPU-PDA synthesis (a), photographs (b) and DLS analysis (c) of WPU and WPU-PDA dispersions.

The white color of the WPU dispersion turned to dark brown following the reaction indicating that the WPU particles were successfully coated with PDA (Figure 9b). The dynamic light scattering (DLS) measurements of WPU-PDA dispersion presented an

increase in the mean particle size due to the coating of the outer surface of the WPU particles with PDA (Figure 9c). Furthermore, the WPU-PDA dispersion showed a uniform distribution of sizes with an average diameter of 275 ± 2 nm, which is evidence for the fact that the dispersion did not contain any particles other than WPU-PDA particles.

Whether the WPU-PDA films had the absorption properties that are required for NIR light-activated photothermal conversion based lysis of bacteria [232] was studied. As compared with the transparent WPU films, the black-colored WPU-PDA films presented a significantly enhanced, broad absorbance in the UV-VIS-NIR region, potentially due to the π-π* transition of the benzenoid ring of the PDA backbone indicating that they can be utilized as NIR light-activated photothermal materials (Figure 10).
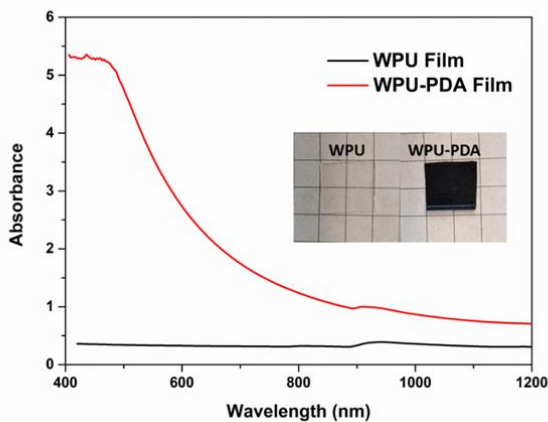
Figure 10. UV-VIS absorption spectra of WPU and WPU-PDA films.

Wetting properties, thermal conductivity values and mechanical properties of WPU-PDA films were evaluated in comparison to WPU films and were listed in Table 7. The contact angle value of the WPU-PDA film decreased relative to the WPU film, indicating an increase in hydrophilicity due to the abundant hydrophilic catechol groups of PDA. The low thermal conductivity of the material plays an important role in the prevention of thermal energy loss

and effective use of locally generated heat [233]. Although the thermal conductivity value of the WPU-PDA film increased relative to WPU films due to the hydrogen bonding, π-π stacking capability and the aromatic content of PDA, it was still an acceptable value for efficient use of the generated heat [234]. Young's modulus and tensile strength of WPU-PDA films decreased slightly compared to WPU films, whereas the elongation at break values of WPU-PDA films were higher than that of WPU films. Although showing an increase in the elastic behavior, films prepared from the hybrid WPU-PDA dispersions mostly retained the mechanical properties of WPU films and were shown to have the mechanical strength required for different applications.

Table 7. Contact angle, thermal conductivity, and mechanical properties of WPU and WPU-PDA films.

	Contact angle (°)	Thermal conductivity (W/m°K)	Young modulus (Mpa)	Tensile Strenght (Mpa)	Elongation at break (%)
WPU	71.2	0.1462	7.3 ± 0.2	15.3 ± 0.5	1357.0 ± 29.7
WPU-PDA	47.8	0.2297	6.4 ± 0.5	9.1 ± 0.2	1400.6 ± 2.9

To examine the light-to-heat conversion capability of WPU-PDA films, samples were irradiated with NIR laser light at 808 nm. As shown in Figure 11a and b, the temperature of the WPU-PDA films increased dramatically and reached almost 155 °C after 4 min of NIR laser irradiation, while any increase in temperature was not observed for WPU films under the same conditions, confirming that the heating was caused by the photothermal activity of the PDA content of the WPU-PDA films. It has been reported that an increase in temperature above 50 °C may induce bacterial death caused by denaturation of bacterial enzymes and disruption of bacterial metabolism [235-236]. Therefore, WPU-PDA films, which achieved high

temperatures in minutes under laser irradiation, were demonstrated to be effective in photothermal therapy for the lysis of bacteria.
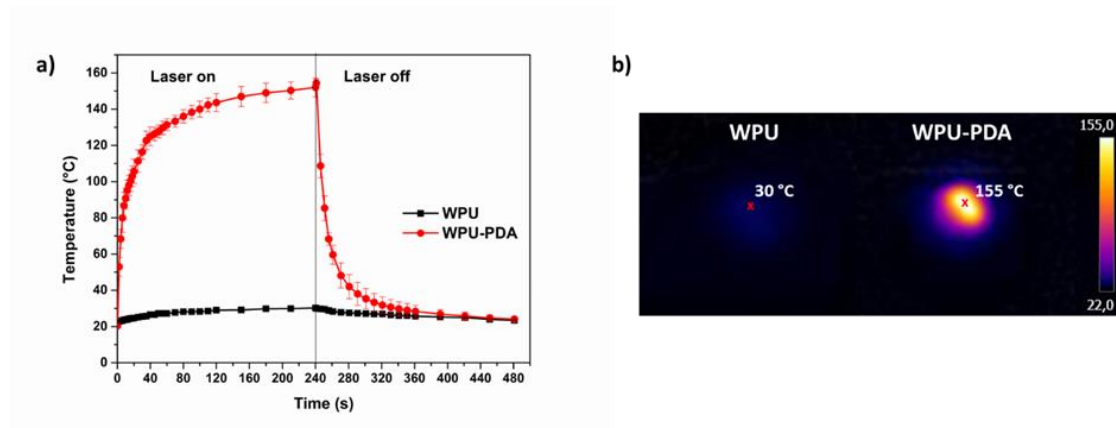
Figure 11. Time-temperature profiles (a), thermal camera images (b) of WPU and WPU-PDA films under NIR laser at 808 nm.

The photothermal reproducibility of WPU-PDA films was tested by periodically exposing the films to NIR light. As demonstrated in Figure 12a, the photothermal effect of WPU-PDA films remained stable after three on-off NIR laser cycles suggesting the reusability of these surfaces for light-activated sterilization. Whether the laser light irradiation and the resulting temperature elevations affected the physical properties of the films was studied by monitoring the physical appearance and molecular weight of the films following each laser on-off cycle (Figure 12b). While the polydispersity index (PDI) and the weight average molecular weight of the films did not change significantly upon multiple consecutive irradiation cycles, the films preserved their mechanical integrity and appearance demonstrating their durability against light-activated temperature elevations.
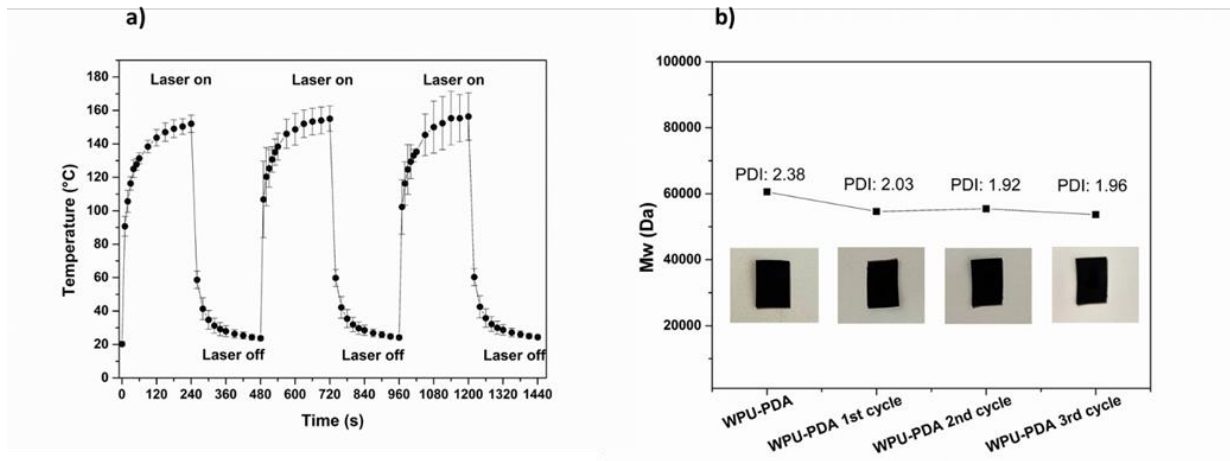
Figure 12. Time temperature profiles (a), GPC analysis and phototgraphs (b) of WPU-PDA films exposed to three consecutive laser on-off cycles.

The NIR-driven antibacterial properties of WPU-PDA films were tested against *S. aureus* by evaluating the ability of films to kill bacteria upon NIR light activation. Bacterial suspensions were placed on WPU-PDA films and the film surfaces were irradiated with NIR laser light continuously. The viability of the bacteria before and after the light activation was determined. After laser treatment for 1 min, the WPU-PDA films presented a significant killing activity on bacteria due to the temperature increase resulting in a 2.8 log reduction in the number of viable bacteria, whereas bacteria alone or bacteria on WPU films were not killed under the same NIR laser light irradiation (Figure 13). Moreover, killing efficiency of WPU-PDA films increased as the duration of laser irradiation increased; 3 min NIR-laser treatment of films resulted in 3.5 log reduction in bacterial viability. Prepared nanoparticle-free one-component polymeric WPU-PDA surface coatings presented comparable/better performance than many nanoparticle-containing photothermal surface coatings reported in the literature [237-239] and were able to kill more than 99.9% of the bacteria on the surface when exposed to laser light for only 5 minutes. With this remarkable light-activated antibacterial

activity, WPU-PDA coatings have a strong potential for utilization on many surfaces requiring disinfection, including surfaces of biomedical devices/implants [240], water membranes [241] or various surfaces in hospital [242-243], food processing [244], and marine environments [245].
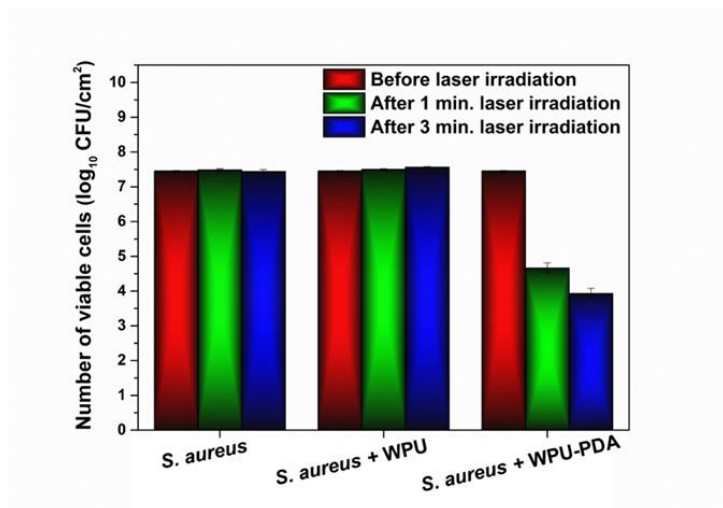
Figure 13. NIR-driven photothermal antibacterial activity of WPU-PDA and WPU films against S. aureus under 808 nm laser irradiation for 1 min and 3 min.

WPU-PDA films, which were proven to show significant photothermal antibacterial properties, were investigated in terms of their reusability following multiple laser treatments (Figure 14). When WPU-PDA films were repeatedly exposed to bacteria and sterilized by laser irradiation, they preserved their photothermal antibacterial activity even in the twentieth cycle. It can be said that WPU-PDA films can retain their strong lethal effect on *S. aureus* upon multiple use and can be utilized on surfaces that need to be re-sterilized due to regeneration of bacterial contamination.
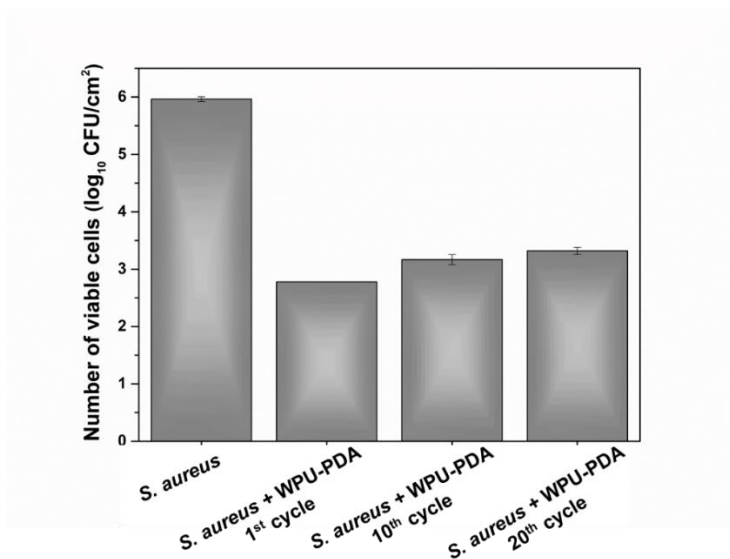
Figure 14. The operational stability of WPU-PDA films under NIR light exposure over multiple bacterial contamination cycles.

The NIR light-activated eradication effect of WPU-PDA films on *S. aureus* biofilms was investigated. Static *S. aureus* biofilms established on WPU and WPU-PDA films were irradiated with NIR laser light and the number of viable bacteria in the biofilms before and after the laser light treatment was determined (Figure 15a). WPU-PDA films presented a significant laser light-activated killing activity on biofilm bacteria resulting in a 3.9 log reduction in viability, whereas the bacteria of the biofilm established on the control WPU film were not affected from the same light-treatment and remained alive. Furthermore, WPU and WPU-PDA surfaces before and after NIR laser exposure were imaged with LSCM by live/dead cell staining. Figure 15b illustrates the representative LSCM images of WPU and WPU-PDA films. While almost all biofilm bacteria on the WPU-PDA film surface were killed and the biofilm was eradicated thanks to the photothermal effect of the WPU-PDA film under NIR laser light irradiation, the biofilm bacteria on control WPU films survived the same light treatment since there was no light-activated temperature increase.
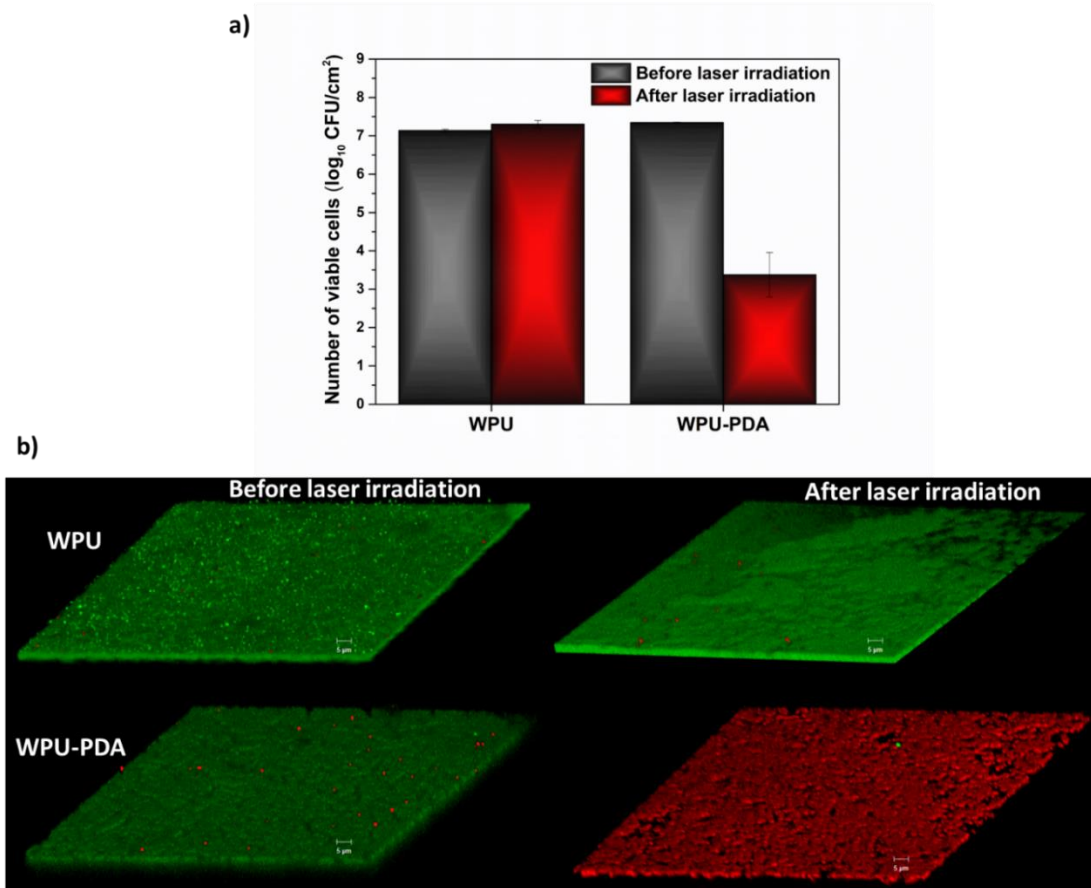
Figure 15. Viability of S. aureus in biofilms established on WPU and WPU-PDA film surfaces before and after 10 min irradiation with 808 nm laser light (a), representative LSCM images of WPU film (top) and WPU-PDA film (bottom) following a 48-h incubation with S. aureus and staining with live-dead cell stain. Images were obtained before and after 10 min laser irradiation at 808 nm, the scale bar is 5 μm (b).

The morphology of the bacteria on samples before and after the NIR irradiation was evaluated by SEM (Figure 16). For WPU-PDA films, the morphology of *S. aureus* was observed as smooth and spherical with a continuous membrane integrity before NIR irradiation. However, following the exposure of the WPU-PDA films to NIR irradiation, *S. aureus* cells were deformed and severely damaged by flattening and wrinkling due to the

hyperthermic effect. These results clearly point out that WPU-PDA films have a strong potential as NIR-driven antibiofilm surfaces that can kill bacteria irreversibly upon NIR light-activation. Among the limited number of coatings that have been reported to remotely eradicate biofilms by light-activation [138, 246-247], WPU-PDA coatings stand out with their polymeric, nanoparticle-free design and easy application.
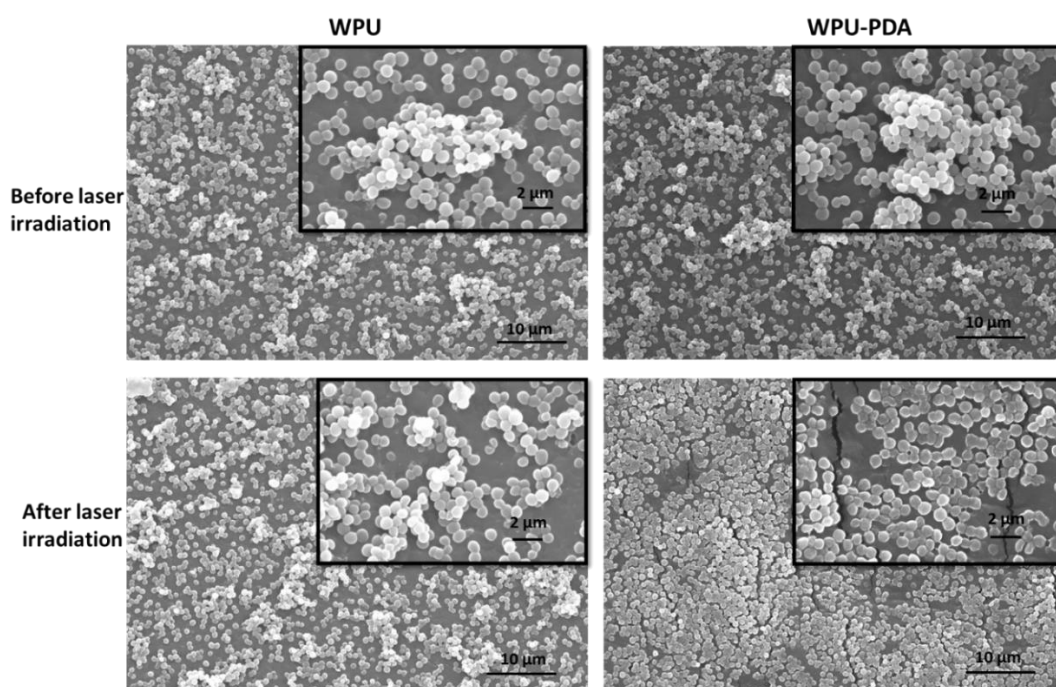
Figure 16. Representative SEM images of S. aureus biofilms on WPU and PUPDA films before (top) and after (bottom) 10 min irradiation with 808 nm laser light.

3. 5.   Conclusions

In summary, WPU-PDA films cast from dispersions of PDA coated WPU solid particles were fabricated as a novel NIR-sensitive antibacterial/antibiofilm surface coating that can be utilized for the physical disinfection of surfaces by photothermal therapy. WPU-PDA films presented a rapid and significant temperature increase upon NIR laser light irradiation.

Furthermore, these films had a significant destructive effect on *S. aureus* resulting in a 3.5 log reduction in the number of viable bacteria under NIR light irradiation with impressive reusability over twenty on-off irradiation cycles. Moreover, bacteria in *S. aureus* biofilms were killed by WPU-PDA hybrid films under laser irradiation due to hyperthermia derived from NIR-stimulated photothermal effect. We believe that the materials presented here have a great potential as disinfectable coatings that can be applied in many areas where non-chemical sterilization is critical, from biomedical surfaces to environmental surfaces.

CHAPTER 4: Antibacterial hybrid coatings from halloysite-immobilized lysostaphin and waterborne polyurethanes

4.1. Abstract

Lysostaphin enzyme is an effective antibacterial agent proven to be promising for the prevention of healthcare-associated infections related to methicillin-resistant *Staphylococcus aureus* (MRSA). Here, safe, and non-toxic antibacterial hybrid coatings consisting of lysostaphin, and waterborne polyurethane (PU) are presented. Lysostaphin was covalently immobilized onto polydopamine functionalized halloysite nanotubes (HNTs) to obtain stable HNT-lysostaphin nanohybrid structures with high effective lysostaphin concentrations, which were then incorporated into PU coatings by a facile spray coating process. Resulting PU/HNT-lysostaphin hybrid coatings presented strong antibacterial activity against *S. aureus* with a >99% killing efficiency. The incorporation of lysostaphin into the polymer matrix via HNTs as a carrier enhanced the stability of the enzyme resulting in non-leaching coatings that presented high operational stability over multiple bacterial incubation cycles and high

61

storage stability without any significant loss of enzymatic activity. Furthermore, PU/HNT-lysostaphin coatings demonstrated significant antibiofilm properties and reduced the formation of *S. aureus* biofilms by 70% relative to neat PU coatings. The lysostaphin based antibacterial hybrid coatings developed in this study, which can be easily applied to surfaces in healthcare facilities and medical devices offer an effective approach for the prevention of *S. aureus* associated nosocomial infections.

4.2. Introduction

Healthcare-associated infections by methicillin-resistant *Staphylococcus aureus* (MRSA) constitute an important public health problem that causes extended hospital stays [248], increased mortality, morbidity [249-251] and substantial economic burden to the healthcare system [252-253]. Contamination of abiotic surfaces in hospital settings with pathogenic bacteria has a main role in the spread of hospital-acquired infections. Bacteria adhering and accumulating on surfaces such as door handles, bed rails, stethoscopes and keyboards are easily transmitted upon being touched and these surfaces act as sources of microbial contamination. Abiotic surfaces in hospital settings are also prone to formation of biofilms resulting from bacterial colonization which have a much higher resistance to antibiotic therapy due to the self-produced extracellular polymer matrix [35, 185, 254]. A promising solution to eliminate the contribution of contaminated surfaces to the proliferation of healthcare-associated infections is the utilization of antibacterial coatings in healthcare settings which can prevent bacteria from adhering to materials surfaces or inactivate already attached bacteria [188, 255].

Utilization of contact-active antibacterial agents in the form of coatings has been one of the most effective methods to combat pathogenic bacteria on surfaces [256]. The desired surface can be adapted with antibacterial agents that kill bacteria by destroying bacterial cell walls upon contact via anchoring of these agents onto the surface. Quaternary ammonium compounds [257-260], N-halamines [261-262], antimicrobial peptides [84, 263-265] and bacteriophages [266-268] have been demonstrated as effective contact-active antibacterial agents that can kill bacteria on surfaces when incorporated into coatings. Moreover, some enzymes which were evolved to protect living organisms from bacterial attack intrinsically exhibit contact-killing activity via disrupting cell integrity or degrading biofilm matrix components [21]. Such enzymes can be incorporated into coating materials directly or as anchored on a support material by non-covalent adsorption [269], ionic interaction [16], encapsulation [270], entrapment [271-272] and covalent attachment [273-276], resulting in antibacterial surfaces. While the immobilization of enzymes on a support material allows a more convenient handling, it also enhances their stability and resistance to environmental conditions. However, the selection of the immobilization method is critical since catalytic activity of the immobilized enzyme may be reduced relative to its free form [277].

Lysostaphin enzyme is a remarkable antibacterial agent effective against methicillin-resistant *S. aureus*. It targets the cell wall and cleaves the pentaglycine cross-bridges found in the staphylococcal peptidoglycans resulting in the rupture of the cell [278-279]. Lysostaphin has a destructive ability on not only planktonic *S. aureus* but also *S. aureus* biofilms on abiotic surfaces [22, 280]. Antibacterial surfaces comprising of lysostaphin encapsulated in a hydrogel [281] or absorbed on a coating material [282-285] have been previously demonstrated. However, since antibacterial coatings obtained by direct noncovalent incorporation of lysostaphin may

63

have significant drawbacks such as leaching of the enzyme from the surface or decrease in antibacterial activity in long-term applications, covalent immobilization of lysostaphin on target surfaces is primarily needed for durable antibacterial coatings. A limited number of studies on the incorporation of lysostaphin into surface coatings via immobilization has been reported including immobilization of lysostaphin onto cellulose fibers [100], paint formulations comprising of carbon nanotube/lysostaphin conjugates [103] and polydopamine-assisted modification of surfaces with lysostaphin [99]. However, these methods may provide limited benefits due to the potential toxicity of the carriers used in immobilization or due to difficulties in the application of such coatings to large surfaces. The utilization of antibacterial coatings especially on hospital setting surfaces and medical devices requires both the use of non-toxic carriers for enzyme immobilization and compatibility of the coating technique for large-surface applications.

Here, halloysite nanotube/lysostaphin (HNT/Lys) nanohybrids were prepared utilizing polydopamine coated HNTs as support materials for the covalent immobilization of lysostaphin. Resulting HNT/Lys nanohybrids alone showed remarkable enzyme stabilities with high effective lysostaphin contents, and they were incorporated onto waterborne polyurethane (PU) based surfaces by spray coating to obtain antibacterial/antibiofilm surfaces. The proposed method enables the development of safe and durable antibacterial coatings that are effective against *S. aureus,* and applicable to large surfaces thanks to their natural, non-toxic, and environmentally friendly components.

4.3. Materials and Methods

4.3.1. Chemicals

HNTs were provided by Eczacıbaşı Esan (Turkey). Dopamine (3-hydroxytyramine hydrochloride) was purchased from Acros Organics Inc. Ultrapure Tris base (Tris(hydroxymethyl)aminomethane) was purchased from MP Biomedicals, LLC. Sodium hydroxide pellets, hydrochloric acid (ACS reagent, 37%), ethylenediamine (EDA) and acetone (99.5%) were purchased from Sigma-Aldrich Inc. Hexamethylene diisocyanate (HDI), and polyester polyol (Desmophen 1652, Mn=2000 g/mol) were purchased from Covestro AG. Sodium 2-[(2-aminoethyl) amino] ethane sulphonate (AEAS, 50 wt% in water) was kindly donated by Evonik Industries. Polyester polyol was dried at 80 °C under vacuum (~2 mbar) for 15 min prior to use. Tryptic soy broth (TSB) and agar powder were purchased from Medimark (Italy). Bradford protein assay kit was purchased from Bio-Rad. Deionized (DI) water was used in all experiments. All chemicals were used without any further purification unless otherwise stated.

4.3.2. Expression and purification of recombinant lysostaphin using auto-induction medium

E. coli TOP10 cells transformed with *p*BAD*Lys* were used as a host to express lysostaphin. For large amounts of soluble and active lysostaphin overexpression, an auto-induction protocol from our previous study was used [286]. The transformants were grown overnight at 37 °C on LB Agar plates supplemented with ampicillin (100 μg/mL). Then, a single colony was used to inoculate a 5 mL LB starter culture containing 100 μg/mL ampicillin at 37 °C and 180 rpm. The starter culture was cultivated at 30 °C in 500 mL of auto-induction engineered For Medium (FM, yeast extract 5 g/L, tryptone 10 g/L, Na$_2$HPO$_4$ 7.10 g/L,

65

KH$_2$PO$_4$ 6.8 g/L, MgSO$_4$ 0.15 g/L, (NH$_4$)$_2$SO$_4$ 3.3 g/L, glucose 0.5 g/L, containing 0.1% (v/v) filter-sterilized arabinose solution), containing 100 µg/mL of ampicillin for 24 hours with vigorous shaking (180 rpm). Stationary-phase cells were harvested from the medium by centrifugation at 4000 rpm for 15 min and 4 °C.

For protein purification, approximately every gram of wet cell paste was resuspended in ice-cold lysis buffer (10 mL, 20 mM Tris-HCl, 500 mM NaCl, pH 7.40, 30 mM imidazole, 1.0 mg/mL lysozyme) and incubated on the ice for 30 min with gentle shaking. The cells were mechanically disrupted by Soniprep 150 sonicator (Sanyo, Tokyo, Japan) on ice with a 10 s burst followed by a 10 s cooling for ten times. Cell debris was separated from the supernatant by centrifugation (11000 rpm, 1 h, 4 °C) in order to obtain the crude extract, and the lysate part was filtered through a 0.45 nm filter.

The clarified extract was purified using the AKTA Primer Plus FPLC system (GE Healthcare, Pittsburgh, PA, USA). The clear lysate was loaded onto a nickel HiTrap™ FF column (5 mL, Amersham Biosciences, Little Chalfont, UK), pre-equilibrated with binding buffer (20 mM Tris–HCl, 200 mM NaCl, 30 mM imidazole, pH 7.40). After loading, the column was washed with 5 column volumes of binding buffer. After no more protein absorption was detected, lysostaphin was eluted with a gradient of imidazole formed by binding buffer and elution buffer (20 mM Tris–HCl, 200 mM NaCl, 500 mM imidazole, pH 7.40). Elution fractions of 1 mL were collected and analyzed by SDS-PAGE.

The protein concentration of each sample was determined by using the Thermo Scientific BCA Protein Assay Kit which contains bovine serum albumin as a standard. The protein samples were concentrated with ultracentrifuge tubes (Vivaspin® Centrifugal Concentrator,

10 kDa). The buffer was exchanged with Tris-HCl buffer (20 mM, pH 7.0) using a PD-10 desalting column (Amersham Biosciences, Little Chalfont, United Kingdom) at 4 °C and the purified protein was stored at 4 °C.

4.3.3. Preparation of PDA functionalized HNTs

Prior to PDA functionalization, HNTs were purified to remove agglomerates and impurities. 5 g of HNTs in 200 mL deionized water were subjected to ultrasound sonication (Qsonica, Q700) for 20 min with 5 s pulse on and 2 s pulse off in an ice bath, then HNTs were treated with 0.01 M NaOH solution at room temperature for 24 h resulting in an increase in hydroxyl groups on the surface, which provides dispersion stability for the purification of HNTs. Base-treated HNTs were centrifuged at 5000 rpm for 5 min and the precipitate which consists of agglomerated HNTs were removed from the medium. The supernatant which consisted of agglomeration-free HNTs was subjected to a second centrifugation at 11000 rpm for 5 min. The precipitate which consisted of the purified HNTs was rinsed with DI water three times to remove unreacted NaOH and dried overnight at 80 °C in a vacuum oven for further use.

Raw HNTs and purified HNTs prepared on specimen stubs were visualized by LEO Supra 35 V P scanning electron microscopy (SEM).

For the functionalization of purified HNTs with PDA, 1 g of purified HNTs in 100 mL of DI water (10 mg/mL) were sonicated for 30 min with 5 s pulse on and 2 s pulse off in an ice bath. Subsequently, 0.2 g dopamine was added into HNT dispersion at 2 mg/mL and the pH was adjusted to 8.5 with Tris base powder. The mixture was stirred at 30 °C for 24 h and PDA functionalized HNTs were separated by centrifugation at 11000 rpm for 5 min.

Separated PDA functionalized HNTs were rinsed with DI water until a clear supernatant was obtained to remove unreacted dopamine and dried overnight at 50 °C in a vacuum oven.

The morphology of PDA functionalized HNTs was investigated in comparison with HNTs using SEM. For this purpose, aqueous dispersions of HNTs and PDA functionalized HNTs (0.01 mg/mL) were ultrasonicated for 5 minutes with 5 seconds pulse on and 3 seconds pulse off in an ice bath, transferred on silicon wafers and air dried. PDA functionalization efficiency was determined by thermogravimetric analysis (TGA) using Shimadzu Corp. DTG-60H (TGA/DTA) instrument by heating samples up to 1000 °C at a rate of 10 °C/min under nitrogen. The percentage of PDA functionalization on HNTs was calculated by the difference between the total weight loss of PDA functionalized HNTs and the total weight loss of uncoated, purified HNTs.

Nicolet IS10 Fourier Transform Infrared (FT-IR) spectroscopy with an ATR system was used for the structural characterization of samples. Samples prepared in dried powder form were directly pressed against the diamond crystal using the attached pressure clamp.

4.3.4. Preparation of HNT-Lys nanohybrids

Lysostaphin was covalently immobilized onto PDA functionalized HNTs by the following procedure: 0.3 g PDA functionalized HNTs were mixed with 3 mL of 0.6 mg/mL lysostaphin solution in Tris buffer (50 mM Tris, 145 mM NaCl) by rotational shaking at RT for 6 h. Resulting HNT-Lys nanohybrids were centrifuged at 5000 rpm for 3 min, rinsed with buffer three times to remove unreacted lysostaphin and dried at RT. HNT-Lys nanohybrids were stored at -20 °C for further use. To evaluate their morphology, aqueous dispersions of HNT-

Lys (0.01 mg/mL) were ultrasonicated for 5 minutes with 5 seconds pulse on and 3 seconds pulse off in an ice bath, transferred on silicon wafers, air dried and visualized with SEM.

The amount of lysostaphin anchored to HNT support was determined by measuring the initial and final concentrations of lysostaphin in the enzyme solution and rinse the solution via Bio-Rad Quick Start™ Bradford Protein Assay [287]. Briefly, the enzyme concentration recovered from the rinse solution was determined by using the calibration curve constituted using bovine serum albumin (BSA) spectroscopically at 595 nm. The concentration of immobilized lysostaphin was calculated by the following equation:

$$The\ concentration\ of\ immobilized\ lysostaphin\ (\frac{mg}{g}) = \frac{(C_0 - C_1)xV}{W}$$

where C_0 and C_1 are enzyme concentrations for the initial solution and recovered buffer, respectively, V is the volume of the enzyme solution used in immobilization, W is the weight of PDA functionalized HNTs used for the immobilization.

4.3.5. Killing efficiency of HNT-Lys nanohybrids

The killing efficiency of the HNT-Lys nanohybrids was determined with a turbidity assay by monitoring the decrease in optical density of a suspension of *S. aureus* ATCC 29213 at 595 nm by the Tecan Infinite M200 plate reader. *S. aureus* ATCC 29213 were grown in 3 mL TSB growth medium overnight at 37 °C on a shaker incubator (200 rpm). Cells were harvested by centrifugation, washed twice in sterile Tris buffer (pH 7.5) and resuspended in Tris buffer at a concentration of 10^7 CFU/mL. Native lysostaphin in Tris buffer and HNT-Lys nanohybrids were placed in a 96-well microplate, where each well contained 7 µg enzyme in 150 µL cell suspension and the plate was covered to prevent evaporation of the

solutions. The turbidity of each well at 595 nm was measured every 3 min for 30 min at 37 °C.

4.3.6.   Synthesis of waterborne polyurethane dispersion

Waterborne PU dispersion was synthesized using the acetone method. First, NCO-terminated polyurethane prepolymer was synthesized by charging a four-necked, 1-L glass round-bottomed-flask equipped with a heating mantle, stirrer, condenser and a thermocouple with 40.00 g of polyester polyol and 6.28 g of HDI, allowing the mixture to polymerize at 80 °C until theoretical NCO content was reached. The NCO content of the reaction mixture was determined by the standard di-butyl amine back titration method (ASTM D2572-97). Upon reaching the theoretical NCO value, the reaction mixture was allowed to cool to 50 °C while dissolving in acetone to obtain a prepolymer solution with 40 wt% solids content. Once the prepolymer was completely dissolved in acetone, the chain extension step was carried out by adding the mixture of 3.02 g AEAS (50 wt% in water) and 0.33 g EDA dropwise into the solution at 50 °C. Then the prepared polyurethane polymer was dispersed in water by slowly adding 110.00 g of distilled water into the flask while cooling the mixture to 40 °C. Finally, acetone was removed from the reaction mixture by vacuum distillation and complete removal of acetone was ensured at 45 °C, 50 mbar. Waterborne polyurethane dispersion product with approximately 30 wt% solids content was obtained by filtering the final dispersion through a 50-micron filter.

4.3.7.   Preparation of PU/HNT-Lys hybrid coatings

Waterborne PU dispersion with a solid polymer content of 30% was coated on a sterile glass substrate (20 mm x 20 mm, Corning Inc) by spin coating at 2000 rpm for 60 s followed by

drying overnight at RT, resulting in substrates coated with PU with a dry thickness of 2 μm. The weight change in the glass substrate after the spin coating with PU and drying was used to determine the amount of coated PU on the surface. Ultrasound sonication was applied to HNT-Lys nanohybrids in DI water mixed at a concentration of 0.02 wt%, 0.05 wt% and 0.1 wt% for 10 min with 5 s pulse on and 2 s pulse off in an ice bath. Sonicated HNT-Lys nanohybrids were sprayed onto PU coatings on glass substrates by using home-built robotic spraying system equipped with an airbrush having a nozzle size of 0.35 mm. The working distance of the spray tip was kept at 50 mm from the substrates and 250 μL dispersions of HNT-Lys were sprayed onto the PU coated glass substrate in 5 s, resulting in hybrid coatings with 4 wt%, 10 wt% and 20 wt% HNT/Lys concentrations. PU/HNT-Lys coated surfaces were dried overnight at RT. PDA functionalized HNT containing PU coatings coded as PU/HNT were prepared by the same method mentioned above and used as control samples lacking lysostaphin for antibacterial tests. As an additional control surface, 1.2 μg/mL of native lysostaphin in Tris buffer were sprayed onto PU coating to prepare PU/Lys coatings at a lysostaphin concentration of 0.08 μg/cm^2, which were used as a second control lacking the HNT support.

The thickness of coated films on glass substrates was analyzed by KLA-Tencor P6 Surface Profilometer. Approximately 1 mm of Z range on the surface was scanned by applying 1 mg force with 50 μm/s velocity.

The surface morphology of coatings was investigated by SEM. Samples were coated with Au-Pd for visualization.

Static contact angle measurements of PU, PU/HNT and PU/HNT-Lys was performed with the sessile-drop method using a Theta Lite Contact Angle Measurement System with an

optical tensiometer. Approximately, 10 µl distilled water was dropped on the surface at room temperature and contact angle values were recorded by the optical tensiometer equipped with a high-resolution digital camera. At least three measurements were taken for each sample and average contact angle values were reported.

4.3.8.   Antibacterial properties of hybrid coatings

The antibacterial activity of PU/HNT-Lys hybrid coatings was determined by quantifying the survival of bacteria in contact with the coating according to ISO 22196 with some modifications [288]. *S. aureus* ATCC 29213 were grown in 3 mL TSB growth medium overnight at 37 °C on a shaker incubator (200 rpm). Cells were harvested by centrifugation, washed twice in sterile Tris buffer (pH=7.5) and resuspended in Tris/TSB (1% v/v) at a concentration of 10^5 CFU/mL. Samples (20 mm x 20 mm) were placed into sterile petri dishes with the coated surface facing up. An aliquot (30 µL) of test inoculums were pipetted onto samples. Then, inoculated samples were covered with parafilm (18 mm x 18 mm) to ensure maximum contact. Petri dishes containing the inoculated samples were incubated at 37 °C under a relative humidity of above 90% for 24 h. To collect microorganisms after incubation, samples with parafilm were immersed into Tris buffer (15 mL) and then sonicated by ultrasound bath for 15 min followed by vortexing for 30 s. Bacterial suspensions were then serially diluted and plated onto TSB agar. Following the incubation of agar plates at 37 °C for 18 h, colonies grown on plates were counted and the number of bacteria was calculated as log CFU/cm^2. Each sample was tested three times.

Antibacterial activity of PU/HNT-Lys hybrid coatings at room temperature was examined by incubating samples with the aqueous bacterial suspension under dynamic contact conditions. Samples prepared by the coating of PU/HNT-Lys on sterile glass substrate (18 mm diameter)

72

were incubated with aqueous suspensions of *S. aureus* ATCC 29213 (10^7 CFU/mL) at room temperature for 24 h on an orbital shaker at 60 rpm; subsequently, aliquots of the bacterial suspensions were serially diluted, plated onto TSB agar and incubated at 37 °C for 18 h. Colonies grown on plates were counted as CFU/mL. Each sample was tested three times.

To visualize bacteria incubated on prepared surfaces, 30 µL of an *S. aureus* suspension (10^5 CFU/mL) was dropped onto 2 cm x 2 cm sample surfaces, covered with parafilm and incubated at 37 °C for 24 h. For the visualization of surface attached bacteria with confocal microscopy, surfaces were stained with BacLight Live/Dead stain (L-7012, Invitrogen, USA) for 10 min in dark at room temperature without any rinsing step. Coated surfaces were then mounted onto coverslips and imaged with a Carl-Zeiss LSM 710 Laser Scanning Confocal Microscope (LSCM) equipped with a Plan-Apochromat 63x/1.40 oil objective. For the visualization of surface attached bacteria with SEM, following the incubation with bacteria, samples were fixed in 2.5% glutaraldehyde in sterile PBS for 2 h at room temperature. After fixation, samples were rinsed twice with sterile PBS followed by dehydration through a series of increasing ethanol concentrations. Dried samples were coated with carbon for SEM visualization.

4.3.9. Stability of PU/HNT-Lys hybrid coatings

To check whether the lysostaphin leaches out from PU/HNT-Lys and PU/Lys coatings, coated glass substrates were immersed in 200 µL Tris buffer (50 mM Tris, 145 mM NaCl) and shaken at 60 rpm at room temperature for 24 h. Following the incubation, both the incubation buffer and coated samples that were dried under nitrogen were tested for their antibacterial activity. Bacterial suspension of 500 µL and 2 mL with a final concentration of 10^7 CFU/mL was mixed with the incubation buffer and dried coatings, respectively, and

incubated at 37 °C with shaking at 200 rpm for 24 h. Following the incubation, aliquots of the bacterial suspensions were serially diluted in Tris buffer, plated, and incubated at 37 °C for 18 h followed by counting of bacterial colonies grown on plates. Each sample was tested three times.

The stability of PU/HNT-Lys coatings against mechanical intervention was evaluated using SEM. Samples (5 mm x 5 mm) were mounted onto the SEM specimen stub and a swab was rubbed onto the entire surface of PU/HNT-Lys coatings to determine the stability of HNT-Lys nanohybrids against physical force. To visualize the morphology of coatings by SEM, the surface of coatings was coated with Au-Pd after swabbing.

To assess the operational stability of the hybrid coatings, multiple cell exposure cycles were performed. PU/HNT-Lys coated glass substrates (18 mm diameter) were placed in bacterial suspensions at a concentration of 10^7 CFU/mL and incubated under dynamic contact conditions at 37 °C and 60 rpm shaking for 6 h. Following the incubation, coated surfaces were washed with Tris buffer, dried under nitrogen gas flow and stored at room temperature for three days until the next cell exposure. After each cycle of cell exposure, the number of bacteria was determined by serial dilution, plating and colony counting. Each sample was tested three times.

4.3.10. Antibiofilm properties of PU/HNT-Lys hybrid coatings

Glass substrates (20 mm x 20 mm) coated with PU/HNT-Lys and PU as a control were placed into petri dishes containing *S. aureus* ATCC 29213 in TSB growth medium (10^8 CFU/mL) and incubated at 37 °C. After 24 h of incubation, bacterial suspensions were replaced with fresh growth medium and incubated for an additional 24 h. Following the incubation,

bacterial suspensions were removed from petri dishes and coated surfaces were rinsed with sterile Tris buffer once to get rid of unattached bacteria. Coated surfaces were stained with BacLight Live/Dead stain (L-7012, Invitrogen, USA) for 10 min in dark at room temperature followed by rinsing with Tris buffer. Coated surfaces were then mounted onto a coverslip and imaged with a Carl-Zeiss LSM 710 Laser Scanning Confocal Microscope equipped with a Plan-Apochromat 63x/1.40 oil objective. Reported images are 3-D renderings of Z-stacks created by using Zen 2010 software. To examine the biofilm formation on surfaces quantitatively, following the biofilm formation, coated surfaces removed from the bacterial suspensions were gently immersed into 15 mL of Tris buffer to eliminate unattached bacteria and agitated in an ultrasound bath for 20 min followed by vortexing for 30 seconds. The viable cell counting method was performed on the Tris buffer solution containing bacteria released from biofilms. Each sample was tested three times.

4.3.11. Statistical analysis

Results were expressed as mean ± standard error of at least three replicates. Statistical significance of differences between means was assessed by one-way ANOVA with Tukey's test at a confidence level of $p < 0.05$ using OriginPro software v.8.5. (OriginLab Corporation, USA).

4.4. Results and Discussions

4.4.1. HNT-Lys nanohybrids

HNTs were functionalized with polydopamine (PDA) via self-oxidation polymerization of the dopamine monomer [220] to create reactive groups on HNTs, through which the lysostaphin enzyme can be covalently coupled, as illustrated Figure 17. The functionalization of HNTs

with PDA has been previously demonstrated for the purpose of coupling HNTs with different molecules [289-290].
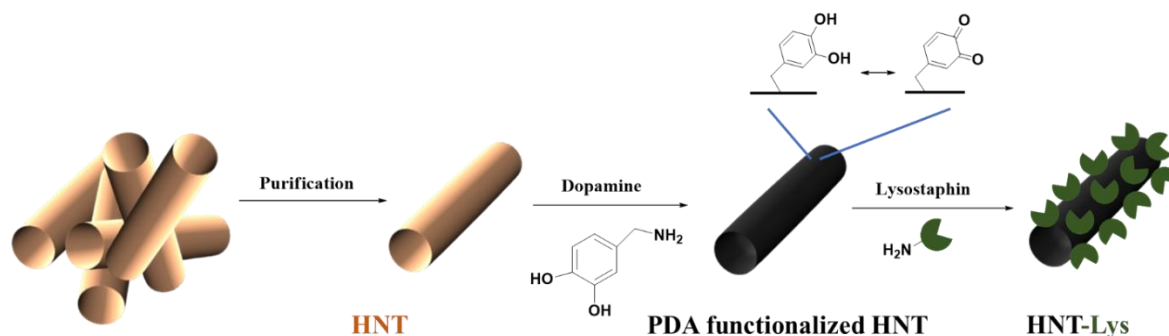
Figure 17. Schematic illustration of the preparation of HNT-Lys nanohybrids.

HNTs were purified by NaOH treatment to improve their hydrophilicity followed by centrifugation of aqueous dispersions to remove agglomerated particles and impurities. The purification protocol resulted in finely dispersed individual nanotubes free of agglomerations (Figure 18). Purified HNTs were mixed with alkaline dopamine solution to induce the self-polymerization of dopamine oxidatively, resulting in PDA functionalized HNTs.
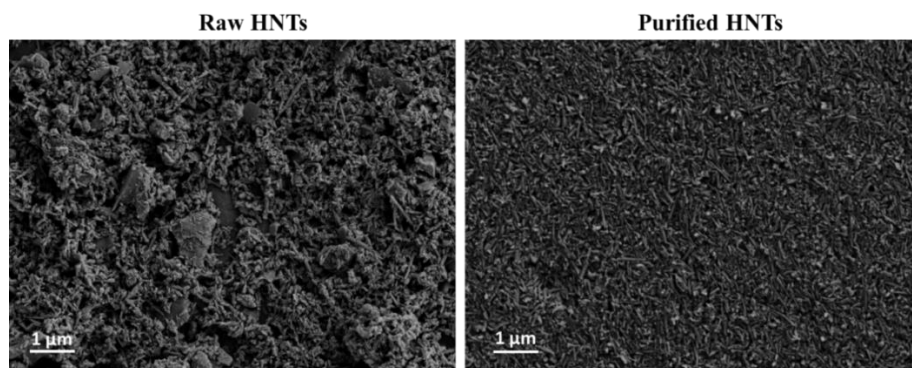
Figure 18. SEM images of raw and purified HNTs.

The presence of the PDA on HNTs was demonstrated by TGA (Figure 19a). PDA functionalized HNTs presented a 7% higher weight loss relative to neat HNTs in the

temperature range of 200 °C to 1000 °C due to the decomposition of PDA. The successful

functionalization of HNTs with PDA was further evidenced with FT-IR by the formation of

new peaks at 1613 cm^{-1}, 1494 cm^{-1} and 1296 cm^{-1}, corresponding to -NH bending, aromatic

C=C bending and C-N stretching of PDA, respectively [291-292] (Figure 19b). The

immobilization of lysostaphin was accomplished via the reaction of PDA functionalized

HNTs and lysostaphin in the dispersion, followed by washing of HNT-Lys nanohybrids by

centrifugation to remove any free unreacted enzyme. The quinone groups of the PDA enabled

the immobilization of lysostaphin via Michael addition and/or Schiff base reactions with

nucleophilic amino-functional groups commonly found in enzymes [293]. The immobilization

of the lysostaphin on the PDA functionalized HNTs was confirmed by FT-IR. Following the

treatment of PDA functionalized HNTs with lysostaphin, an additional peak arising from the

protein-specific amide I band associated with stretching vibration of C=O [294] at 1635 cm^{-1}

provided a strong evidence for the successful immobilization of lysostaphin on HNTs (Figure

19c). Furthermore, the amount of lysostaphin immobilized onto PDA functionalized HNTs

was quantified with a colorimetric protein assay. Analysis of the protein content of HNT-Lys

nanohybrids demonstrated that each gram of HNTs contained 6 mg of lysostaphin.
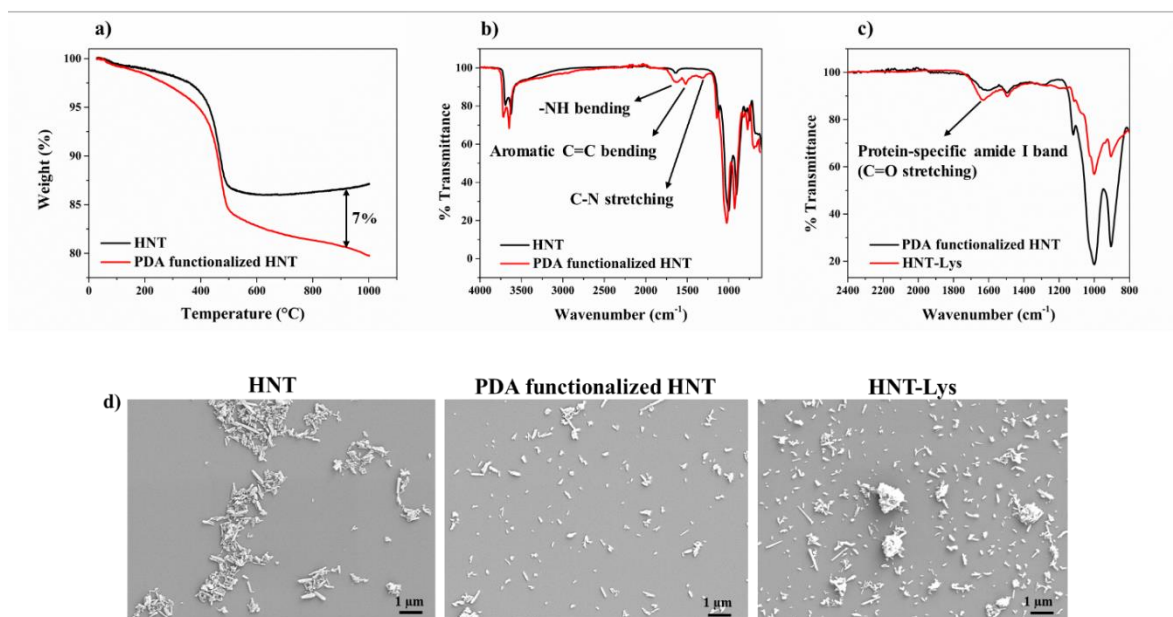
Figure 19. TGA analysis of raw HNT and PDA functionalized HNT (a), FT-IR analysis of raw HNT and PDA functionalized HNT (b), FT-IR analysis of PDA functionalized HNT and HNT-Lys nanohybrids (c) SEM images of HNT, PDA functionalized HNT and HNT-Lys (d).

SEM visualization of nanohybrids have revealed that the PDA functionalized HNTs were finely dispersed without any agglomerated particles (Figure 19d). Potentially the hydrophilic character of the PDA improved the dispersibility of HNTs in water. Following the immobilization of the lysostaphin on PDA functionalized HNTs, HNT-Lys nanohybrids were still finely dispersed, but agglomerations were also visible due to hydrophobic lysostaphin coating on the nanotubes which might have reduced the aqueous dispersibility.

The enzymatic and antibacterial activity of lysostaphin in HNT-Lys nanohybrids was investigated. The enzymatic activity of native and immobilized lysostaphin was tested against *S. aureus* by a turbidity assay which monitors cell lysis based on the reduction of the optical density in the bacterial suspension. HNT-Lys nanohybrids presented significant enzymatic activity on *S. aureus* as shown by the time-based decrease in optical density

78

demonstrating that the immobilization of lysostaphin on the HNT surface did not prevent the cell lysis (Figure 20). The decrease in the optical density of native lysostaphin was more pronounced, indicating that the enzymatic activity of HNT-Lys against *S. aureus* was reduced upon immobilization. The degree of freedom of the enzyme, which provides easy access to the target cell, was higher in the case of the native enzyme that is free in solution. When the enzyme is anchored onto a support surface, loss of activity is expectable due to the limitation of the dynamic motion, steric hindrance that restrains contact with the target cell, and blockage of enzymes active center [295-296]. However, while HNT-Lys samples have partially lost some of their enzymatic activity, they still had a significant destructive effect on *S. aureus*.
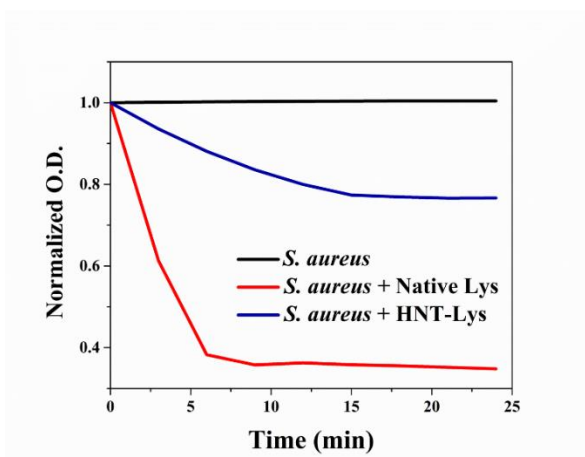
Figure 20. Enzymatic activity of native lysostaphin (red) and immobilized lysostaphin (blue) determined by the decrease in turbidity at 595 nm. The amount of enzyme was 7 μg for each sample.

4.4.2.   Antibacterial properties of PU/HNT-Lys hybrid coatings

HNT-Lys nanohybrids, which were active against *S. aureus*, were utilized in the design of durable antibacterial coatings. Waterborne PUs, which are widely utilized in industrial

applications due to their chemical and physical properties, as well as environmentally friendly nature, were synthesized and used as the polymeric base coating material. The design and fabrication of PU/HNT-Lys based antibacterial surface coatings was demonstrated in Figure 21. The glass substrate was coated with waterborne PU with a coating thickness of about 2 microns by spin coating. Subsequently, HNT-Lys nanohybrids, which were subjected to sonication in an aqueous dispersion were sprayed onto the PU coating. Non-covalent interactions such as H-bonding and electrostatic interactions allowed a secure assembly between PU and HNT-Lys nanohybrids resulting in PU/HNT-Lys hybrid coatings.
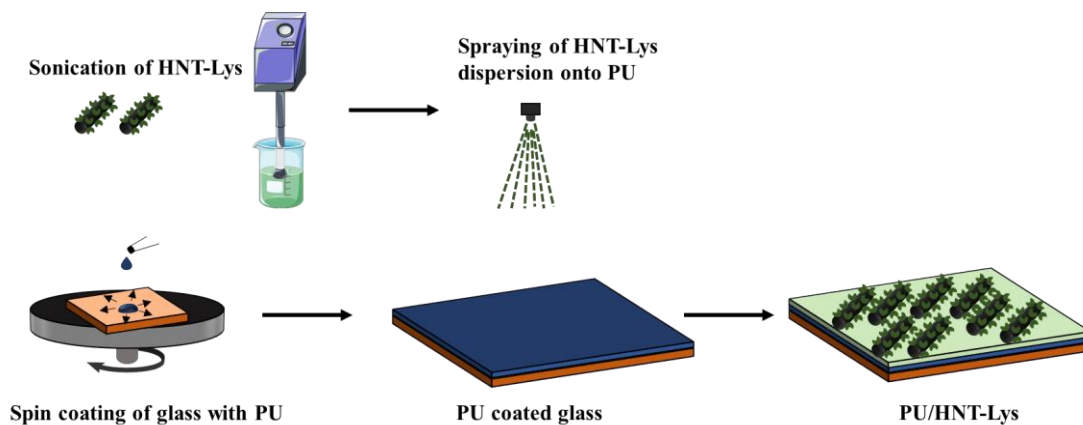
Figure 21. Schematic illustration of the design and fabrication of PU/HNT-Lys hybrid coatings.

SEM image of the coated surface exhibited that HNT-Lys nanohybrids were successfully embedded onto the PU surface with a homogeneous distribution (Figure 22a). The presence of the HNT-Lys nanohybrids on PU was further demonstrated by FT-IR spectroscopy (Figure 22b). The formation of the new peaks at 3200 cm^{-1} and 3100 cm^{-1}, which are protein-specific peaks Amide A and Amide B peaks, respectively, indicates that lysostaphin is present on the surface and HNT-Lys nanohybrids have been successfully incorporated onto the PU surface.

Hydrophilicities of PU, PU/HNT and PU/HNT-Lys surfaces were analyzed by water contact angle measurements and the results were demonstrated in Figure 22c. Due to the increase in hydrophilicity caused by catechol groups in polydopamine, the contact angle decreased when the PDA functionalized HNTs were sprayed onto the PU surface. However, the contact angle of PU/HNT-Lys surface was found to be higher than that of the PU and PU/HNT surfaces, indicating a decrease in hydrophilicity of the surface.

The antimicrobial activity of PU/HNT-Lys hybrid coatings was evaluated on *S. aureus* by quantifying the survival of bacteria held in contact with the coated surfaces for 24 h according to ISO 22196 standard protocol. PU/HNT-Lys coated surfaces containing 4 wt.% HNT/Lys nanohybrids with a lysostaphin concentration of 0.08 μg/cm^2 were incubated with *S. aureus* (10^5 CFU/mL) at 37 °C for 24 h followed by serial dilution and colony counting. PU and PU coated glass substrates sprayed with PDA functionalized HNTs (PU/HNT) were used as control samples lacking lysostaphin. As shown in Figure 23a, while PU and PU/HNT films did not display any antibacterial activity, the number of viable cells in contact with PU/HNT-Lys decreased by about two logs, demonstrating a significant reduction in the number of bacteria. The enzymatic activity of HNT immobilized lysostaphin incorporated into PU allowed the lysis of bacteria in contact with the coating resulting in strong antibacterial activity on *S. aureus*.
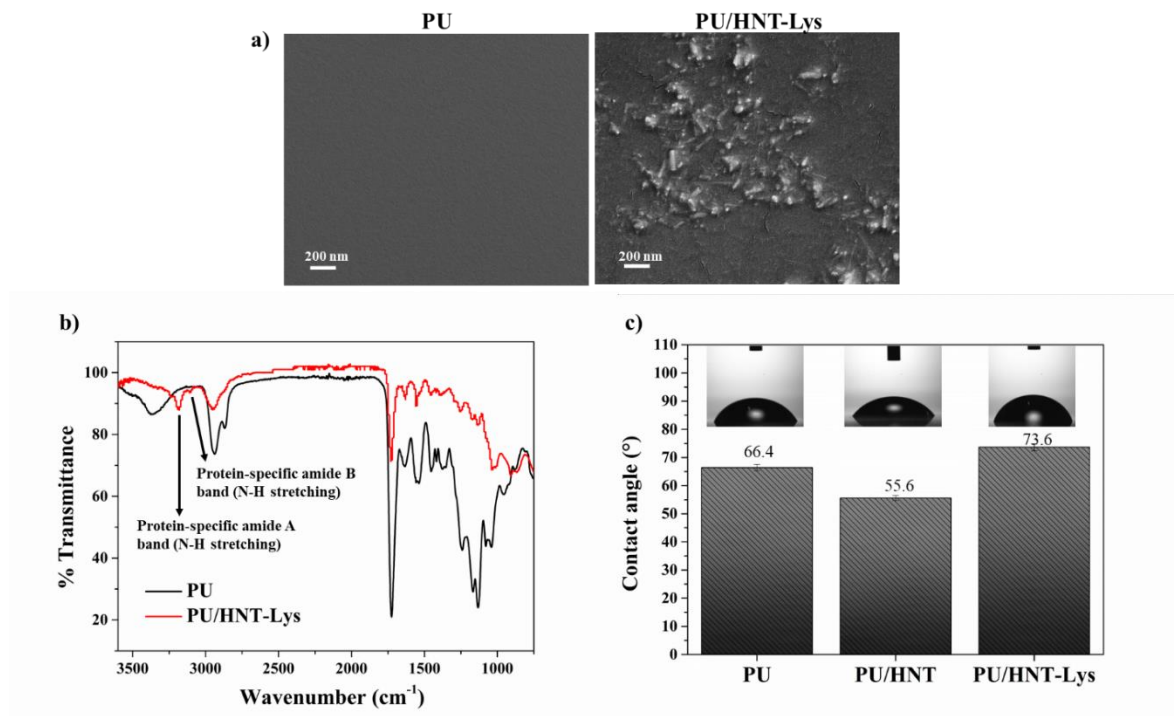
Figure 22. SEM images (a), FT-IR analysis (b) and water contact angle measurements (c) of PU, PU/HNT and PU/HNT-Lys hybrid coatings (c).

The antimicrobial activity of PU/HNT-Lys hybrid coatings was evaluated on *S. aureus* by quantifying the survival of bacteria held in contact with the coated surfaces for 24 h according to ISO 22196 standard protocol. PU/HNT-Lys coated surfaces containing 4 wt.% HNT/Lys nanohybrids with a lysostaphin concentration of 0.08 μg/cm^2 were incubated with *S. aureus* (10^5 CFU/mL) at 37 °C for 24 h followed by serial dilution and colony counting. PU and PU coated glass substrates sprayed with PDA functionalized HNTs (PU/HNT) were used as control samples lacking lysostaphin. As shown in Figure 23a, while PU and PU/HNT films did not display any antibacterial activity, the number of viable cells in contact with PU/HNT-Lys decreased by about two logs, demonstrating a significant reduction in the number of bacteria. The enzymatic activity of HNT immobilized lysostaphin incorporated into PU

82

allowed the lysis of bacteria in contact with the coating resulting in strong antibacterial activity on *S. aureus*.

Bacteria, that were incubated on the surfaces for 24 hours were visualized by LSCM with live/dead staining (Figure 23b). While the majority of the bacteria incubated on the PU/HNT-Lys surface was dead, the bacteria incubated on the PU and PU/HNT surfaces were alive, which has clearly demonstrated the killing activity of the PU/HNT-Lys hybrid coating on *S. aureus*. The damage on the bacteria caused by the contact-killing effect of HNT-Lys nanohybrids was further visualized with SEM. While bacteria on PU and PU/HNT surfaces preserved their spherical shape, the morphology of bacteria which were in contact with PU/HNT-Lys hybrid coatings was significantly changed (Figure 23c). This clearly indicated the antibacterial effectiveness of the PU/HNT-Lys hybrid coating due to the lysostaphin as a contact-killing agent.
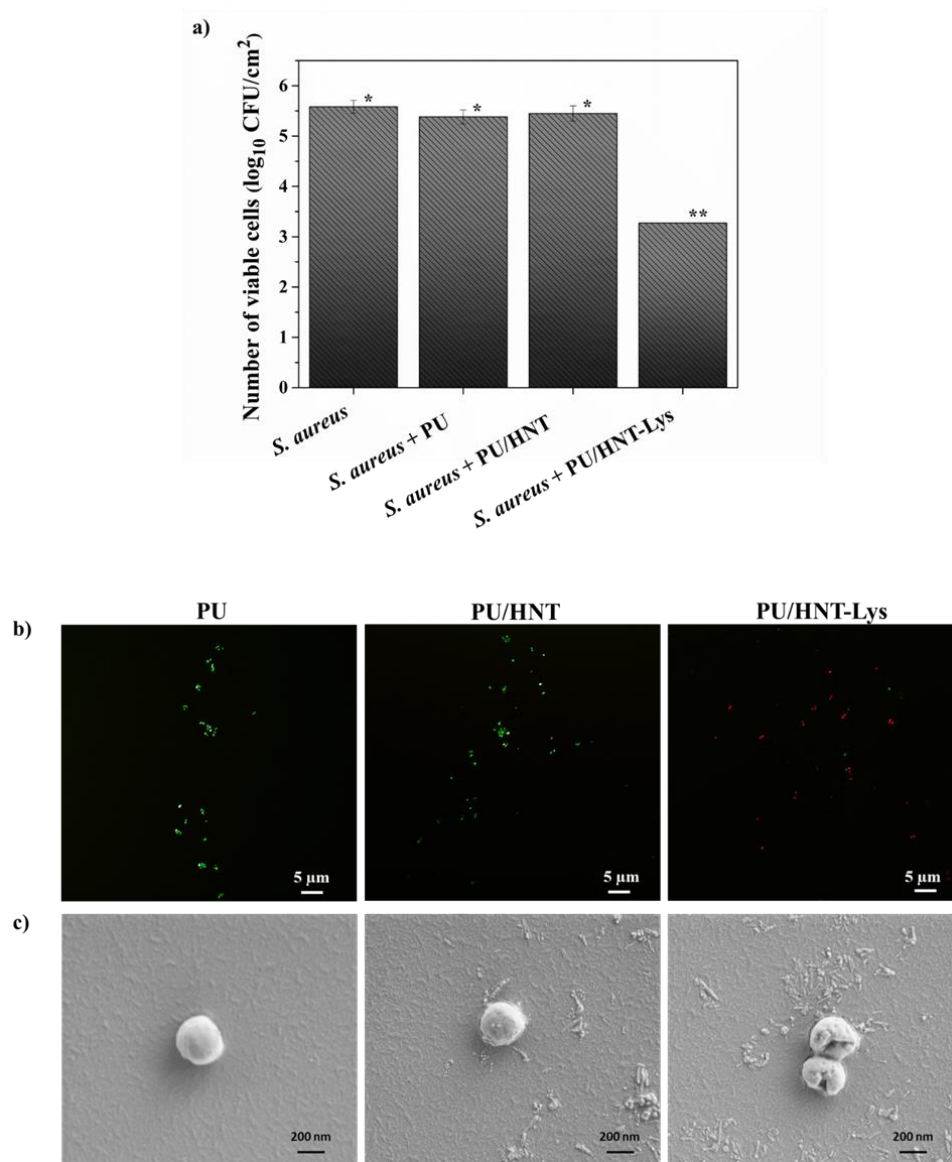
Figure 23. Viability of S. aureus incubated with glass substrates coated with PU, PU/HNT and PU/HNT-Lys at 37 °C for 24 h according to ISO 22196. Values sharing a common symbol are not significantly different (n = 3) (a), LSCM images of bacteria on PU, PU/HNT and PU/HNT-Lys surfaces (b) and SEM images of bacteria on PU, PU/HNT and PU/HNT-Lys surfaces (c).

PU/HNT-Lys hybrid coatings, which have been proven to show antibacterial activity at 37 °C on *S. aureus,* were also tested for their antibacterial activity at room temperature.

PU/HNT-Lys coated glass surfaces of equal sizes were incubated with aqueous suspensions of *S. aureus* (10^7 CFU/mL) under dynamic contact conditions for 24 hours at room temperature, followed by serial dilution and viable-cell counting. The PU/HNT-Lys hybrid coatings caused a decrease in the number of live cells by approximately 99% (Figure 24), demonstrating that PU/HNT-Lys coatings presented significant killing efficiency at room temperature and can be easily utilized in applications where antibacterial activity at ambient temperature is required.
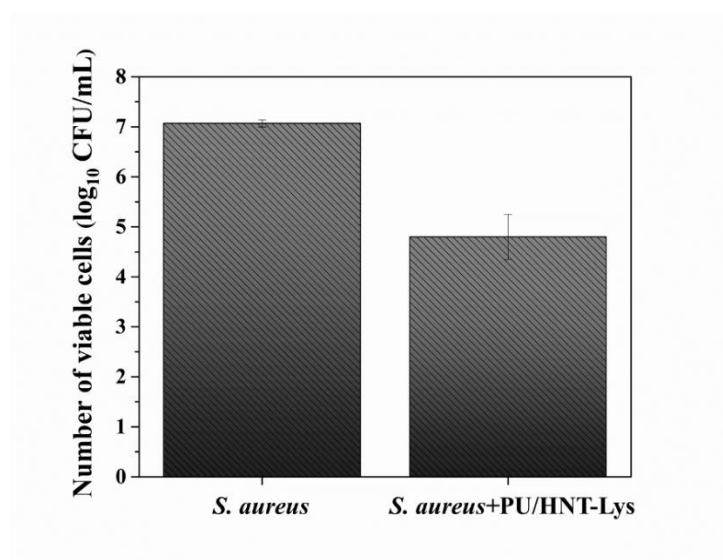
Figure 24. Viability of S. aureus (10^7 CFU/mL) incubated in the presence of PU/HNT-Lys for 24 h at room temperature. Nanocomposite coatings contained 4 wt% HNT-Lys nanohybrids and the lysostaphin concentration was 0.08 µg/cm².

To determine the effect of the enzyme content on the killing efficiency of the hybrid coatings, HNT-Lys nanohybrids were sprayed onto the PU surface to result in coatings with a lysostaphin concentration of 0.04 µg/cm², 0.08 µg/cm², 0.19 µg/cm², 0.38 µg/cm² and viability assays were performed based on ISO 22196 for the resulting coatings. Contrary to

expectations, the antibacterial activity of the hybrid coatings decreased as the enzyme content on the PU coating surface increased (Figure 25a). This result may be explained by the fact that HNT-Lys nanohybrids tend to form agglomerates as the amount of nanohybrids sprayed onto the surfaces increases. Thus, the direct contact of the enzyme with the target cell may be restricted due to steric hindrance, thereby reducing the enzyme activity [297]. The formation of agglomerates was clearly observed with increasing nanohybrid concentrations as shown in Figure 25b. Although the antibacterial activity increased by decreased lysostaphin concentration, 0.08 $\mu g/cm^2$ was determined to be an optimal concentration, below which antibacterial activity of nanocomposite coatings starts to decrease again, potentially because the lysostaphin concentration present in the coating was below the effective lysostaphin concentration and was not sufficient to kill bacteria. Since the highest antibacterial activity was observed in coatings containing 4 wt% HNT-Lys at a lysostaphin concentration of 0.08 $\mu g/cm^2$, all further experiments were performed at this concentration.
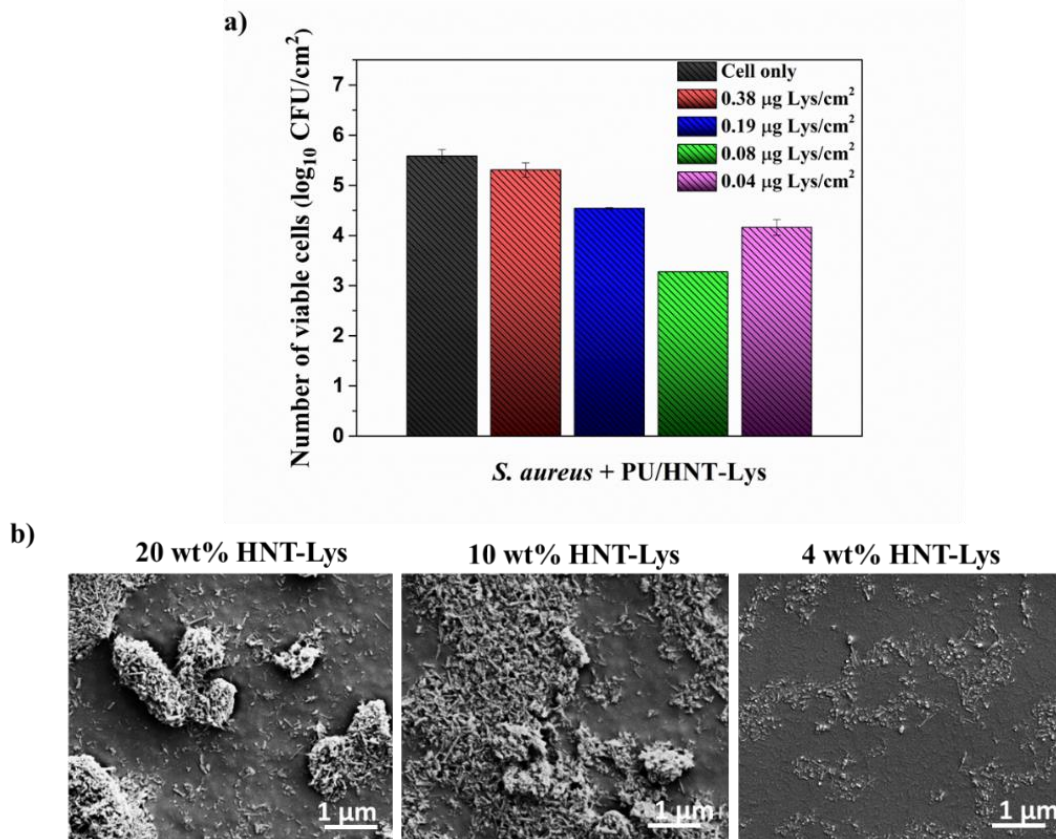
Figure 25. a) The effect of concentration of HNT-Lys on the viability of S. aureus incubated at 37 °C for 24 h. The experiments were carried out according to the ISO 22196 standard protocol. The HNT-Lys nanohybrid concentrations were 20 wt%, 10 wt%, and 4 wt%, and the lysostaphin concentration in the nanocomposites tested were 0.38 µg/cm², 0.19 µg/cm², 0.08 µg/cm² and 0.04 µg/cm², respectively, b) SEM images of PU/HNT-Lys nanocomposite coatings prepared with different concentrations of HNT-Lys.

4.4.3. Stability of PU/HNT-Lys hybrid coatings

Considering that PU/HNT-Lys coatings are designed via non-covalent interactions between HNT-Lys nanohybrids and the PU surface, it was critical to demonstrate that nanohybrids remain on the surface during/after the application and maintain their enzymatic activity under different conditions, mimicking the use of these coatings in real world applications. To

evaluate the adhesion and mechanical stability of HNT-Lys nanohybrids on the coating surface, PU/HNT-Lys coatings were subjected to incubation in an aqueous buffer for 24 hours and to rubbing of the surface with a swab, respectively. Following these applications, the tendency of HNT-Lys nanohybrids to leach out of the surface was examined qualitatively by SEM. As seen in Figure 26a, HNT-Lys nanohybrids did not leach out and remained on the surface in both cases, demonstrating the durability of the coatings.

Whether the lysostaphin was leaching from the PU/HNT-Lys hybrid coatings during aqueous incubation was also quantitatively determined. In order to demonstrate the effect of the PDA functionalized HNT-assisted immobilization of the lysostaphin on the stability of resulting coatings, PU/HNT-Lys coatings were evaluated in comparison to PU/Lys coatings, in which the same amount of lysostaphin was directly sprayed onto the PU from an aqueous solution without HNTs. Following a 24 h incubation of both coated surfaces in a buffer, both the incubation buffer, which would contain any lysostaphin leached out, and the coated surfaces were subjected to a viability assay under dynamic conditions. While the antibacterial activity of PU/HNT-Lys coatings were still significantly active against *S. aureus*, PU/Lys coatings entirely lost their antibacterial activity following the incubation (Figure 26b). The killing efficiencies of the incubation buffers that could potentially contain leached out lysostaphin further confirmed the stability of PU/HNT-Lys coatings. While the buffer obtained from the incubation of PU/HNT-Lys coated surfaces showed a very weak killing efficiency on *S. aureus*, the buffer, in which PU/Lys coated surfaces was incubated resulted in 95% killing activity, demonstrating that most of the enzyme from the PU/Lys surface has migrated into the incubation buffer (Figure 26c). The native lysostaphin which adhered to the PU only by physical adsorption without being immobilized on HNTs presented weak interactions with

88

the coating material [99, 298] and was easily removed from the surface in the case of PU/Lys coatings. On the other hand, lysostaphin was not found to leach out of the surface when it was immobilized with the aid of HNTs due to the ability of these nanohybrids to form strong non-covalent interactions with the PU. These results suggest that the covalent immobilization of the enzyme on the HNT support significantly enhanced its adhesion stability on the surface, resulting in durable, non-leaching antibacterial coatings effective against *S. aureus*.
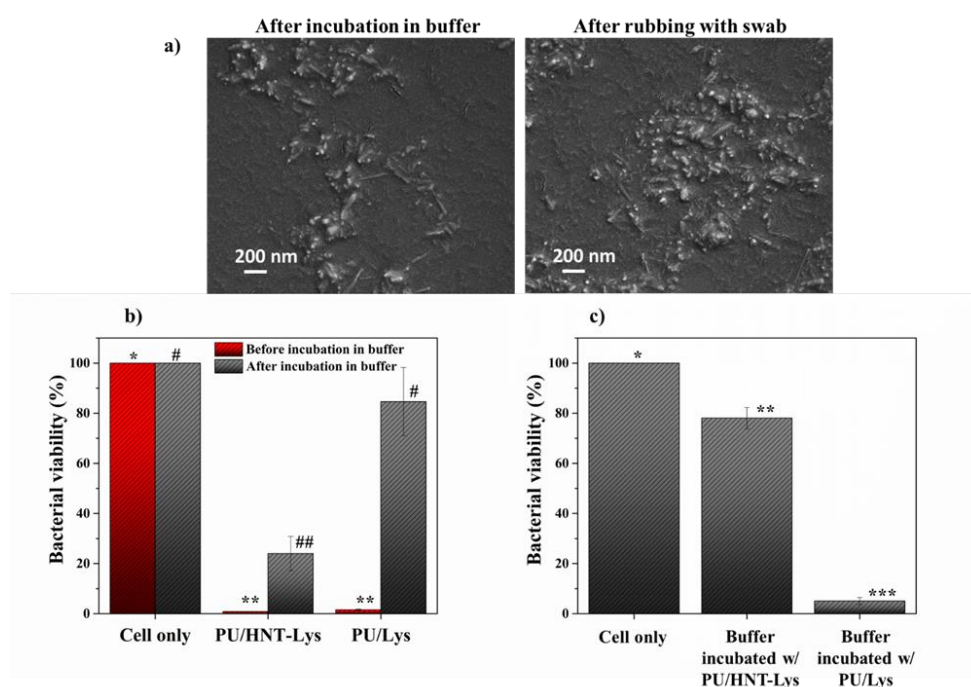
Figure 26. a) SEM images of PU/HNT-Lys coated surfaces following incubation with aqueous buffer (left) and rubbing with a swab (right), b) killing efficiency of PU/HNT-Lys and PU/Lys coated surfaces following the incubation with aqueous buffer, c) killing efficiency of the buffer incubated with PU/HNT-Lys and PU/Lys coated surfaces. Values sharing a common symbol are not significantly different (n = 3).

The prolonged use of the enzyme-based antibacterial coatings is challenging as it involves continuous exposure of the immobilized enzyme to bacteria; therefore, it is a fundamental

requirement for the coating material to have operational stability. To assess the reusability of PU/HNT-Lys hybrid coatings, multiple incubation cycles of the same set of coated surfaces were performed with *S. aureus*. In each cycle, coatings were incubated with a cell suspension (10^7 CFU/mL) for six hours followed by cell counting to determine the antimicrobial activity of the coatings. Coated surfaces were rinsed with buffer, dried and kept at room temperature for three days between each cycle. As shown in Figure 27a, at the end of three operation cycles, PU/HNT-Lys surfaces presented only a slight decrease in enzymatic activity and were still active against *S. aureus* demonstrating 1.5 log killing efficiency. These results demonstrated the reusability of the PU/HNT-Lys coatings, which retain their powerful destructive effect on *S. aureus* upon multiple use.
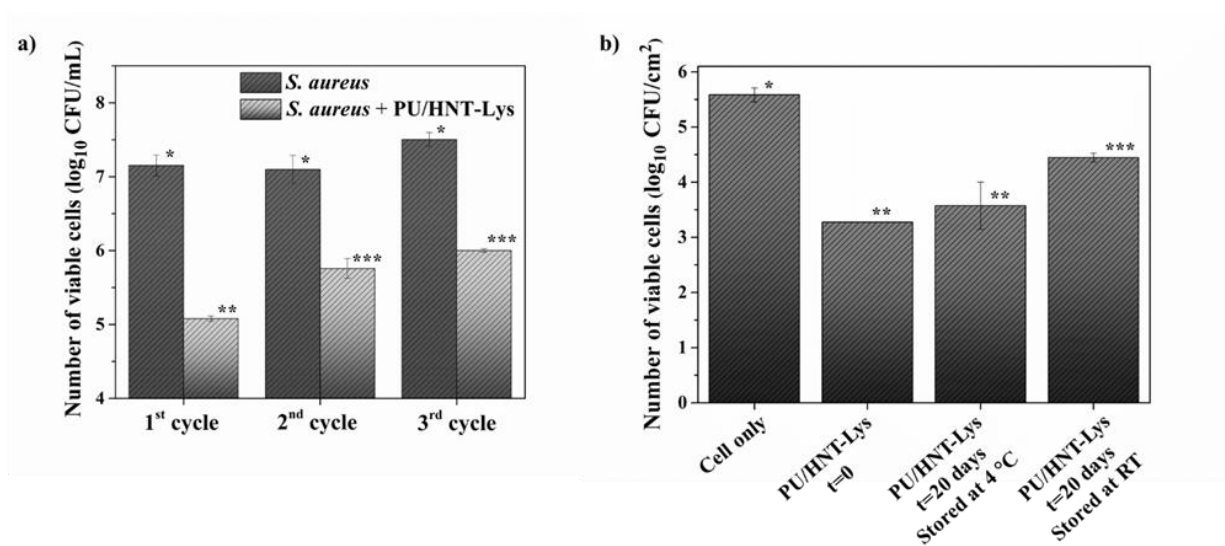
Figure 27. a) Operational stability of PU/HNT-Lys hybrid coatings over three cycles, b) Storage stability of PU/HNT-Lys hybrid coatings stored at 4 °C and RT for 20 days. Values sharing a common symbol are not significantly different (n = 3).

Finally, the storage stability of PU/HNT-Lys hybrid coatings was studied over 20 days (Figure 27b). PU/HNT-Lys coatings that were stored at 4 °C and at RT in dry form for 20

days were subjected to a viability assay, and their antibacterial activity was evaluated. Coatings stored for 20 days at 4 °C reduced the number of viable bacteria by the same ratio as freshly prepared coatings. While coatings stored for 20 days at RT presented a minimal decrease in antibacterial activity, they were still active in killing *S. aureus* on the surface demonstrating the stability of these coatings over time.

4.4.4. Antibiofilm properties of PU/HNT-Lys hybrid coatings

Biofilms of *S. aureus* formed by aggregates of surface attached bacteria embedded in a self-produced extracellular matrix are resistant to many antibacterial agents and are important causes of surface-associated infections [184]. Lysostaphin has a strong eradicative effect on not only planktonic *S. aureus* but also biofilms originating from *S. aureus* on abiotic surfaces [22]. The effectiveness of PU/HNT-Lys coatings on the inhibition of biofilm formation was investigated. Glass substrates coated with PU/HNT-Lys and control PU were incubated with *S. aureus* for 48 h to allow static biofilm formation, rinsed to remove unadhered cells, stained with live-dead cell stain and visualized with laser scanning confocal microscopy (LSCM). Figure 28a demonstrates the representative LSCM images of stained surfaces. The dark green background experienced in LSCM images for neat PU and PU/HNT-Lys samples resulted from the non-specific binding between PU and the stain and should not be confused with cell viability. While the neat PU surface was highly colonized with light green live cells, PU/HNT-Lys coated surface significantly impaired the attachment of cells and caused a significant reduction in the number of colonized bacteria due to its antibiofilm activity. Furthermore, the biofilm formation on these surfaces was quantitatively examined by dispersing the surface attached bacteria followed by colony-counting. PU/HNT-Lys coatings showed 70% reduction in biofilm formation compared to neat PU coatings (Figure 28b).

These results clearly indicate that PU/HNT-Lys hybrid coatings have a significant effect on the prevention of biofilm formation and have strong potential as antibiofilm coatings effective against *S. aureus*.
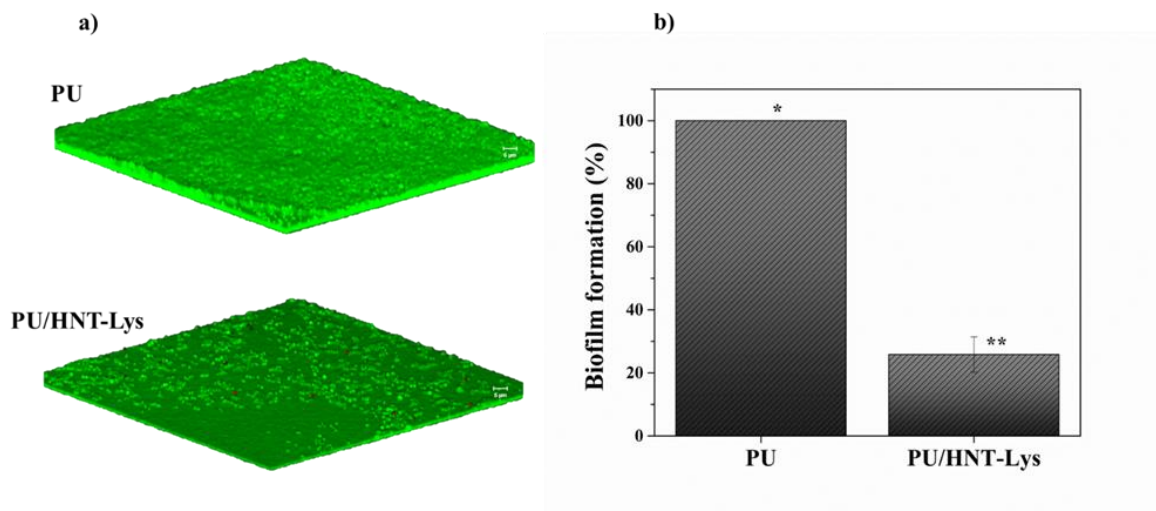
Figure 28. Representative LSCM images of surfaces coated with neat PU film (top) and PU/HNT-Lys (bottom) following a 48 h incubation with S. aureus and staining with live-dead cell stain (a) biofilm formation on PU and PU/HNT-Lys coated surfaces (b). Scale bar is 5 μm. Values sharing a common symbol are not significantly different (n = 3).

4.5. Conclusion

Novel lysostaphin containing waterborne polyurethane hybrid coatings with antibacterial and antibiofilm properties were fabricated by the covalent immobilization of lysostaphin on PDA functionalized HNTs and incorporation of resulting nanohybrids into polyurethane coatings. These coatings presented a strong antibacterial effect on both planktonic and biofilm form of methicillin-resistant *S. aureus*, the primary source of healthcare-associated infections, by

direct-contact killing mechanism without the release of antibacterial agents. Moreover, lysostaphin containing hybrid coatings prepared in this study were demonstrated to have storage and operational stability, which can be safely used as durable and effective coating materials in areas related to human health. These novel hybrid coatings, consisting of natural and safe ingredients, have a great potential to combat *S. aureus* related infections as they can easily be applied to surfaces in healthcare environments and medical devices.

CHAPTER 5: Lysostaphin-functionalized waterborne polyurethane-polydopamine coatings effective against *S. aureus* Biofilms

5.1. Abstract

Hybrid waterborne polyurethane-polydopamine (WPU-PDA) matrix, showing the adhesive properties of PDA in its entirety, was utilized for the immobilization of lysostaphin (Lys), an important anti-staphylococcal agent, to obtain highly effective antibacterial and antibiofilm surface coatings. WPU-PDA matrix prepared by the encapsulation of WPU particles with PDA in aqueous dispersion was applied as coatings on substrates and the facile incubation of the WPU-PDA coated surfaces with Lys in aqueous solution resulted in WPU-PDA/Lys coatings that contain immobilized Lys on the surface. WPU-PDA/Lys coatings showed strong anti-*S. aureus* activity with a 4-log reduction in the number of cells. Furthermore, WPU-PDA/Lys coatings were demonstrated to be durable without any enzyme leakage and their antibacterial activity was preserved for at least 30 days and over multiple exposures to bacteria. WPU-PDA/Lys coatings presented significant antibiofilm activity against *S. aureus*

with a 3.5 log reduction in the number of surface-attached bacteria. WPU-PDA/Lys coatings that are easy-to-apply to almost any surface, non-toxic, and environmentally friendly, provide promising antibacterial and antibiofilm surfaces, that are effective on *S. aureus*.

5.2. Introduction

Biofilms, defined as organized surface-attached bacterial aggregates, cause significant problems in different application areas in marine [299], food [300] and healthcare industries [301-303]. Following the adhesion of planktonic cells to biotic or abiotic surfaces, the bacteria population increases via formation of colonies surrounded by a polymeric extracellular matrix [304]. The three-dimensional extracellular polymeric matrix, which acts as a physical and chemical barrier, protects the biofilms from attack by antibiofilm therapies and extreme environmental conditions, making biofilms very difficult to eradicate [35]. Current antimicrobial treatments using antibiotics are often unsuitable for infections caused by biofilms due to their complex physical and biological properties.

Surface coatings, that can prevent bacteria from adhering to the surface or target the extracellular polymeric substances (EPS) of existing biofilms, are promising approaches to prevent biofilm-induced problems. Reduction of the interactions between the surface and bacteria via a hydrophobic surface [305], a negatively charged surface [306] or integration of polyethylene glycol (PEG) to the surface may provide an anti-adhesive layer [307-308] that inhibits bacterial adhesion; thus biofilm formation may be prevented at an initial step. However, the effectiveness of anti-adhesive surfaces is limited, as even a small number of bacteria adhered to the surface can trigger biofilm formation. Active coatings containing antimicrobial agents are more promising because they destroy the biofilm integrity by

degrading the structural components of the EPS. Coatings based on polycationic biocides [309-311] for killing bacteria via electrostatic interactions and coatings based on antimicrobial peptides [85, 312-313] for blocking the bacterial function via penetration into the cell membrane are some examples of antibiofilm coatings. Furthermore, another strategy that has proven effective in combating biofilms has been the integration of enzymes active against biofilm forming bacteria into surface coatings. The control of biofilms with enzymes is an important approach, as enzymes are environmentally friendly due to their non-toxic nature and their biodegradability. Quorum-sensing-degrading enzymes [314] and Dispersin B [315] that were non-covalently immobilized onto surfaces have been demonstrated as effective contact-active antibacterial/antibiofilm agents. However, in coatings obtained via non-covalent incorporation of enzymes onto surfaces, the enzyme may leak from the surface, or the enzymatic activity may decrease over time. Therefore, covalent immobilization of enzymes onto target surfaces has an important advantage for obtaining durable active coatings. Covalent immobilization of enzymes including cellobiose dehydrogenase (CDH) [316], nuclease [317], acylase [318], and glycoside hydrolase [319] have been demonstrated to result in coatings that are effective against biofilms. The covalent incorporation of the enzyme on the coating surface offers an alternative approach in that the enzyme is more stable with minimization of enzyme leaching and provides long-term use.

Lysostaphin (Lys) is a proteolytic enzyme, that can degrade biofilms by disrupting the peptide bonds of the proteinaceous substances that make up the EPS content of biofilms [21]. Lys is highly selective for *S. aureus*, the best-known example of staphylococcal strains, and eradicates *S. aureus* biofilms effectively [320]. In limited number of studies, Lys was incorporated into surface coatings via Lys-functionalized nanoparticles or pre-

functionalization of the surface with an adhesive polymeric layer, and antibiofilm surfaces, that can effectively eradicate *S. aureus* biofilms were obtained [99, 101, 191]. However, the immobilization of the Lys onto a nanoparticle and its subsequent dispersion in the coating material can cause formation of aggregates and heterogeneous distribution of the nanoparticles into the coating material decreasing the effectiveness of the enzyme. A nanoparticle-free approach to incorporate Lys into a surface coating, that does not require prior functionalization of surfaces and can be easily applied to large-area surfaces would have great potential as effective and practical antibiofilm coatings for eradication of *S. aureus* biofilms.

In this study, a hybrid waterborne polyurethane and polydopamine (WPU-PDA) polymer matrix [321] was utilized as a scaffold for the immobilization of Lys, resulting in a single-component, nanoparticle-free surface coating that can be easily applied to large-surface areas and presents effective antibiofilm activity against *S. aureus*. The WPU-PDA is obtained by coating the WPU particles with polydopamine and can be applied to any surface as a single component coating. Surfaces onto which this hybrid polymer is applied exhibit intrinsically adhesive properties, allowing Lys to be immobilized homogeneously via a facile incubation, that preserved its antibiofilm activity. The WPU-PDA-Lys coatings presented here offer a practical and effective solution on surfaces that are prone to *S. aureus* biofilm formation.

5.3. Materials and Methods

5.3.1. Materials

3-hydroxytyramine hydrochloride (dopamine) and Tris(hydroxymethyl)aminomethane (ultrapure Tris base) were purchased from Acros Organics Inc and MP Biomedicals, LLC,

respectively. Acetone with 99.5% purity, sodium hydroxide, ethylenediamine (EDA), hydrochloric acid (37%), and Lys were supplied from Sigma-Aldrich Inc. Agar powder and Tryptic soy broth (TSB) were purchased from Medimark. Sodium 2-[(2-aminoethyl) amino] ethane sulphonate (AEAS) (50 wt % in water) was donated by Evonik Industries. Hexamethylene diisocyanate (HDI) was purchased from Covestro AG. Polyester polyol (Desmophen 1652, M_n=2000 g/mol) was supplied from Covestro AG and dried at 80 °C for 15 min under vacuum (~2 mbar) before use.

5.3.2. Synthesis of WPU-PDA dispersion

The WPU dispersion was synthesized using the acetone method [191]. The NCO-terminated polyurethane prepolymer was prepared via the pre-polymerization reaction between polyester polyol (170.8 g) and HDI (29.0 g). The reaction temperature was first set to 80 °C until the theoretical NCO content of 3.86 % (determined by the back titration method following ASTM D2572-97) was reached, then the prepolymer was dissolved in acetone at 50 °C resulting in 40 wt % solid content. Chain extension of the prepolymer was performed by the dropwise addition of a mixture of AEAS (13.3 g) and EDA (1.9 g) at 50 °C. Then, distilled water was slowly added into the reaction mixture at 40 °C and acetone was removed by vacuum distillation. Finally, filtration of the product through a 50 μm filter resulted in a WPU dispersion with approximately 35 wt % solid content and a pH of 7.0.

WPU-PDA dispersions were prepared as reported earlier [321]. An aqueous dopamine solution was mixed with the WPU dispersion at 6 mg/mL dopamine concentration and 6 wt % total solid content, and the pH was adjusted to 8.5. A dark   brown WPU-PDA dispersion was obtained after a 24 h stirring reaction at 40 °C.

5.3.3. Preparation and characterization of WPU-PDA/Lys coatings

The WPU-PDA dispersion was spin coated (SPIN-COATER KW-4A) onto a sterile glass substrate (18 mm diameter, Corning Inc.) at 2000 rpm for 60 s and the substrate was dried overnight at room temperature. The thickness of the coating on the substrate was measured as 2 µm by a KLA-Tencor P6 Surface Profilometer.

To covalently immobilize the Lys, WPU-PDA coated substrates were immersed into 1 mL Lys solution with a concentration of 0.16 mg/mL in Tris buffer (50 mM Tris, 145 mM NaCl) and shaken at 500 rpm at room temperature for 4 h. Resulting WPU-PDA/Lys coated substrates were removed and washed with 1 mL Tris buffer by shaking for 10 min to remove any unreacted Lys from the surface and drying at room temperature. Lys was directly immobilized onto WPU coatings by the same method to prepare WPU/Lys coated substrates as a control surface.

Fourier Transform Infrared (FT-IR) spectra of the coated substrates were acquired using Nicolet IS10 equipped with an ATR system.

To determine the immobilization efficiency of the Lys on the WPU-PDA coatings, the concentration of the Lys solution before and after the reaction with WPU-PDA coated surfaces was determined with the Bio-Rad Quick Start™ Bradford Protein Assay (BSA). The amount of the Lys immobilized onto the WPU-PDA coated substrate was calculated from the difference of the amount of the Lys in the initial solution and the solution collected after the reaction. The Lys concentration on the WPU-PDA-Lys coatings was reported in $\mu g/cm^2$.

Immobilization of the Lys to the WPU-PDA surface was evaluated by the decrease in optical density of *S. aureus* (ATCC 29213) suspensions mixed with the Lys solution collected from

the reaction with the WPAU-PDA coated substrates using Tecan Infinite M200 plate reader. *S. aureus* (ATCC 29213) grown on TSB agar plates were inoculated into TSB (3 mL) and grown overnight at 37 °C on a shaker incubator (200 rpm). Cells harvested by centrifugation were washed twice in sterile Tris buffer (pH 7.5) and resuspended in Tris buffer at a concentration of 10^7 CFU/mL. The initial Lys solution and the Lys solution collected after the reaction with the WPU-PDA coated substrates were placed in a 96-well microplate and the plate was covered to prevent any evaporation. The optical density of the suspensions at 595 nm was monitored for 30 min at 37 °C.

5.3.4. Antibacterial properties of WPU-PDA/Lys coatings

The antibacterial activity of WPU-PDA/Lys coatings was determined with the ISO 22196 standard protocol with some modifications [288]. *S. aureus* (ATCC 29213) grown on TSB agar plates were inoculated into TSB (3 mL) and grown overnight at 37 °C on a shaker incubator (200 rpm). Following the incubation, centrifugation was applied to collect grown cells; subsequently, collected cells were rinsed twice in sterile Tris buffer and resuspended in Tris/TSB (1 %, v/v) at a concentration of 10^5 CFU/mL. 30 µL aliquot of the of bacterial suspension was transferred onto coated glass substrates (20 mm × 20 mm), which were placed into petri dishes, and samples were covered with parafilm (15 mm × 15 mm). Incubation of samples was performed at 37 °C under a relative humidity of above 90% for 24 h. The coated glass substrates and parafilm used as a cover were transferred into Tris buffer (2 mL) and bath sonication was carried out for 15 min followed by vortexing for 30 s. Serial dilutions of the bacterial suspension were plated onto TSB agar and the number of bacteria was determined as log CFU/cm^2 by counting the colonies that were grown on agar during the

incubation at 37 °C for 18 h. Mean and standard error calculated from three different measurements were reported.

5.3.5. Stability of WPU-PDA/Lys coatings

To determine whether the immobilized Lys remains stable on the surface, a turbidity assay was performed. WPU/Lys and WPU-PDA/Lys coated substrates, which contained 6 µg/cm^2 enzyme on the surface were incubated with 2 mL Tris buffer for 24 h. The buffer incubated with the coated substrates were removed and subjected to a turbidity assay; the coated substrates were dried at room temperature. 50 µL of the buffer incubated with the coated substrates was placed in a 96-well microplate, mixed with 150 µL of *S. aureus* (10^7 CFU/mL) and the optical density at 595 nm was monitored for 30 min at 37 °C. Furthermore, a viability assay was applied to the WPU/Lys and WPU-PDA/Lys coated substrates that have been incubated with buffer. The substrates were added into 500 µL bacterial suspensions with a concentration of 10^7 CFU/mL and incubated at 37 °C with shaking at 200 rpm for 24 h. Serial dilutions of the bacterial suspensions were plated and incubated at 37 °C for 18 h for colony counting. Mean and standard error calculated from three different measurements were reported.

The operational stability of the coatings over multiple exposures to *S. aureus* was determined via the ISO 22196 standard protocol with some modifications. Coated substrates (20 mm x 20 mm) were exposed to bacteria (30 µL) at 10^5 CFU/mL, covered with parafilm (15 mm × 15 mm) and incubated at 37 °C under a relative humidity of above 90 % for 24 h. Following the incubation, bacteria on the coated substrates were transferred to Tris buffer for quantification as detailed above, and the coated substrates were prepared for the second cycle

of exposure to *S. aureus* by washing with Tris buffer and drying under nitrogen flow. This process was repeated three times for each sample.

The storage stability of the coatings was studied over 30 d. WPU-PDA/Lys coatings that were stored at room temperature for 30 d were subjected to a viability assay via the ISO 22196 protocol as detailed above. Mean and standard error calculated from three different measurements were reported.

5.3.6. Antibiofilm properties of WPU-PDA/Lys coatings

Glass substrates (18 mm diameter) coated with WPU-PDA/Lys, prepared by incubation with 0.16 mg/mL, 0.31 mg/mL or 0.54 mg/mL Lys solution and containing 6 µg/cm^2, 13 µg/cm^2 and 20 µg/cm^2 enzyme on their surfaces, respectively, were immersed into petri dishes containing suspensions of *S. aureus* (ATCC 29213) in TSB growth medium (10^8 CFU/mL). To allow biofilm formation, petri dishes were incubated at 37 °C without shaking. After 24 h, bacterial suspensions were replaced with fresh TSB and incubated for an additional 24 h. To quantify the biofilm formation, coated substrates were removed from the petri dishes and gently washed once with 15 mL Tris buffer to eliminate unattached bacteria. Substrates were then immersed into 15 mL fresh Tris buffer and agitated in an ultrasound bath for 20 min followed by vortexing for 30 seconds to transfer surface-attached biofilm bacteria into the buffer. Serial dilution and colony counting was performed on the buffer containing bacteria released from the biofilms. Mean and standard error calculated from three different measurements were reported.

Scanning electron microscope (SEM) imaging of the biofilm formation on surfaces was performed using LEO Supra 35 V P scanning electron microscope. Following the static

biofilm formation substrates were gently rinsed with Tris buffer and fixed in 2.5 % glutaraldehyde in PBS for 2 h at room temperature. Fixed samples were washed twice with sterile PBS and dehydrated in a series of increasing ethanol concentrations. Before the SEM visualization samples were coated with Au-Pd.

Biofilms formed on the substrates were visualized with laser scanning confocal microscopy (LSCM). Substrates were washed with sterile Tris buffer once to remove unattached bacteria, stained with BacLight Live/Dead stain (L-7012, Invitrogen, USA) for 10 min in dark at room temperature, and finally rinsed with Tris buffer to remove the excess stain. Samples mounted onto a coverslip were imaged with a Carl-Zeiss LSM 710 Laser Scanning Confocal Microscope equipped with a Plan-Apochromat 63x/1.40 oil objective. 3-D renderings of Z-stacks created by using Zen 2010 software were reported.

5.4.   Results and Discussions

5.4.1.   WPU-PDA/Lys coatings

To obtain a polymeric matrix, that can be easily applied as a coating and presents adhesion properties allowing the immobilization of Lys, hybrid waterborne polyurethane/polydopamine was prepared.   The excellent adhesion properties of polydopamine originating from its catechol groups [231] were aimed to be imparted to waterborne polyurethane. The stable, hybrid dispersion of the WPU-PDA polymeric matrix, was obtained by encapsulating WPU particles with polydopamine via a one-pot polymerization of the dopamine monomer in the WPU dispersion, as reported previously [321-322]. A substrate was coated with the WPU-PDA polymer matrix via spin coating followed by

the incubation of the WPU-PDA coated substrate with an aqueous Lys solution, resulting in WPU-PDA-Lys coatings (Figure 29).
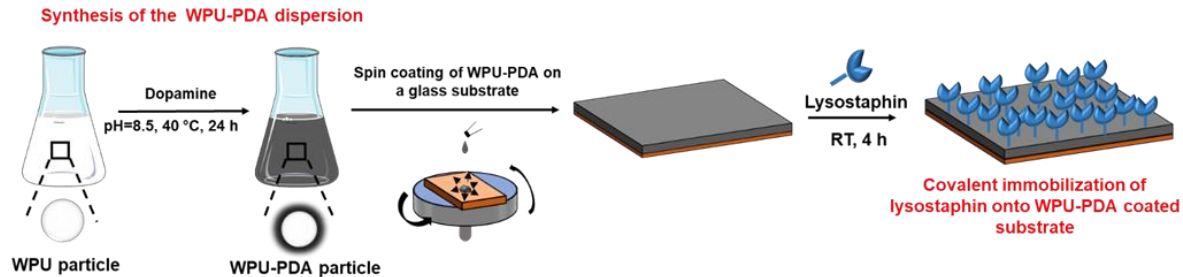
Figure 29. Preparation of the WPU-PDA/Lys coated surfaces.

The PDA component of the hybrid matrix was utilized for the covalent immobilization of the Lys via Michael addition and/or Schiff base reactions between the quinone groups of the PDA and nucleophilic amino-functional groups of the enzyme [293].
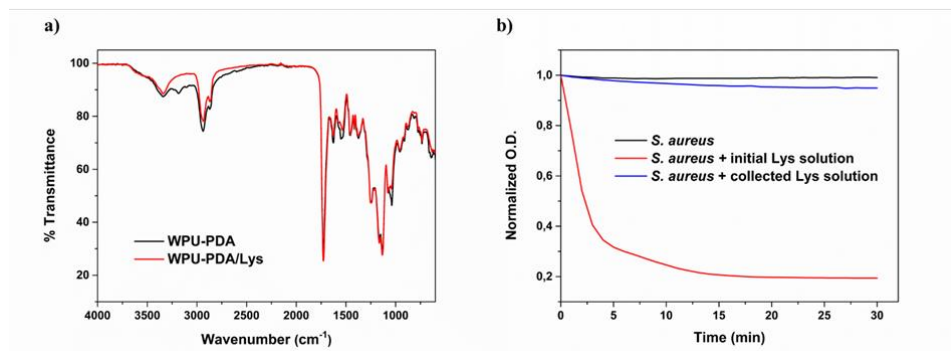
Figure 30. FT-IR analysis of WPU-PDA and WPU-PDA/Lys coated surfaces (a), Enzymatic activity of the initial Lys solution (red) and the solution that was collected from the reaction of WPU-PDA coated surface and the Lys solution (blue) as determined by the decrease in OD$_{595\ nm}$ of S. aureus incubated with each of these solutions (b).

The successful immobilization of Lys onto the WPU-PDA coating was evidenced by FT-IR (Figure 30a). The disappearance of the peak at 3175 cm^{-1} in the WPU-PDA spectrum

corresponding to the amino group of the PDA [323] confirmed the reaction between the PDA and the functional groups of the Lys. The efficiency of the Lys immobilization on the WPU-PDA coating was determined to be 96 % by the BSA assay, resulting in a Lys concentration of 6 μg/cm^2 on the coating surface. The immobilization of Lys was further confirmed with a turbidity assay, which monitors the decrease in optical density due to the Lys-based cell lysis. The enzymatic activity of the initial Lys solution and the wash solution collected from the WPU-PDA surface after the reaction with the Lys solution was tested against *S. aureus.* The initial Lys solution showed a very strong enzymatic activity on *S. aureus*, resulting in a significant decrease in optical density. On the other hand, the wash solution collected after the reaction was completed presented a negligible enzymatic activity, demonstrating that most of the Lys was immobilized on the WPU-PDA surface (Figure 30b).

5.4.2. Antibacterial properties of WPU-PDA/Lys coatings

The antibacterial activity of the WPU-PDA/Lys coating was evaluated against *S. aureus* by determining the viability of the bacteria that have been in contact with this surface according to the ISO 22196 standard protocol. As illustrated in Figure 31, while WPU and WPU-PDA control samples, which did not contain Lys enzyme, did not show any killing activity on *S. aureus* cells, WPU-PDA/Lys coatings demonstrated strong antibacterial effect against *S. aureus* with a 4-log reduction in the number of viable bacteria. The facile immobilization of the Lys onto the WPA-PDU coating resulted in a surface containing Lys, which preserved its enzymatic activity and can kill *S. aureus* effectively.
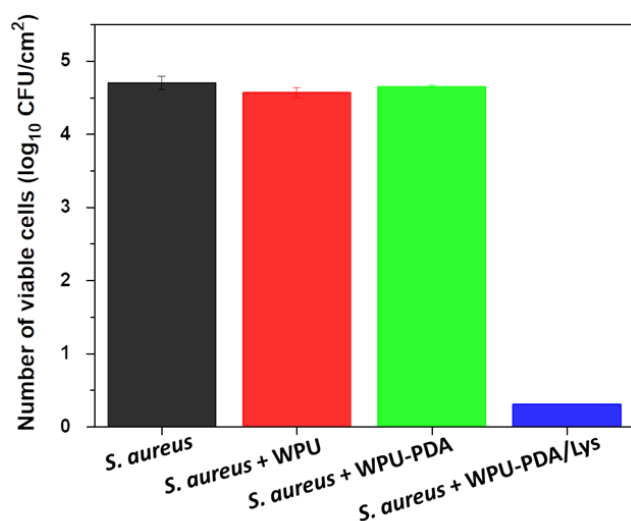
Figure 31. Viability of S. aureus incubated with WPU, WPU-PDA and WPU-PDA/Lys coated substrates at 37 °C for 24 h according to ISO 22196.

5.4.3. Stability of WPU-PDA/Lys coatings

The stability of the Lys immobilized onto the coating, as well as the durability of its enzymatic activity was studied. WPU-PDA-Lys surfaces were incubated in an aqueous buffer, which was then tested in terms of its cell lysis activity on *S. aureus*. WPU-Lys surfaces, which were prepared via dip coating of the same amount of Lys directly onto the WPU coating was used as a control. As shown in Figure 32a, the buffer in which the WPU/Lys surfaces was incubated killed the *S. aureus*, confirming that the Lys bound to the surface via non-covalent interactions was not stable and migrated to the incubation buffer [298]. On the other hand, the buffer in which the WPU-PDA/Lys coated surfaces were incubated presented very low antibacterial activity on *S. aureus*, demonstrating that the Lys in the WPU-PDA/Lys coatings remained stable due to covalent immobilization. As a further confirmation of the enzyme stability of WPU-PDA/Lys coatings, the resulting WPU/Lys and

106

WPU-PDA/Lys coatings treated with the aqueous buffer were tested in terms of their killing activity on *S. aureus*. While the WPU-PDA/Lys coatings washed with the buffer presented killing activity on *S. aureus*, WPU/Lys coatings did not show any antibacterial activity following the treatment with buffer (Figure 32b). These results suggest that the PDA on the WPU-PDA constitutes a scaffold for the covalent binding of the Lys enzyme, and as a result, non-leaching and durable Lys-containing coatings that are effective against *S. aureus* were obtained.
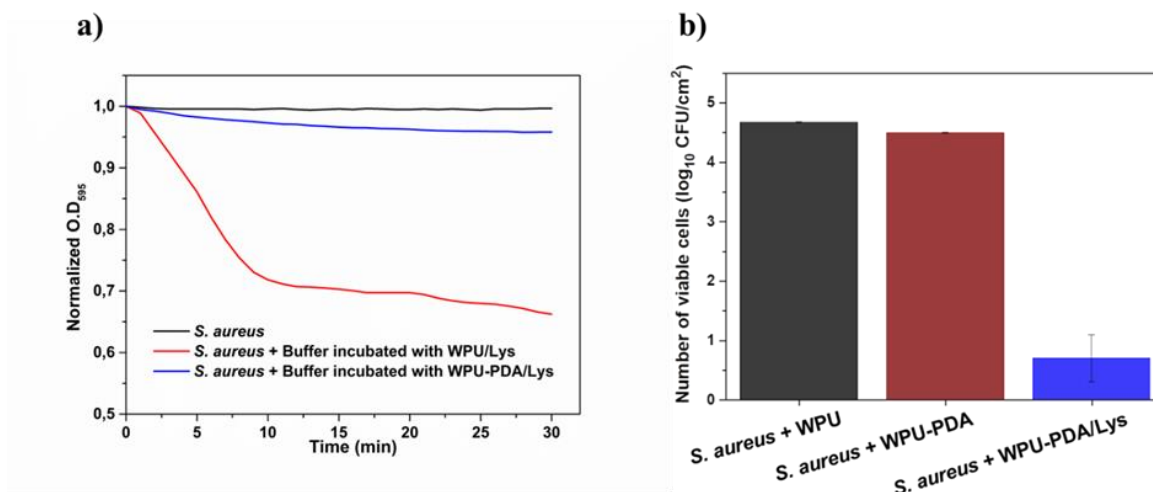
Figure 32. a) Killing efficiency of the buffer incubated with the WPU/Lys and WPU-PDA/Lys coated surfaces, b) Viability of S. aureus incubated with WPU, WPU-PDA/Lys and WPU-PDA/Lys coated surfaces which were treated with aqueous buffer.

It is critical that the enzyme in enzyme-based antibacterial coatings maintains its activity over multiple exposures to bacteria. To evaluate the operational stability of WPU-PDA/Lys coatings, they were challenged with *S. aureus* over multiple incubation cycles. In each cycle, coated surfaces were incubated with suspensions of *S. aureus* for 24 h, rinsed with buffer, dried and re-exposed to the same number of bacteria. As shown in Figure 33a, after

challenging the same coatings with bacteria by three operational cycles, only a slight decrease in antibacterial activity of WPU-PDA/Lys coatings was observed; the coatings still presented strong killing effect on *S. aureus* with a 3.5 log reduction in number of bacteria.

The storage stability of the WPU-PDA/Lys coatings was determined by storing the coated surfaces at room temperature for 30 d, and then applying a viability assay to these coatings. As indicated in Figure 33b, the killing efficiency of the coatings stored for 30 d at room temperature remained almost the same as the freshly prepared coating, demonstrating the strong storage stability of these coatings.
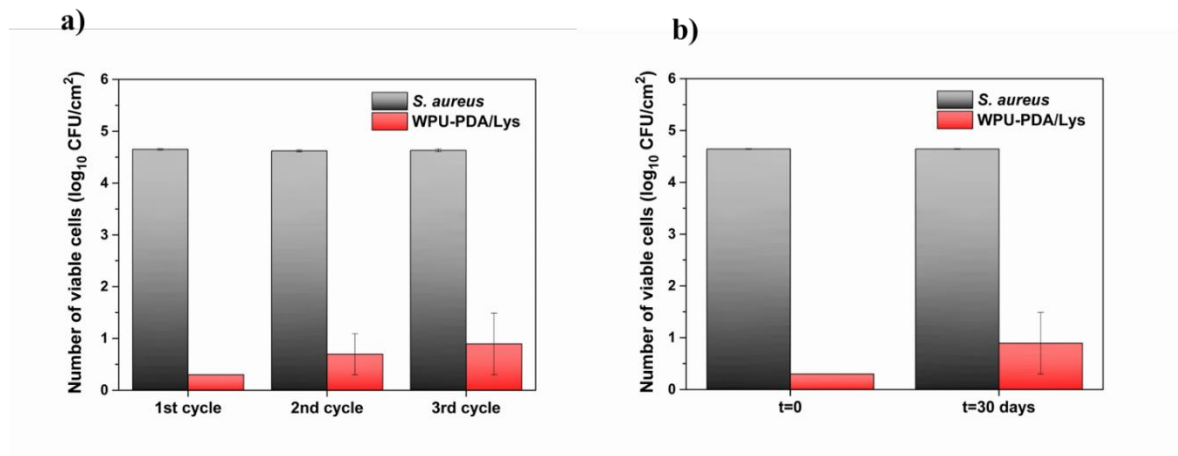
Figure 33. a) Operational stability of WPU-PDA/Lys coatings over three cycles, b) Storage stability of WPU-PDA/Lys coatings stored at RT for 30 d.

5.4.4. Antibiofilm properties of WPU-PDA/Lys coatings

The antibiofilm activity of WPU-PDA/Lys coatings on *S. aureus* biofilms was also investigated. To determine the effect of the Lys content of the coatings on the formation of biofilms, WPU-PDA/Lys coatings of different Lys concentrations were prepared. WPU-PDA/Lys coatings, as well as WPU and WPU-PDA control coatings were statically incubated with *S. aureus* for 48 h to allow formation of bacterial biofilms on their surfaces

and then rinsed to remove any unadhered cells. Finally, the number of viable surface attached bacteria was counted to quantitatively determine the biofilm formation on these surfaces. As the Lys content increased in the coating, the degree of the biofilm formation on the surfaces has decreased. WPU-PDA/Lys coatings with a Lys content of 20 $\mu g/cm^2$ on the surface resulted in a 3.5 log reduction in the number of surface-attached bacteria, which clearly shows that WPU-PDA/Lys coatings were highly effective on *S. aureus* biofilms (Figure 34).
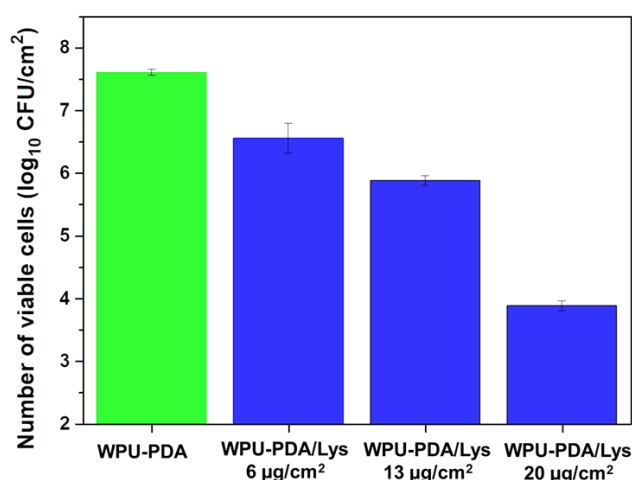
Figure 34. Biofilm formation on the WPU-PDA control surface and WPU-PDA/Lys coated surfaces at different Lys concentrations.

The morphology of the biofilm bacteria on the WPU, WPU-PDA and WPU-PDA/Lys coated surfaces incubated with *S. aureus* to allow static biofilm formation was investigated using SEM (Figure 35). WPU and WPU-PDA coated control surfaces, which were lacking the Lys were highly colonized with aggregates of healthy bacteria without any structural deformation. However, for the WPU-PDA/Lys coatings, significantly less bacteria were observed on the surface, demonstrating that the Lys on the coatings have prevented biofilm

formation. Furthermore, distortions in the spherical shape of the surface-attached cells indicated that Lys has presented a killing activity by breaking down the cell walls.
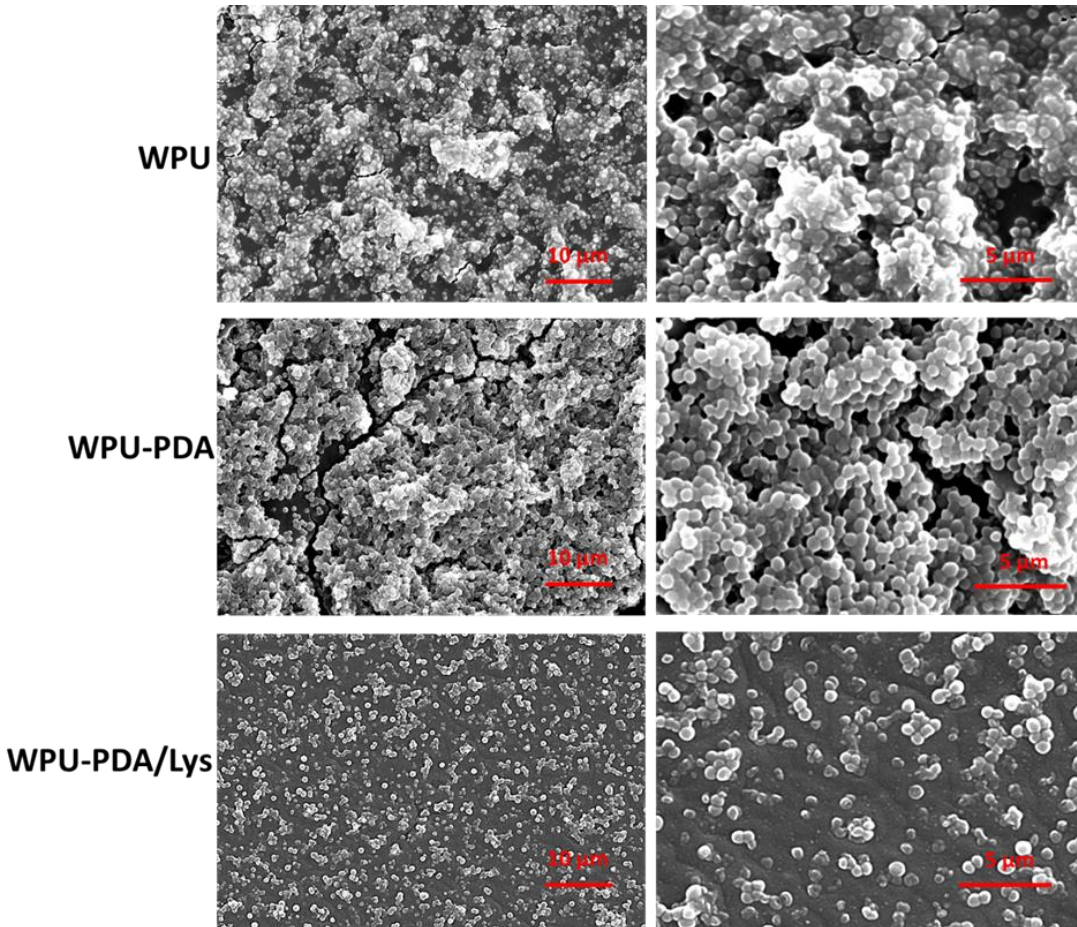
Figure 35. Representative SEM images of surfaces coated with WPU, WPU-PDA and WPU-PDA/Lys following a 48-h incubation with S. aureus.

Coating samples were also stained with live/dead indicator dyes and imaged with laser scanning confocal microscopy (LSCM). Figure 36 illustrates the representative LSCM images of WPU, WPU-PDA and WPU-PDA/Lys coatings. Both WPU and WPU-PDA coated surfaces were colonized by live bacteria, whereas the WPU-PDA/Lys coating inhibited the bacterial attachment on the surfaces as seen by the significant reduction in the number of colonized bacteria. Also, the small number of bacteria attached to WPU-PDA/Lys

surfaces were almost entirely dead. These results demonstrated that WPU-PDA/Lys coatings have a significant effect on both inhibition of biofilm formation and the destruction of surface-attached bacteria indicating that these coatings can be utilized as effective antibiofilm coating against *S. aureus*.
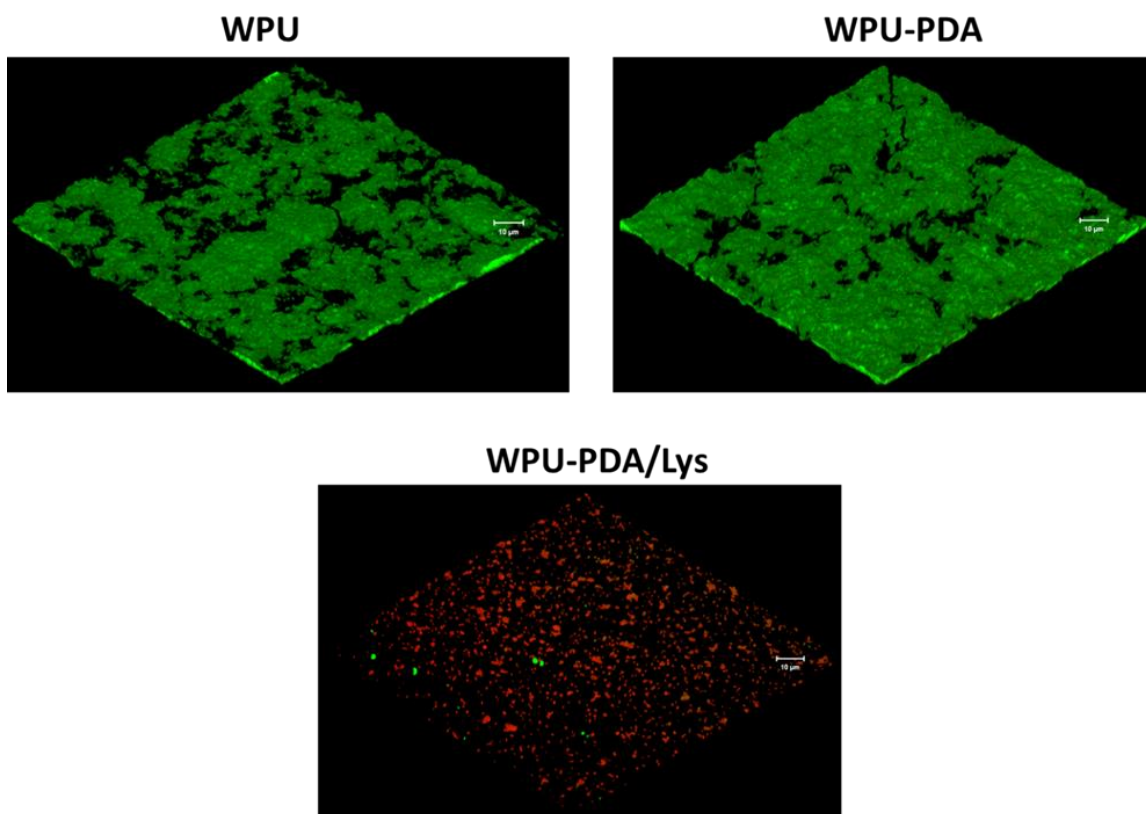
Figure 36. Representative LSCM images of surfaces coated with WPU, WPU-PDA and WPU-PDA/Lys following a 48-h incubation with S. aureus.

5.5. Conclusions

WPUs, which stand out in a variety of industrial applications due to their environmental friendliness as well as their excellent chemical and physical properties, were functionalized with polydopamine, resulting in a one-component polymeric coating that allowed facile covalent immobilization of the Lys enzyme. Non-leaching, antibacterial Lys coatings

presented strong antibacterial effect on *S. aureus*, resulting in a 4-log reduction in the number of viable bacteria. Furthermore, the WPU-PDA/Lys coatings were shown to have a durable enzymatic activity allowing strong storage and operational stability. Biofilm formation was significantly inhibited with a 3.5 log reduction in the number of surface-attached bacteria, and the bacteria attached to the WPU-PDA/Lys coatings were shown to be killed by the Lys on the surface. We believe that the WPU-PDA/Lys coatings presented here have the potential to be used on a variety of large-area surfaces, ranging from healthcare to indoor applications, where inhibition and eradication of biofilms are required, thanks to their strong antibacterial/antibiofilm activity, ease of applicability and the environmentally friendly nature.

CHAPTER 6: Overall conclusions

The overall conclusions of the thesis can be stated in the order of the chapters as below:

- Antimicrobial crv-HNT/PE thin film coatings were prepared by multiple self-assembly of CHI and carvacrol-loaded HNTs onto the polyethylene surface by spray LbL. The viability of *A. hydrophila* on the coated film and the aerobic count on chicken meat surfaces packaged with the resulting material was decreased by 85% and 48%, respectively. Furthermore, the antibiofilm properties of films were confirmed by observation of less colonized bacteria on the surface. As a result of the encapsulation of carvacrol in the nano-carrier, sustained release of carvacrol was ensured and thus the films were provided with long-term antimicrobial properties.

- WPU-PDA hybrid coatings were fabricated to destroy pathogenic bacteria physically by utilizing the NIR-sensitive properties of the surface. Thanks to the effective photothermal activity of the PDA, the temperature of the hybrid coatings reached almost 155 °C after 4 minutes of NIR laser irradiation, which is an effective temperature for the lysis of bacteria irreversibly. Moreover, the photothermal stability of hybrid coatings was maintained after repeated laser irradiation. WPU-PDA hybrid coatings demonstrated strong antibacterial activity, resulting in 3.5 logs reduction in bacterial viability under NIR light irradiation and this activity was maintained up to twenty-irradiation cycles as well. In addition, the *S. aureus* biofilms were completely destroyed under laser irradiation, and the hybrid coatings showed impressive antibiofilm properties.

- PU/Lys-HNT hybrid coatings were designed to combat MRSA by utilizing the contact-killing property of lysostaphin. Hybrid coatings demonstrated effective antimicrobial activity against *S. aureus* by >99% killing efficiency. Besides, coatings maintained their activity over multiple incubation cycles without leaching of the enzyme due to covalent bonding. Storage stability was confirmed by no change in antimicrobial effect after 20 days as well. Moreover, the decrease in biofilm formation by 70% was proof of the antibiofilm effectiveness of hybrid coatings.

- WPU-PDA/Lys coatings, in which lysostaphin acts as the contact-killing agent, showed a significantly lethal effect on *S. aureus* with excellent storage and operational stability, resulting in a 4 log decrease in the number of viable bacteria. In addition, surface-attached bacteria on WPU-PDA/Lys coatings were significantly killed, resulting 3.5 logs reduction in the number of bacteria, which means WPU-PDA/Lys coatings had a significantly destructive effect on biofilms.

REFERENCES

(1) Verderosa, A. D.; Totsika, M.; Fairfull-Smith, K. E. Bacterial Biofilm Eradication Agents: A Current Review. *Frontiers in Chemistry* **2019,** *7* (824).

(2) WHO. Foodborne disease health topic. *Retrieved from https://www.who.int/health-topics/foodborne-diseases* **2018,** *Accessed 2021 November 07*.

(3) Jarvis, W. R. Selected Aspects of the Socioeconomic Impact of Nosocomial Infections: Morbidity, Mortality, Cost, and Prevention. *Infection Control & Hospital Epidemiology* **1996,** *17* (8), 552-557.

(4) Barrasa-Villar, J. I.; Aibar-Remón, C.; Prieto-Andrés, P.; Mareca-Doñate, R.; Moliner-Lahoz, J. Impact on Morbidity, Mortality, and Length of Stay of Hospital-Acquired Infections by Resistant Microorganisms. *Clinical Infectious Diseases* **2017,** *65* (4), 644-652.

(5) Hetrick, E. M.; Schoenfisch, M. H. Reducing implant-related infections: active release strategies. *Chemical Society Reviews* **2006,** *35* (9), 780-789.

(6) Holcapkova, P.; Hurajova, A.; Bazant, P.; Pummerova, M.; Sedlarik, V. Thermal stability of bacteriocin nisin in polylactide-based films. *Polymer degradation and stability* **2018,** *158*, 31-39.

(7) Scaffaro, R.; Maio, A.; Nostro, A. Poly (lactic acid)/carvacrol-based materials: Preparation, physicochemical properties, and antimicrobial activity. *Applied Microbiology and Biotechnology* **2020,** *104* (5), 1823-1835.

(8) Jones, A. Killer plastics: Antimicrobial additives for polymers. *Plastics Engineering* **2008,** *64* (8), 34-40.

(9) Zou, Y.; Zhang, Y.; Yu, Q.; Chen, H. Photothermal bactericidal surfaces: killing bacteria using light instead of biocides. *Biomaterials science* **2021,** *9* (1), 10-22.

(10) Xia, M.-Y.; Xie, Y.; Yu, C.-H.; Chen, G.-Y.; Li, Y.-H.; Zhang, T.; Peng, Q. Graphene-based nanomaterials: the promising active agents for antibiotics-independent antibacterial applications. *Journal of Controlled Release* **2019,** *307*, 16-31.

(11) Oruc, B.; Unal, H. Fluorophore-Decorated Carbon Nanotubes with Enhanced Photothermal Activity as Antimicrobial Nanomaterials. *ACS Omega* **2019,** *4* (3), 5556-5564.

(12) Ye, L.; Cao, Z.; Liu, X.; Cui, Z.; Li, Z.; Liang, Y.; Zhu, S.; Wu, S. Noble metal-based nanomaterials as antibacterial agents. *Journal of Alloys and Compounds* **2022,** *904*, 164091.

(13) Sun, H.; Lv, F.; Liu, L.; Gu, Q.; Wang, S. Conjugated polymer materials for photothermal therapy. *Advanced Therapeutics* **2018,** *1* (6), 1800057.

(14) Lin, F.; Duan, Q.-Y.; Wu, F.-G. Conjugated Polymer-Based Photothermal Therapy for Killing Microorganisms. *ACS Applied Polymer Materials* **2020,** *2* (10), 4331-4344.

(15) Buruaga-Ramiro, C.; Valenzuela, S. V.; Valls, C.; Roncero, M. B.; Pastor, F. I. J.; Díaz, P.; Martinez, J. Development of an antimicrobial bioactive paper made from bacterial cellulose. *International Journal of Biological Macromolecules* **2020,** *158*, 587-594.

(16) Diaz-Gomez, L.; Concheiro, A.; Alvarez-Lorenzo, C. Functionalization of titanium implants with phase-transited lysozyme for gentle immobilization of antimicrobial lysozyme. *Applied Surface Science* **2018,** *452*, 32-42.

(17) Steiert, E.; Radi, L.; Fach, M.; Wich, P. R. Protein-Based Nanoparticles for the Delivery of Enzymes with Antibacterial Activity. *Macromolecular rapid communications* **2018,** *39* (14), 1800186.

(18) Elena, P.; Miri, K. Formation of contact active antimicrobial surfaces by covalent grafting of quaternary ammonium compounds. *Colloids and Surfaces B: Biointerfaces* **2018,** *169*, 195-205.

(19) Zhang, T.; Gu, J.; Liu, X.; Wei, D.; Zhou, H.; Xiao, H.; Zhang, Z.; Yu, H.; Chen, S. Bactericidal and antifouling electrospun PVA nanofibers modified with a quaternary ammonium salt and zwitterionic sulfopropylbetaine. *Materials Science and Engineering: C* **2020,** *111*, 110855.

(20) Yang, W.; Zhang, N.; Wang, Q.; Wang, P.; Yu, Y. Development of an eco-friendly antibacterial textile: lysozyme immobilization on wool fabric. *Bioprocess and biosystems engineering* **2020,** *43* (9), 1639-1648.

(21) Thallinger, B.; Prasetyo, E. N.; Nyanhongo, G. S.; Guebitz, G. M. Antimicrobial enzymes: an emerging strategy to fight microbes and microbial biofilms. *Biotechnology journal* **2013,** *8* (1), 97-109.

(22) Wu, J. A.; Kusuma, C.; Mond, J. J.; Kokai-Kun, J. F. Lysostaphin disrupts Staphylococcus aureus and Staphylococcus epidermidis biofilms on artificial surfaces. *Antimicrobial agents and chemotherapy* **2003,** *47* (11), 3407-14.

(23) Bridier, A.; Briandet, R.; Thomas, V.; Dubois-Brissonnet, F. Resistance of bacterial biofilms to disinfectants: a review. *Biofouling* **2011,** *27* (9), 1017-1032.

(24) Dancer, S. J. Controlling hospital-acquired infection: focus on the role of the environment and new technologies for decontamination. *Clinical microbiology reviews* **2014,** *27* (4), 665-690.

(25) WHO. Health care-associated infections fact sheet **2016**.

(26) Van Boeckel, T. P.; Pires, J.; Silvester, R.; Zhao, C.; Song, J.; Criscuolo, N. G.; Gilbert, M.; Bonhoeffer, S.; Laxminarayan, R. Global trends in antimicrobial resistance in animals in low-and middle-income countries. *Science* **2019,** *365* (6459), eaaw1944.

(27) Husman, T. Health effects of indoor-air microorganisms. *Scandinavian journal of work, environment & health* **1996**, 5-13.

(28) Joardder, M. U.; Masud, M. H. A brief history of food preservation. In *Food Preservation in Developing Countries: Challenges and Solutions*; Springer: 2019; pp 57-66.

(29) Baldevraj, R. M.; Jagadish, R. Incorporation of chemical antimicrobial agents into polymeric films for food packaging. *Multifunctional and nanoreinforced polymers for food packaging* **2011**, 368-420.

(30) Ding, X.; Duan, S.; Ding, X.; Liu, R.; Xu, F. J. Versatile antibacterial materials: an emerging arsenal for combatting bacterial pathogens. *Advanced Functional Materials* **2018,** *28* (40), 1802140.

(31) Tiller, J. C. Antimicrobial surfaces. *Bioactive surfaces* **2010**, 193-217.

(32) Ibelli, T.; Templeton, S.; Levi-Polyachenko, N. Progress on utilizing hyperthermia for mitigating bacterial infections. *International Journal of Hyperthermia* **2018,** *34* (2), 144-156.

(33) Zilberman, M.; Elsner, J. J. Antibiotic-eluting medical devices for various applications. *Journal of Controlled Release* **2008,** *130* (3), 202-215.

(34) Gold, H. S.; Moellering Jr, R. C. Antimicrobial-drug resistance. *New England journal of medicine* **1996,** *335* (19), 1445-1453.

(35) Flemming, H. C.; Wingender, J.; Szewzyk, U.; Steinberg, P.; Rice, S. A.; Kjelleberg, S. Biofilms: an emergent form of bacterial life. *Nature reviews. Microbiology* **2016,** *14* (9), 563-75.

(36) Wang, B.; Liu, H.; Zhang, B.; Han, Y.; Shen, C.; Lin, Q.; Chen, H. Development of antibacterial and high light transmittance bulk materials: Incorporation and sustained release of hydrophobic or hydrophilic antibiotics. *Colloids and Surfaces B: Biointerfaces* **2016,** *141*, 483-490.

(37) Zhuk, I.; Jariwala, F.; Attygalle, A. B.; Wu, Y.; Libera, M. R.; Sukhishvili, S. A. Self-defensive layer-by-layer films with bacteria-triggered antibiotic release. *ACS nano* **2014,** *8* (8), 7733-7745.

(38) Albright, V.; Zhuk, I.; Wang, Y.; Selin, V.; van de Belt-Gritter, B.; Busscher, H. J.; van der Mei, H. C.; Sukhishvili, S. A. Self-defensive antibiotic-loaded layer-by-layer coatings: Imaging of localized bacterial acidification and pH-triggering of antibiotic release. *Acta biomaterialia* **2017,** *61*, 66-74.

(39) Wang, B.; Liu, H.; Wang, Z.; Shi, S.; Nan, K.; Xu, Q.; Ye, Z.; Chen, H. A self-defensive antibacterial coating acting through the bacteria-triggered release of a hydrophobic antibiotic from layer-by-layer films. *Journal of Materials Chemistry B* **2017,** *5* (7), 1498-1506.

(40) Geuli, O.; Metoki, N.; Zada, T.; Reches, M.; Eliaz, N.; Mandler, D. Synthesis, coating, and drug-release of hydroxyapatite nanoparticles loaded with antibiotics. *Journal of Materials Chemistry B* **2017,** *5* (38), 7819-7830.

(41) Fathi, M.; Akbari, B.; Taheriazam, A. Antibiotics drug release controlling and osteoblast adhesion from Titania nanotubes arrays using silk fibroin coating. *Materials Science and Engineering: C* **2019,** *103*, 109743.

(42) Li, D.; Lv, P.; Fan, L.; Huang, Y.; Yang, F.; Mei, X.; Wu, D. The immobilization of antibiotic-loaded polymeric coatings on osteoarticular Ti implants for the prevention of bone infections. *Biomaterials science* **2017,** *5* (11), 2337-2346.

(43) Hirschfeld, J.; Akinoglu, E. M.; Wirtz, D. C.; Hoerauf, A.; Bekeredjian-Ding, I.; Jepsen, S.; Haddouti, E.-M.; Limmer, A.; Giersig, M. Long-term release of antibiotics by carbon

nanotube-coated titanium alloy surfaces diminish biofilm formation by Staphylococcus epidermidis. *Nanomedicine: Nanotechnology, Biology and Medicine* **2017,** *13* (4), 1587-1593.

(44) Aguilera-Correa, J. J.; Garcia-Casas, A.; Mediero, A.; Romera, D.; Mulero, F.; Cuevas-López, I.; Jiménez-Morales, A.; Esteban, J. A new antibiotic-loaded sol-gel can prevent bacterial prosthetic joint infection: From in vitro studies to an in vivo model. *Frontiers in Microbiology* **2020**, 2935.

(45) Mittapally, S.; Taranum, R.; Parveen, S. Metal ions as antibacterial agents. *Journal of Drug Delivery and Therapeutics* **2018,** *8* (6-s), 411-419.

(46) Xu, Z.; Zhang, C.; Wang, X.; Liu, D. Release strategies of silver ions from materials for bacterial killing. *ACS Applied Bio Materials* **2021,** *4* (5), 3985-3999.

(47) Rai, M.; Kon, K.; Ingle, A.; Duran, N.; Galdiero, S.; Galdiero, M. Broad-spectrum bioactivities of silver nanoparticles: the emerging trends and future prospects. *Applied microbiology and biotechnology* **2014,** *98* (5), 1951-1961.

(48) Wang, R.; Neoh, K. G.; Kang, E. T.; Tambyah, P. A.; Chiong, E. Antifouling coating with controllable and sustained silver release for long-term inhibition of infection and encrustation in urinary catheters. *Journal of Biomedical Materials Research Part B: Applied Biomaterials* **2015,** *103* (3), 519-528.

(49) Zhang, X.; Li, Z.; Yuan, X.; Cui, Z.; Bao, H.; Li, X.; Liu, Y.; Yang, X. Cytotoxicity and antibacterial property of titanium alloy coated with silver nanoparticle-containing polyelectrolyte multilayer. *Materials Science and Engineering: C* **2013,** *33* (5), 2816-2820.

(50) Yun'an Qing, L. C.; Li, R.; Liu, G.; Zhang, Y.; Tang, X.; Wang, J.; Liu, H.; Qin, Y. Potential antibacterial mechanism of silver nanoparticles and the optimization of orthopedic implants by advanced modification technologies. *International journal of nanomedicine* **2018,** *13*, 3311.

(51) Gunputh, U. F.; Le, H.; Handy, R. D.; Tredwin, C. Anodised TiO2 nanotubes as a scaffold for antibacterial silver nanoparticles on titanium implants. *Materials Science and Engineering: C* **2018,** *91*, 638-644.

(52) Meghana, S.; Kabra, P.; Chakraborty, S.; Padmavathy, N. Understanding the pathway of antibacterial activity of copper oxide nanoparticles. *RSC advances* **2015,** *5* (16), 12293-12299.

(53) Phan, D.-N.; Dorjjugder, N.; Saito, Y.; Khan, M. Q.; Ullah, A.; Bie, X.; Taguchi, G.; Kim, I.-S. Antibacterial mechanisms of various copper species incorporated in polymeric nanofibers against bacteria. *Materials Today Communications* **2020,** *25*, 101377.

(54) Li, M.; Gao, L.; Schlaich, C.; Zhang, J.; Donskyi, I. S.; Yu, G.; Li, W.; Tu, Z.; Rolff, J.; Schwerdtle, T. Construction of functional coatings with durable and broad-spectrum antibacterial potential based on mussel-inspired dendritic polyglycerol and in situ-formed copper nanoparticles. *ACS applied materials & interfaces* **2017,** *9* (40), 35411-35418.

(55) Fang, F. C. Perspectives series: host/pathogen interactions. Mechanisms of nitric oxide-related antimicrobial activity. *The Journal of clinical investigation* **1997,** *99* (12), 2818-2825.

(56) Carpenter, A. W.; Schoenfisch, M. H. Nitric oxide release: Part II. Therapeutic applications. *Chemical Society Reviews* **2012,** *41* (10), 3742-3752.

(57) Riccio, D. A.; Schoenfisch, M. H. Nitric oxide release: Part I. Macromolecular scaffolds. *Chemical Society Reviews* **2012,** *41* (10), 3731-3741.

(58) Sadrearhami, Z.; Shafiee, F. N.; Ho, K. K.; Kumar, N.; Krasowska, M.; Blencowe, A.; Wong, E. H.; Boyer, C. Antibiofilm nitric oxide-releasing polydopamine coatings. *ACS applied materials & interfaces* **2019,** *11* (7), 7320-7329.

(59) Ho, K. K.; Ozcelik, B.; Willcox, M. D.; Thissen, H.; Kumar, N. Facile solvent-free fabrication of nitric oxide (NO)-releasing coatings for prevention of biofilm formation. *Chemical Communications* **2017,** *53* (48), 6488-6491.

(60) Bakkali, F.; Averbeck, S.; Averbeck, D.; Idaomar, M. Biological effects of essential oils–a review. *Food and chemical toxicology* **2008,** *46* (2), 446-475.

(61) Calo, J. R.; Crandall, P. G.; O'Bryan, C. A.; Ricke, S. C. Essential oils as antimicrobials in food systems–A review. *Food control* **2015,** *54*, 111-119.

(62) Ju, J.; Chen, X.; Xie, Y.; Yu, H.; Guo, Y.; Cheng, Y.; Qian, H.; Yao, W. Application of essential oil as a sustained release preparation in food packaging. *Trends in Food Science & Technology* **2019,** *92*, 22-32.

(63) Pandey, A. K.; Kumar, P.; Singh, P.; Tripathi, N. N.; Bajpai, V. K. Essential oils: Sources of antimicrobials and food preservatives. *Frontiers in microbiology* **2017,** *7*, 2161.

(64) Maes, C.; Bouquillon, S.; Fauconnier, M.-L. Encapsulation of essential oils for the development of biosourced pesticides with controlled release: A review. *Molecules* **2019,** *24* (14), 2539.

(65) Makwana, S.; Choudhary, R.; Dogra, N.; Kohli, P.; Haddock, J. Nanoencapsulation and immobilization of cinnamaldehyde for developing antimicrobial food packaging material. *LWT-Food science and technology* **2014,** *57* (2), 470-476.

(66) Granata, G.; Stracquadanio, S.; Leonardi, M.; Napoli, E.; Consoli, G. M. L.; Cafiso, V.; Stefani, S.; Geraci, C. Essential oils encapsulated in polymer-based nanocapsules as potential candidates for application in food preservation. *Food chemistry* **2018,** *269*, 286-292.

(67) Saucedo-Zuñiga, J.; Sánchez-Valdes, S.; Ramírez-Vargas, E.; Guillen, L.; Ramos-deValle, L.; Graciano-Verdugo, A.; Uribe-Calderón, J.; Valera-Zaragoza, M.; Lozano-Ramírez, T.; Rodríguez-González, J. Controlled release of essential oils using laminar nanoclay and porous halloysite/essential oil composites in a multilayer film reservoir. *Microporous and Mesoporous Materials* **2021,** *316*, 110882.

(68) WILLIAMS, J. F.; WORLEY, S. D. Infection-resistant nonleachable materials for urologic devices. *Journal of endourology* **2000,** *14* (5), 395-400.

(69) Kenawy, E.-R.; Worley, S.; Broughton, R. The chemistry and applications of antimicrobial polymers: a state-of-the-art review. *Biomacromolecules* **2007,** *8* (5), 1359-1384.

(70) Jennings, M. C.; Minbiole, K. P.; Wuest, W. M. Quaternary ammonium compounds: an antimicrobial mainstay and platform for innovation to address bacterial resistance. *ACS infectious diseases* **2015,** *1* (7), 288-303.

(71) Wang, B.; Xu, Q.; Ye, Z.; Liu, H.; Lin, Q.; Nan, K.; Li, Y.; Wang, Y.; Qi, L.; Chen, H. Copolymer brushes with temperature-triggered, reversibly switchable bactericidal and antifouling properties for biomaterial surfaces. *ACS Applied Materials & Interfaces* **2016,** *8* (40), 27207-27217.

(72) Vaterrodt, A.; Thallinger, B.; Daumann, K.; Koch, D.; Guebitz, G. M.; Ulbricht, M. Antifouling and antibacterial multifunctional polyzwitterion/enzyme coating on silicone catheter material prepared by electrostatic layer-by-layer assembly. *Langmuir* **2016,** *32* (5), 1347-1359.

(73) Abid, C. Z.; Jain, S.; Jackeray, R.; Chattopadhyay, S.; Singh, H. Formulation and characterization of antimicrobial quaternary ammonium dendrimer in poly (methyl methcarylate) bone cement. *Journal of Biomedical Materials Research Part B: Applied Biomaterials* **2017,** *105* (3), 521-530.

(74) Peng, Z.; Ao, H.; Wang, L.; Guo, S.; Tang, T. Quaternised chitosan coating on titanium provides a self-protective surface that prevents bacterial colonisation and implant-associated infections. *Rsc Advances* **2015,** *5* (67), 54304-54311.

(75) Waßmann, M.; Winkel, A.; Haak, K.; Dempwolf, W.; Stiesch, M.; Menzel, H. Influence of quaternization of ammonium on antibacterial activity and cytocompatibility of thin copolymer layers on titanium. *Journal of Biomaterials science, Polymer edition* **2016,** *27* (15), 1507-1519.

(76) Saini, S.; Falco, Ç. Y.; Belgacem, M. N.; Bras, J. Surface cationized cellulose nanofibrils for the production of contact active antimicrobial surfaces. *Carbohydrate polymers* **2016,** *135*, 239-247.

(77) Zhang, T.; Jin, Z.; Jia, Z.; Xu, X.; Chen, Y.; Peng, W.; Zhang, J.; Wang, H.; Li, S.; Wen, J. Preparation of antimicrobial PVDF and EVOH membranes by grafting quaternary ammonium compounds. *Reactive and Functional Polymers* **2022,** *170*, 105117.

(78) Valiei, A.; Okshevsky, M.; Lin, N.; Tufenkji, N. Anodized aluminum with nanoholes impregnated with quaternary ammonium compounds can kill pathogenic bacteria within seconds of contact. *ACS applied materials & interfaces* **2018,** *10* (48), 41207-41214.

(79) Bahar, A. A.; Ren, D. Antimicrobial peptides. *Pharmaceuticals* **2013,** *6* (12), 1543-1575.

(80) da Cunha, N. B.; Cobacho, N. B.; Viana, J. F.; Lima, L. A.; Sampaio, K. B.; Dohms, S. S.; Ferreira, A. C.; de la Fuente-Núñez, C.; Costa, F. F.; Franco, O. L. The next generation of antimicrobial peptides (AMPs) as molecular therapeutic tools for the treatment of diseases with social and economic impacts. *Drug discovery today* **2017,** *22* (2), 234-248.

(81) Mahlapuu, M.; Håkansson, J.; Ringstad, L.; Björn, C. Antimicrobial peptides: an emerging category of therapeutic agents. *Frontiers in cellular and infection microbiology* **2016,** *6*, 194.

(82) Huerta-Cantillo, J.; Navarro-García, F. Properties and design of antimicrobial peptides as potential tools against pathogens and malignant cells. *Investigación en Discapacidad* **2016,** *5* (2), 96-115.

(83) Gao, G.; Lange, D.; Hilpert, K.; Kindrachuk, J.; Zou, Y.; Cheng, J. T. J.; Kazemzadeh-Narbat, M.; Yu, K.; Wang, R.; Straus, S. K.; Brooks, D. E.; Chew, B. H.; Hancock, R. E. W.; Kizhakkedathu, J. N. The biocompatibility and biofilm resistance of implant coatings based on hydrophilic polymer brushes conjugated with antimicrobial peptides. *Biomaterials* **2011,** *32* (16), 3899-3909.

(84) Monteiro, C.; Costa, F.; Pirttilä, A. M.; Tejesvi, M. V.; Martins, M. C. L. Prevention of urinary catheter-associated infections by coating antimicrobial peptides from crowberry endophytes. *Scientific Reports* **2019,** *9* (1), 10753.

(85) Mishra, B.; Basu, A.; Chua, R. R. Y.; Saravanan, R.; Tambyah, P. A.; Ho, B.; Chang, M. W.; Leong, S. S. J. Site specific immobilization of a potent antimicrobial peptide onto silicone catheters: evaluation against urinary tract infection pathogens. *Journal of Materials Chemistry B* **2014,** *2* (12), 1706-1716.

(86) Lim, K.; Chua, R. R. Y.; Ho, B.; Tambyah, P. A.; Hadinoto, K.; Leong, S. S. J. Development of a catheter functionalized by a polydopamine peptide coating with antimicrobial and antibiofilm properties. *Acta biomaterialia* **2015,** *15*, 127-138.

(87) Acosta, S.; Ibañez-Fonseca, A.; Aparicio, C.; Rodríguez-Cabello, J. C. Antibiofilm coatings based on protein-engineered polymers and antimicrobial peptides for preventing implant-associated infections. *Biomaterials science* **2020,** *8* (10), 2866-2877.

(88) Yazici, H.; Habib, G.; Boone, K.; Urgen, M.; Utku, F. S.; Tamerler, C. Self-assembling antimicrobial peptides on nanotubular titanium surfaces coated with calcium phosphate for local therapy. *Materials Science and Engineering: C* **2019,** *94*, 333-343.

(89) Cao, P.; Li, W.-W.; Morris, A. R.; Horrocks, P. D.; Yuan, C.-Q.; Yang, Y. Investigation of the antibiofilm capacity of peptide-modified stainless steel. *Royal Society open science* **2018,** *5* (3), 172165.

(90) Nguyen, H. H.; Kim, M. An overview of techniques in enzyme immobilization. *Applied Science and Convergence Technology* **2017,** *26* (6), 157-163.

(91) Tully, J.; Yendluri, R.; Lvov, Y. Halloysite clay nanotubes for enzyme immobilization. *Biomacromolecules* **2016,** *17* (2), 615-621.

(92) Ahmad, R.; Sardar, M. Enzyme immobilization: an overview on nanoparticles as immobilization matrix. *Biochemistry and Analytical Biochemistry* **2015,** *4* (2), 1.

(93) Park, J.-M.; Kim, M.; Park, H.-S.; Jang, A.; Min, J.; Kim, Y.-H. Immobilization of lysozyme-CLEA onto electrospun chitosan nanofiber for effective antibacterial applications. *International Journal of Biological Macromolecules* **2013,** *54*, 37-43.

(94) Bayazidi, P.; Almasi, H.; Purfathi, B. Immobilized lysozyme onto bacterial cellulose nanofibers as active and reinforcing agent of sodium caseinate based films: physical characteristics and antimicrobial activity. *Journal of Food and Bioprocess Engineering* **2021,** *4* (1), 11-18.

(95) Levashov, P. A.; Matolygina, D. A.; Ovchinnikova, E. D.; Adamova, I. Y.; Gasanova, D. A.; Smirnov, S. A.; Nelyub, V. A.; Belogurova, N. G.; Tishkov, V. I.; Eremeev, N. L. The bacteriolytic activity of native and covalently immobilized lysozyme against Gram-positive

and Gram-negative bacteria is differentially affected by charged amino acids and glycine. *FEBS Open bio* **2019,** *9* (3), 510-518.

(96) Wang, P.; Zhang, C.; Zou, Y.; Li, Y.; Zhang, H. Immobilization of lysozyme on layer-by-layer self-assembled electrospun films: Characterization and antibacterial activity in milk. *Food Hydrocolloids* **2021,** *113*, 106468.

(97) Kara, F.; Aksoy, E. A.; Calamak, S.; Hasirci, N.; Aksoy, S. Immobilization of heparin on chitosan-grafted polyurethane films to enhance anti-adhesive and antibacterial properties. *Journal of Bioactive and Compatible Polymers* **2016,** *31* (1), 72-90.

(98) Tavakolian, M.; Okshevsky, M.; van de Ven, T. G.; Tufenkji, N. Developing antibacterial nanocrystalline cellulose using natural antibacterial agents. *ACS applied materials & interfaces* **2018,** *10* (40), 33827-33838.

(99) Yeroslavsky, G.; Girshevitz, O.; Foster-Frey, J.; Donovan, D. M.; Rahimipour, S. Antibacterial and Antibiofilm Surfaces through Polydopamine-Assisted Immobilization of Lysostaphin as an Antibacterial Enzyme. *Langmuir* **2015,** *31* (3), 1064-1073.

(100) Miao, J.; Pangule, R. C.; Paskaleva, E. E.; Hwang, E. E.; Kane, R. S.; Linhardt, R. J.; Dordick, J. S. Lysostaphin-functionalized cellulose fibers with antistaphylococcal activity for wound healing applications. *Biomaterials* **2011,** *32* (36), 9557-9567.

(101) Ehsani, G.; Farahnak, M.; Norouzian, D.; Ehsani, P. Immobilization of recombinant lysostaphin on nanoparticle through biotin–streptavidin conjugation technology as a geometrical progressed confrontation against Staphylococcus aureus infection. *Biotechnology and Applied Biochemistry* **2020**.

(102) Satishkumar, R.; Vertegel, A. Antibody-directed targeting of lysostaphin adsorbed onto polylactide nanoparticles increases its antimicrobial activity against S. aureus in vitro. *Nanotechnology* **2011,** *22* (50), 505103.

(103) Pangule, R. C.; Brooks, S. J.; Dinu, C. Z.; Bale, S. S.; Salmon, S. L.; Zhu, G.; Metzger, D. W.; Kane, R. S.; Dordick, J. S. Antistaphylococcal Nanocomposite Films Based on Enzyme−Nanotube Conjugates. *ACS Nano* **2010,** *4* (7), 3993-4000.

(104) Devlin, H.; Fulaz, S.; Hiebner, D. W.; O'Gara, J. P.; Casey, E. Enzyme-Functionalized Mesoporous Silica Nanoparticles to Target Staphylococcus aureus and Disperse Biofilms. *International journal of nanomedicine* **2021,** *16*, 1929.

(105) Wang, Y.; Jin, Y.; Chen, W.; Wang, J.; Chen, H.; Sun, L.; Li, X.; Ji, J.; Yu, Q.; Shen, L. Construction of nanomaterials with targeting phototherapy properties to inhibit resistant bacteria and biofilm infections. *Chemical Engineering Journal* **2019,** *358*, 74-90.

(106) Feng, Y.; Liu, L.; Zhang, J.; Aslan, H.; Dong, M. Photoactive antimicrobial nanomaterials. *Journal of Materials Chemistry B* **2017,** *5* (44), 8631-8652.

(107) Qing, G.; Zhao, X.; Gong, N.; Chen, J.; Li, X.; Gan, Y.; Wang, Y.; Zhang, Z.; Zhang, Y.; Guo, W. Thermo-responsive triple-function nanotransporter for efficient chemo-photothermal therapy of multidrug-resistant bacterial infection. *Nature communications* **2019,** *10* (1), 1-12.

(108) Huang, W. C.; Tsai, P. J.; Chen, Y. C. Multifunctional Fe3O4@ Au nanoeggs as photothermal agents for selective killing of nosocomial and antibiotic-resistant bacteria. *Small* **2009,** *5* (1), 51-56.

(109) Yougbaré, S.; Mutalik, C.; Krisnawati, D. I.; Kristanto, H.; Jazidie, A.; Nuh, M.; Cheng, T.-M.; Kuo, T.-R. Nanomaterials for the Photothermal Killing of Bacteria. *Nanomaterials* **2020,** *10* (6), 1123.

(110) Liu, Y.; Bhattarai, P.; Dai, Z.; Chen, X. Photothermal therapy and photoacoustic imaging via nanotheranostics in fighting cancer. *Chemical Society Reviews* **2019,** *48* (7), 2053-2108.

(111) Zhu, J.; Wang, Y.; Huo, D.; Ding, Q.; Lu, Z.; Hu, Y. Epitaxial growth of gold on silver nanoplates for imaging-guided photothermal therapy. *Materials Science and Engineering: C* **2019,** *105*, 110023.

(112) Cabana, S.; Lecona-Vargas, C. S.; Meléndez-Ortiz, H. I.; Contreras-García, A.; Barbosa, S.; Taboada, P.; Magarinos, B.; Bucio, E.; Concheiro, A.; Alvarez-Lorenzo, C. Silicone rubber films functionalized with poly (acrylic acid) nanobrushes for immobilization of gold nanoparticles and photothermal therapy. *Journal of Drug Delivery Science and Technology* **2017,** *42*, 245-254.

(113) Jin, C.; Su, K.; Tan, L.; Liu, X.; Cui, Z.; Yang, X.; Li, Z.; Liang, Y.; Zhu, S.; Yeung, K. W. K. Near-infrared light photocatalysis and photothermy of carbon quantum dots and au nanoparticles loaded titania nanotube array. *Materials & Design* **2019,** *177*, 107845.

(114) Luo, J.; Deng, W.; Yang, F.; Wu, Z.; Huang, M.; Gu, M. Gold nanoparticles decorated graphene oxide/nanocellulose paper for NIR laser-induced photothermal ablation of pathogenic bacteria. *Carbohydrate polymers* **2018,** *198*, 206-214.

(115) Zhu, Y.; Ramasamy, M.; Yi, D. K. Antibacterial activity of ordered gold nanorod arrays. *ACS applied materials & interfaces* **2014,** *6* (17), 15078-15085.

(116) Yang, T.; Wang, D.; Liu, X. Assembled gold nanorods for the photothermal killing of bacteria. *Colloids and Surfaces B: Biointerfaces* **2019,** *173*, 833-841.

(117) Rovati, D.; Albini, B.; Galinetto, P.; Grisoli, P.; Bassi, B.; Pallavicini, P.; Dacarro, G.; Taglietti, A. High stability thiol-coated gold nanostars monolayers with photo-thermal antibacterial activity and wettability control. *Nanomaterials* **2019,** *9* (9), 1288.

(118) Khantamat, O.; Li, C.-H.; Yu, F.; Jamison, A. C.; Shih, W.-C.; Cai, C.; Lee, T. R. Gold nanoshell-decorated silicone surfaces for the near-infrared (NIR) photothermal destruction of the pathogenic bacterium E. faecalis. *ACS applied materials & interfaces* **2015,** *7* (7), 3981-3993.

(119) Gupta, K.; Singh, R.; Pandey, A.; Pandey, A. Photocatalytic antibacterial performance of TiO2 and Ag-doped TiO2 against S. aureus. P. aeruginosa and E. coli. *Beilstein journal of nanotechnology* **2013,** *4* (1), 345-351.

(120) Wang, X.; Su, K.; Tan, L.; Liu, X.; Cui, Z.; Jing, D.; Yang, X.; Liang, Y.; Li, Z.; Zhu, S. Rapid and highly effective noninvasive disinfection by hybrid Ag/CS@ MnO2 nanosheets using near-infrared light. *ACS applied materials & interfaces* **2019,** *11* (16), 15014-15027.

(121) Liu, Y.; Li, F.; Guo, Z.; Xiao, Y.; Zhang, Y.; Sun, X.; Zhe, T.; Cao, Y.; Wang, L.; Lu, Q. Silver nanoparticle-embedded hydrogel as a photothermal platform for combating bacterial infections. *Chemical Engineering Journal* **2020,** *382*, 122990.

(122) Zhang, J.; Feng, Y.; Mi, J.; Shen, Y.; Tu, Z.; Liu, L. Photothermal lysis of pathogenic bacteria by platinum nanodots decorated gold nanorods under near infrared irradiation. *Journal of Hazardous Materials* **2018,** *342*, 121-130.

(123) Yang, K.; Feng, L.; Shi, X.; Liu, Z. Nano-graphene in biomedicine: theranostic applications. *Chemical Society Reviews* **2013,** *42* (2), 530-547.

(124) Zhang, L.; Xia, J.; Zhao, Q.; Liu, L.; Zhang, Z. Functional graphene oxide as a nanocarrier for controlled loading and targeted delivery of mixed anticancer drugs. *small* **2010,** *6* (4), 537-544.

(125) Fan, X.; Yang, F.; Nie, C.; Yang, Y.; Ji, H.; He, C.; Cheng, C.; Zhao, C. Mussel-inspired synthesis of NIR-responsive and biocompatible Ag–graphene 2D nanoagents for versatile bacterial disinfections. *ACS applied materials & interfaces* **2018,** *10* (1), 296-307.

(126) Kurapati, R.; Vaidyanathan, M.; Raichur, A. M. Synergistic photothermal antimicrobial therapy using graphene oxide/polymer composite layer-by-layer thin films. *RSC Advances* **2016,** *6* (46), 39852-39860.

(127) Jia, X.; Ahmad, I.; Yang, R.; Wang, C. Versatile graphene-based photothermal nanocomposites for effectively capturing and killing bacteria, and for destroying bacterial biofilms. *Journal of Materials Chemistry B* **2017,** *5* (13), 2459-2467.

(128) Jiang, Q.; Ghim, D.; Cao, S.; Tadepalli, S.; Liu, K.-K.; Kwon, H.; Luan, J.; Min, Y.; Jun, Y.-S.; Singamaneni, S. Photothermally Active Reduced Graphene Oxide/Bacterial Nanocellulose Composites as Biofouling-Resistant Ultrafiltration Membranes. *Environmental Science & Technology* **2019,** *53* (1), 412-421.

(129) Feng, Y.; Chen, Q.; Yin, Q.; Pan, G.; Tu, Z.; Liu, L. Reduced graphene oxide functionalized with gold nanostar nanocomposites for synergistically killing bacteria through intrinsic antimicrobial activity and photothermal ablation. *ACS Applied Bio Materials* **2019,** *2* (2), 747-756.

(130) Jiang, N.; Wang, Y.; Chan, K. C.; Chan, C. Y.; Sun, H.; Li, G. Additive manufactured graphene coating with synergistic photothermal and superhydrophobic effects for bactericidal applications. *Global Challenges* **2020,** *4* (1), 1900054.

(131) Liang, Y.; Zhao, X.; Hu, T.; Han, Y.; Guo, B. Mussel-inspired, antibacterial, conductive, antioxidant, injectable composite hydrogel wound dressing to promote the regeneration of infected skin. *Journal of colloid and interface science* **2019,** *556*, 514-528.

(132) Soni, R.; Joshi, S. R.; Karmacharya, M.; Min, H.; Kim, S.-K.; Kumar, S.; Kim, G.-H.; Cho, Y.-K.; Lee, C. Y. Superhydrophobic and Self-Sterilizing Surgical Masks Spray-Coated with Carbon Nanotubes. *ACS Applied Nano Materials* **2021,** *4* (8), 8491-8499.

(133) Feng, L.; Zhu, C.; Yuan, H.; Liu, L.; Lv, F.; Wang, S. Conjugated polymer nanoparticles: preparation, properties, functionalization and biological applications. *Chemical Society Reviews* **2013,** *42* (16), 6620-6633.

(134) Xu, L.; Cheng, L.; Wang, C.; Peng, R.; Liu, Z. Conjugated polymers for photothermal therapy of cancer. *Polymer Chemistry* **2014,** *5* (5), 1573-1580.

(135) Huang, J.; Kaner, R. B. Flash welding of conducting polymer nanofibres. *Nature Materials* **2004,** *3* (11), 783-786.

(136) Gueye, M. N.; Carella, A.; Faure-Vincent, J.; Demadrille, R.; Simonato, J.-P. Progress in understanding structure and transport properties of PEDOT-based materials: A critical review. *Progress in Materials Science* **2020,** *108*, 100616.

(137) Zeng, X.; Luo, M.; Liu, G.; Wang, X.; Tao, W.; Lin, Y.; Ji, X.; Nie, L.; Mei, L. Polydopamine-modified black phosphorous nanocapsule with enhanced stability and photothermal performance for tumor multimodal treatments. *Advanced science* **2018,** *5* (10), 1800510.

(138) Yuan, Z.; Tao, B.; He, Y.; Mu, C.; Liu, G.; Zhang, J.; Liao, Q.; Liu, P.; Cai, K. Remote eradication of biofilm on titanium implant via near-infrared light triggered photothermal/photodynamic therapy strategy. *Biomaterials* **2019,** *223*, 119479.

(139) Liu, Y.; Ai, K.; Liu, J.; Deng, M.; He, Y.; Lu, L. Dopamine-melanin colloidal nanospheres: an efficient near-infrared photothermal therapeutic agent for in vivo cancer therapy. *Advanced materials* **2013,** *25* (9), 1353-1359.

(140) Yan, L. X.; Chen, L. J.; Zhao, X.; Yan, X. P. pH switchable nanoplatform for in vivo persistent luminescence imaging and precise photothermal therapy of bacterial infection. *Advanced Functional Materials* **2020,** *30* (14), 1909042.

(141) Kim, S. H.; Kang, E. B.; Jeong, C. J.; Sharker, S. M.; In, I.; Park, S. Y. Light controllable surface coating for effective photothermal killing of bacteria. *ACS applied materials & interfaces* **2015,** *7* (28), 15600-15606.

(142) Pan, Q.; Zhang, S.; Li, R.; He, Y.; Wang, Y. A low-cost and reusable photothermal membrane for solar-light induced anti-bacterial regulation. *Journal of Materials Chemistry B* **2019,** *7* (18), 2948-2953.

(143) Tondro, G.; Behzadpour, N.; Keykhaee, Z.; Akbari, N.; Sattarahmady, N. Carbon@ polypyrrole nanotubes as a photosensitizer in laser phototherapy of Pseudomonas aeruginosa. *Colloids and Surfaces B: Biointerfaces* **2019,** *180*, 481-486.

(144) Behzadpour, N.; Sattarahmady, N.; Akbari, N. Antimicrobial photothermal treatment of pseudomonas aeruginosa by a carbon nanoparticles-polypyrrole nanocomposite. *Journal of Biomedical Physics & Engineering* **2019,** *9* (6), 661.

(145) Jeong, C. J.; Sharker, S. M.; In, I.; Park, S. Y. Iron oxide@ PEDOT-based recyclable photothermal nanoparticles with poly (vinylpyrrolidone) sulfobetaines for rapid and effective antibacterial activity. *ACS Applied Materials & Interfaces* **2015,** *7* (18), 9469-9478.

(146) Ko, Y.; Kim, J.; Jeong, H. Y.; Kwon, G.; Kim, D.; Ku, M.; Yang, J.; Yamauchi, Y.; Kim, H.-Y.; Lee, C. Antibacterial poly (3, 4-ethylenedioxythiophene): poly (styrene-sulfonate)/agarose nanocomposite hydrogels with thermo-processability and self-healing. *Carbohydrate polymers* **2019,** *203*, 26-34.

(147) Lei, W.; Ren, K.; Chen, T.; Chen, X.; Li, B.; Chang, H.; Ji, J. Polydopamine nanocoating for effective photothermal killing of bacteria and fungus upon near-infrared irradiation. *Advanced Materials Interfaces* **2016,** *3* (22), 1600767.

(148) Ren, X.; Gao, R.; van der Mei, H. C.; Ren, Y.; Peterson, B. W.; Busscher, H. J. Eradicating infecting bacteria while maintaining tissue integration on photothermal nanoparticle-coated titanium surfaces. *ACS applied materials & interfaces* **2020,** *12* (31), 34610-34619.

(149) Yuce, S.; Demirel, O.; Alkan Tas, B.; Sungur, P.; Unal, H. Halloysite Nanotube/Polydopamine Nanohybrids as Clay-Based Photothermal Agents for Antibacterial Applications. *ACS Applied Nano Materials* **2021,** *4* (12), 13432-13439.

(150) Malhotra, B.; Keshwani, A.; Kharkwal, H. Antimicrobial food packaging: Potential and pitfalls. *Frontiers in microbiology* **2015,** *6*, 611.

(151) Robertson, G. L. *Food packaging: principles and practice*, CRC press: 2005.

(152) Sung, S.-Y.; Sin, L. T.; Tee, T.-T.; Bee, S.-T.; Rahmat, A.; Rahman, W.; Tan, A.-C.; Vikhraman, M. Antimicrobial agents for food packaging applications. *Trends in Food Science & Technology* **2013,** *33* (2), 110-123.

(153) Bai, Z.; Cristancho, D. E.; Rachford, A. A.; Reder, A. L.; Williamson, A.; Grzesiak, A. L. Controlled release of antimicrobial ClO2 gas from a two-layer polymeric film system. *Journal of agricultural and food chemistry* **2016,** *64* (45), 8647-8652.

(154) Gamage, G. R.; Park, H.-J.; Kim, K. M. Effectiveness of antimicrobial coated oriented polypropylene/polyethylene films in sprout packaging. *Food Research International* **2009,** *42* (7), 832-839.

(155) Lantano, C.; Alfieri, I.; Cavazza, A.; Corradini, C.; Lorenzi, A.; Zucchetto, N.; Montenero, A. Natamycin based sol–gel antimicrobial coatings on polylactic acid films for food packaging. *Food chemistry* **2014,** *165*, 342-347.

(156) Manso, S.; Becerril, R.; Nerín, C.; Gómez-Lus, R. Influence of pH and temperature variations on vapor phase action of an antifungal food packaging against five mold strains. *Food Control* **2015,** *47*, 20-26.

(157) Muriel-Galet, V.; Cerisuelo, J. P.; López-Carballo, G.; Lara, M.; Gavara, R.; Hernández-Muñoz, P. Development of antimicrobial films for microbiological control of packaged salad. *International Journal of Food Microbiology* **2012,** *157* (2), 195-201.

(158) Sundaram, J.; Pant, J.; Goudie, M. J.; Mani, S.; Handa, H. Antimicrobial and physicochemical characterization of biodegradable, nitric oxide-releasing nanocellulose–chitosan packaging membranes. *Journal of agricultural and food chemistry* **2016,** *64* (25), 5260-5266.

(159) Solano, A. C. V.; de Rojas Gante, C. Two different processes to obtain antimicrobial packaging containing natural oils. *Food and Bioprocess Technology* **2012,** *5* (6), 2522-2528.

(160) Guo, M.; Jin, T. Z.; Yang, R. Antimicrobial polylactic acid packaging films against Listeria and Salmonella in culture medium and on ready-to-eat meat. *Food and Bioprocess Technology* **2014,** *7* (11), 3293-3307.

(161) Theinsathid, P.; Visessanguan, W.; Kruenate, J.; Kingcha, Y.; Keeratipibul, S. Antimicrobial activity of lauric arginate-coated polylactic acid films against Listeria monocytogenes and Salmonella Typhimurium on cooked sliced ham. *Journal of food science* **2012,** *77* (2), M142-M149.

(162) Anthierens, T.; Billiet, L.; Devlieghere, F.; Du Prez, F. Poly (butylene adipate) functionalized with quaternary phosphonium groups as potential antimicrobial packaging material. *Innovative Food Science & Emerging Technologies* **2012,** *15*, 81-85.

(163) Muriel-Galet, V.; Talbert, J. N.; Hernandez-Munoz, P.; Gavara, R.; Goddard, J. Covalent immobilization of lysozyme on ethylene vinyl alcohol films for nonmigrating antimicrobial packaging applications. *Journal of Agricultural and Food Chemistry* **2013,** *61* (27), 6720-6727.

(164) Veluchamy, P.; Sivakumar, P. M.; Doble, M. Immobilization of subtilisin on polycaprolactam for antimicrobial food packaging applications. *Journal of agricultural and food chemistry* **2011,** *59* (20), 10869-10878.

(165) Decher, G.; Schlenoff, J. B. *Multilayer thin films: sequential assembly of nanocomposite materials*, John Wiley & Sons: 2006.

(166) Decher, G. Fuzzy nanoassemblies: toward layered polymeric multicomposites. *science* **1997,** *277* (5330), 1232-1237.

(167) Gezgin, Z.; Lee, T.-C.; Huang, Q. Engineering functional nanothin multilayers on food packaging: Ice-nucleating polyethylene films. *Journal of agricultural and food chemistry* **2013,** *61* (21), 5130-5138.

(168) Richardson, J. J.; Cui, J.; Bjornmalm, M.; Braunger, J. A.; Ejima, H.; Caruso, F. Innovation in layer-by-layer assembly. *Chemical Reviews* **2016,** *116* (23), 14828-14867.

(169) Xiao, F.-X.; Pagliaro, M.; Xu, Y.-J.; Liu, B. Layer-by-layer assembly of versatile nanoarchitectures with diverse dimensionality: a new perspective for rational construction of multilayer assemblies. *Chemical Society Reviews* **2016,** *45* (11), 3088-3121.

(170) Azlin-Hasim, S.; Cruz-Romero, M. C.; Cummins, E.; Kerry, J. P.; Morris, M. A. The potential use of a layer-by-layer strategy to develop LDPE antimicrobial films coated with silver nanoparticles for packaging applications. *Journal of colloid and interface science* **2016,** *461*, 239-248.

(171) Huang, W.; Xu, H.; Xue, Y.; Huang, R.; Deng, H.; Pan, S. Layer-by-layer immobilization of lysozyme–chitosan–organic rectorite composites on electrospun nanofibrous mats for pork preservation. *Food Research International* **2012,** *48* (2), 784-791.

(172) Joshi, A.; Abdullayev, E.; Vasiliev, A.; Volkova, O.; Lvov, Y. Interfacial modification of clay nanotubes for the sustained release of corrosion inhibitors. *Langmuir* **2013,** *29* (24), 7439-7448.

(173) Lvov, Y. M.; DeVilliers, M. M.; Fakhrullin, R. F. The application of halloysite tubule nanoclay in drug delivery. *Expert opinion on drug delivery* **2016,** *13* (7), 977-986.

(174) Owoseni, O.; Nyankson, E.; Zhang, Y.; Adams, S. J.; He, J.; McPherson, G. L.; Bose, A.; Gupta, R. B.; John, V. T. Release of surfactant cargo from interfacially-active halloysite clay nanotubes for oil spill remediation. *Langmuir* **2014,** *30* (45), 13533-13541.

(175) Vergaro, V.; Lvov, Y. M.; Leporatti, S. Halloysite clay nanotubes for resveratrol delivery to cancer cells. *Macromolecular bioscience* **2012,** *12* (9), 1265-1271.

(176) Hendessi, S.; Sevinis, E. B.; Unal, S.; Cebeci, F. C.; Menceloglu, Y. Z.; Unal, H. Antibacterial sustained-release coatings from halloysite nanotubes/waterborne polyurethanes. *Progress in Organic Coatings* **2016,** *101*, 253-261.

(177) Shemesh, R.; Krepker, M.; Nitzan, N.; Vaxman, A.; Segal, E. Active packaging containing encapsulated carvacrol for control of postharvest decay. *Postharvest Biology and Technology* **2016,** *118*, 175-182.

(178) Shemesh, R.; Krepker, M.; Natan, M.; Danin-Poleg, Y.; Banin, E.; Kashi, Y.; Nitzan, N.; Vaxman, A.; Segal, E. Novel LDPE/halloysite nanotube films with sustained carvacrol release for broad-spectrum antimicrobial activity. *RSC advances* **2015,** *5* (106), 87108-87117.

(179) Dierendonck, M.; De Koker, S.; De Rycke, R.; De Geest, B. G. Just spray it–LbL assembly enters a new age. *Soft Matter* **2014,** *10* (6), 804-807.

(180) Schlenoff, J. B.; Dubas, S. T.; Farhat, T. Sprayed polyelectrolyte multilayers. *Langmuir* **2000,** *16* (26), 9968-9969.

(181) Isonhood, J. H.; Drake, M. Aeromonas species in foods. *Journal of Food Protection* **2002,** *65* (3), 575-582.

(182) Lynch, M. J.; Swift, S.; Kirke, D. F.; Keevil, C. W.; Dodd, C. E.; Williams, P. The regulation of biofilm development by quorum sensing in Aeromonas hydrophila. *Environmental microbiology* **2002,** *4* (1), 18-28.

(183) Flemming, H.-C.; Wingender, J.; Szewzyk, U.; Steinberg, P.; Rice, S. A.; Kjelleberg, S. Biofilms: an emergent form of bacterial life. *Nature Reviews Microbiology* **2016,** *14* (9), 563.

(184) Moormeier, D. E.; Bayles, K. W. Staphylococcus aureus biofilm: a complex developmental organism. *Molecular microbiology* **2017,** *104* (3), 365-376.

(185) Abdallah, M.; Benoliel, C.; Drider, D.; Dhulster, P.; Chihib, N.-E. Biofilm formation and persistence on abiotic surfaces in the context of food and medical environments. *Archives of microbiology* **2014,** *196* (7), 453-472.

(186) Khatoon, Z.; McTiernan, C. D.; Suuronen, E. J.; Mah, T.-F.; Alarcon, E. I. Bacterial biofilm formation on implantable devices and approaches to its treatment and prevention. *Heliyon* **2018,** *4* (12), e01067.

(187) Ahmed, W.; Zhai, Z.; Gao, C. Adaptive antibacterial biomaterial surfaces and their applications. *Materials Today Bio* **2019,** *2*, 100017.

(188) Wei, T.; Yu, Q.; Chen, H. Responsive and Synergistic Antibacterial Coatings: Fighting against Bacteria in a Smart and Effective Way. *Advanced Healthcare Materials* **2019,** *8* (3), 1801381.

(189) Riool, M.; de Breij, A.; Drijfhout, J. W.; Nibbering, P. H.; Zaat, S. A. Antimicrobial peptides in biomedical device manufacturing. *Frontiers in chemistry* **2017,** *5*, 63.

(190) Yasir, M.; Dutta, D.; Hossain, K. R.; Chen, R.; Ho, K. K.; Kuppusamy, R.; Clarke, R. J.; Kumar, N.; Willcox, M. D. Mechanism of action of surface immobilized antimicrobial peptides against Pseudomonas aeruginosa. *Frontiers in microbiology* **2020,** *10*, 3053.

(191) Alkan-Tas, B.; Durmus-Sayar, A.; Duman, Z. E.; Sevinis-Ozbulut, E. B.; Unlu, A.; Binay, B.; Unal, S.; Unal, H. Antibacterial hybrid coatings from halloysite-immobilized lysostaphin and waterborne polyurethanes. *Progress in Organic Coatings* **2021,** *156*, 106248.

(192) Wang, J.; Qin, L.; Lin, J.; Zhu, J.; Zhang, Y.; Liu, J.; Van der Bruggen, B. Enzymatic construction of antibacterial ultrathin membranes for dyes removal. *Chemical Engineering Journal* **2017,** *323*, 56-63.

(193) Lee, D.; Seo, Y.; Khan, M. S.; Hwang, J.; Jo, Y.; Son, J.; Lee, K.; Park, C.; Chavan, S.; Gilad, A. A. Use of nanoscale materials for the effective prevention and extermination of bacterial biofilms. *Biotechnology and bioprocess engineering* **2018,** *23* (1), 1-10.

(194) Makvandi, P.; Jamaledin, R.; Jabbari, M.; Nikfarjam, N.; Borzacchiello, A. Antibacterial quaternary ammonium compounds in dental materials: A systematic review. *Dental Materials* **2018,** *34* (6), 851-867.

(195) Zhang, H.; Wang, G.; Liu, P.; Tong, D.; Ding, C.; Zhang, Z.; Xie, Y.; Tang, H.; Ji, F. Vancomycin-loaded titanium coatings with an interconnected micro-patterned structure for prophylaxis of infections: an in vivo study. *RSC advances* **2018,** *8* (17), 9223-9231.

(196) Zhang, X.; Song, G.; Qiao, H.; Lan, J.; Wang, B.; Yang, H.; Ma, L.; Wang, S.; Wang, Z.; Lin, H. Novel ternary vancomycin/strontium doped hydroxyapatite/graphene oxide bioactive composite coatings electrodeposited on titanium substrate for orthopedic applications. *Colloids and Surfaces A: Physicochemical and Engineering Aspects* **2020,** *603*, 125223.

(197) Hernando-Amado, S.; Coque, T. M.; Baquero, F.; Martínez, J. L. Defining and combating antibiotic resistance from One Health and Global Health perspectives. *Nat Microbiol* **2019,** *4* (9), 1432-1442.

(198) Gellci, K.; Mehrmohammadi, M. Photothermal Therapy. In *Encyclopedia of Cancer*; Schwab, M., Ed.; Springer Berlin Heidelberg: Berlin, Heidelberg, 2014; pp 1-5.

(199) Kim, J. U.; Lee, S.; Kang, S. J.; Kim, T.-i. Materials and design of nanostructured broadband light absorbers for advanced light-to-heat conversion. *Nanoscale* **2018,** *10* (46), 21555-21574.

(200) Jiang, T.; He, J.; Sun, L.; Wang, Y.; Li, Z.; Wang, Q.; Sun, Y.; Wang, W.; Yu, M. Highly efficient photothermal sterilization of water mediated by Prussian blue nanocages. *Environmental Science: Nano* **2018,** *5* (5), 1161-1168.

(201) Ren, Y.; Liu, H.; Liu, X.; Zheng, Y.; Li, Z.; Li, C.; Yeung, K. W. K.; Zhu, S.; Liang, Y.; Cui, Z. Photoresponsive materials for antibacterial applications. *Cell Reports Physical Science* **2020**, 100245.

(202) Zhong, H.; Zhu, Z.; Lin, J.; Cheung, C. F.; Lu, V. L.; Yan, F.; Chan, C.-Y.; Li, G. Reusable and recyclable graphene masks with outstanding superhydrophobic and photothermal performances. *ACS nano* **2020,** *14* (5), 6213-6221.

(203) De Sio, L.; Ding, B.; Focsan, M.; Kogermann, K.; Pascoal-Faria, P.; Petronela, F.; Mitchell, G.; Zussman, E.; Pierini, F. Personalized Reusable Face Masks with Smart Nano-Assisted Destruction of Pathogens for COVID-19: A Visionary Road. *Chemistry–A European Journal* **2021,** *27* (20), 6112-6130.

(204) Jin, C.; Su, K.; Tan, L.; Liu, X.; Cui, Z.; Yang, X.; Li, Z.; Liang, Y.; Zhu, S.; Yeung, K. W. K.; Wu, S. Near-infrared light photocatalysis and photothermy of carbon quantum dots and au nanoparticles loaded titania nanotube array. *Materials & Design* **2019,** *177*, 107845.

(205) Qu, Y.; Wei, T.; Zhao, J.; Jiang, S.; Yang, P.; Yu, Q.; Chen, H. Regenerable smart antibacterial surfaces: full removal of killed bacteria via a sequential degradable layer. *Journal of Materials Chemistry B* **2018,** *6* (23), 3946-3955.

(206) Liu, Y.; Li, F.; Guo, Z.; Xiao, Y.; Zhang, Y.; Sun, X.; Zhe, T.; Cao, Y.; Wang, L.; Lu, Q.; Wang, J. Silver nanoparticle-embedded hydrogel as a photothermal platform for combating bacterial infections. *Chemical Engineering Journal* **2020,** *382*, 122990.

(207) Kim, J. T.; Kim, B. K.; Kim, E. Y.; Kwon, S. H.; Jeong, H. M. Synthesis and properties of near IR induced self-healable polyurethane/graphene nanocomposites. *European polymer journal* **2013,** *49* (12), 3889-3896.

(208) Li, M.; Li, L.; Su, K.; Liu, X.; Zhang, T.; Liang, Y.; Jing, D.; Yang, X.; Zheng, D.; Cui, Z.; Li, Z.; Zhu, S.; Yeung, K. W. K.; Zheng, Y.; Wang, X.; Wu, S. Highly Effective and Noninvasive Near-Infrared Eradication of a Staphylococcus aureus Biofilm on Implants by a Photoresponsive Coating within 20 Min. *Advanced Science* **2019,** *6* (17), 1900599.

(209) Wang, X.; Su, K.; Tan, L.; Liu, X.; Cui, Z.; Jing, D.; Yang, X.; Liang, Y.; Li, Z.; Zhu, S.; Yeung, K. W. K.; Zheng, D.; Wu, S. Rapid and Highly Effective Noninvasive Disinfection by Hybrid Ag/CS@MnO2 Nanosheets Using Near-Infrared Light. *ACS Applied Materials & Interfaces* **2019,** *11* (16), 15014-15027.

(210) Bilici, K.; Atac, N.; Muti, A.; Baylam, I.; Dogan, O.; Sennaroglu, A.; Can, F.; Acar, H. Y. Broad spectrum antibacterial photodynamic and photothermal therapy achieved with indocyanine green loaded SPIONs under near infrared irradiation. *Biomaterials science* **2020,** *8* (16), 4616-4625.

(211) Maaoui, H.; Jijie, R.; Pan, G.-H.; Drider, D.; Caly, D.; Bouckaert, J.; Dumitrascu, N.; Chtourou, R.; Szunerits, S.; Boukherroub, R. A 980 nm driven photothermal ablation of virulent and antibiotic resistant Gram-positive and Gram-negative bacteria strains using Prussian blue nanoparticles. *Journal of colloid and interface science* **2016,** *480*, 63-68.

(212) Shvedova, A. A.; Kagan, V. E.; Fadeel, B. Close encounters of the small kind: adverse effects of man-made materials interfacing with the nano-cosmos of biological systems. *Annu Rev Pharmacol Toxicol* **2010,** *50*, 63-88.

(213) Lai, D. Y. Approach to using mechanism-based structure activity relationship (SAR) analysis to assess human health hazard potential of nanomaterials. *Food Chem Toxicol* **2015,** *85*, 120-6.

(214) Qi, J.; Fang, Y.; Kwok, R. T. K.; Zhang, X.; Hu, X.; Lam, J. W. Y.; Ding, D.; Tang, B. Z. Highly Stable Organic Small Molecular Nanoparticles as an Advanced and Biocompatible Phototheranostic Agent of Tumor in Living Mice. *ACS Nano* **2017,** *11* (7), 7177-7188.

(215) Cheng, L.; Wang, C.; Feng, L.; Yang, K.; Liu, Z. Functional Nanomaterials for Phototherapies of Cancer. *Chemical Reviews* **2014,** *114* (21), 10869-10939.

(216) d'Ischia, M.; Napolitano, A.; Ball, V.; Chen, C.-T.; Buehler, M. J. Polydopamine and eumelanin: From structure–property relationships to a unified tailoring strategy. *Accounts of chemical research* **2014,** *47* (12), 3541-3550.

(217) Qiu, W.-Z.; Yang, H.-C.; Xu, Z.-K. Dopamine-assisted co-deposition: an emerging and promising strategy for surface modification. *Advances in colloid and interface science* **2018,** *256*, 111-125.

(218) Lee, H.; Dellatore, S. M.; Miller, W. M.; Messersmith, P. B. Mussel-Inspired Surface Chemistry for Multifunctional Coatings. *Science* **2007,** *318* (5849), 426-430.

(219) Ball, V.; Del Frari, D.; Michel, M.; Buehler, M. J.; Toniazzo, V.; Singh, M. K.; Gracio, J.; Ruch, D. Deposition mechanism and properties of thin polydopamine films for high added value applications in surface science at the nanoscale. *BioNanoScience* **2012,** *2* (1), 16-34.

(220) Liu, Y.; Ai, K.; Lu, L. Polydopamine and Its Derivative Materials: Synthesis and Promising Applications in Energy, Environmental, and Biomedical Fields. *Chemical Reviews* **2014,** *114* (9), 5057-5115.

(221) Mazrad, Z. A. I.; Choi, C. A.; Kwon, Y. M.; In, I.; Lee, K. D.; Park, S. Y. Design of Surface-Coatable NIR-Responsive Fluorescent Nanoparticles with PEI Passivation for Bacterial Detection and Killing. *ACS Applied Materials & Interfaces* **2017,** *9* (38), 33317-33326.

(222) Fan, X.-L.; Li, H.-Y.; Ye, W.-Y.; Zhao, M.-Q.; Huang, D.-n.; Fang, Y.; Zhou, B.-Q.; Ren, K.-F.; Ji, J.; Fu, G.-S. Magainin-modified polydopamine nanoparticles for photothermal killing of bacteria at low temperature. *Colloids and Surfaces B: Biointerfaces* **2019,** *183*, 110423.

(223) Hu, D.; Zou, L.; Li, B.; Hu, M.; Ye, W.; Ji, J. Photothermal Killing of Methicillin-Resistant Staphylococcus aureus by Bacteria-Targeted Polydopamine Nanoparticles with Nano-Localized Hyperpyrexia. *ACS Biomaterials Science & Engineering* **2019,** *5* (10), 5169-5179.

(224) Gao, G.; Jiang, Y.-W.; Jia, H.-R.; Wu, F.-G. Near-infrared light-controllable on-demand antibiotics release using thermo-sensitive hydrogel-based drug reservoir for combating bacterial infection. *Biomaterials* **2019,** *188*, 83-95.

(225) Liang, Y.; Zhao, X.; Hu, T.; Chen, B.; Yin, Z.; Ma, P. X.; Guo, B. Adhesive hemostatic conducting injectable composite hydrogels with sustained drug release and photothermal antibacterial activity to promote full-thickness skin regeneration during wound healing. *Small* **2019,** *15* (12), 1900046.

(226) Tao, B.; Lin, C.; Yuan, Z.; He, Y.; Chen, M.; Li, K.; Hu, J.; Yang, Y.; Xia, Z.; Cai, K. Near infrared light-triggered on-demand Cur release from Gel-PDA@Cur composite hydrogel for antibacterial wound healing. *Chemical Engineering Journal* **2021,** *403*, 126182.

(227) Xi, Y.; Ge, J.; Wang, M.; Chen, M.; Niu, W.; Cheng, W.; Xue, Y.; Lin, C.; Lei, B. Bioactive anti-inflammatory, antibacterial, antioxidative silicon-based nanofibrous dressing

enables cutaneous tumor photothermo-chemo therapy and infection-induced wound healing. *ACS nano* **2020,** *14* (3), 2904-2916.

(228) Yuan, Z.; Tao, B.; He, Y.; Liu, J.; Lin, C.; Shen, X.; Ding, Y.; Yu, Y.; Mu, C.; Liu, P. Biocompatible MoS2/PDA-RGD coating on titanium implant with antibacterial property via intrinsic ROS-independent oxidative stress and NIR irradiation. *Biomaterials* **2019,** *217*, 119290.

(229) Tas, C. E.; Berksun, E.; Koken, D.; Unal, S.; Unal, H. Photothermal Waterborne Polydopamine/Polyurethanes with Light-to-Heat Conversion Properties. *ACS Applied Polymer Materials* **2021**.

(230) Anıl, D.; Berksun, E.; Durmuş-Sayar, A.; Sevinis¸-Özbulut, E. B.; Ünal, S. Chapter 11 - Recent advances in waterborne polyurethanes and their nanoparticle-containing dispersions. In *Handbook of Waterborne Coatings*; Zarras, P.; Soucek, M. D.; Tiwari, A., Eds.; Elsevier: 2020; pp 249-302.

(231) Lee, H. A.; Park, E.; Lee, H. Polydopamine and its derivative surface chemistry in material science: a focused review for studies at KAIST. *Advanced Materials* **2020,** *32* (35), 1907505.

(232) Wang, Y.; Li, S.; Liu, L.; Feng, L. Photothermal-Responsive Conjugated Polymer Nanoparticles for the Rapid and Effective Killing of Bacteria. *ACS Applied Bio Materials* **2018,** *1* (1), 27-32.

(233) Wu, D.; Qu, D.; Jiang, W.; Chen, G.; An, L.; Zhuang, C.; Sun, Z. Self-floating nanostructured Ni–NiO x/Ni foam for solar thermal water evaporation. *Journal of Materials Chemistry A* **2019,** *7* (14), 8485-8490.

(234) Xu, Y.; Wang, X.; Zhou, J.; Song, B.; Jiang, Z.; Lee, E. M.; Huberman, S.; Gleason, K. K.; Chen, G. Molecular engineered conjugated polymer with high thermal conductivity. *Science advances* **2018,** *4* (3), eaar3031.

(235) Leuenberger, P.; Ganscha, S.; Kahraman, A.; Cappelletti, V.; Boersema, P. J.; von Mering, C.; Claassen, M.; Picotti, P. Cell-wide analysis of protein thermal unfolding reveals determinants of thermostability. *Science* **2017,** *355* (6327).

(236) Dill, K. A.; Ghosh, K.; Schmit, J. D. Physical limits of cells and proteomes. *Proceedings of the National Academy of Sciences* **2011,** *108* (44), 17876-17882.

(237) Zhao, Y.-Q.; Sun, Y.; Zhang, Y.; Ding, X.; Zhao, N.; Yu, B.; Zhao, H.; Duan, S.; Xu, F.-J. Well-defined gold nanorod/polymer hybrid coating with inherent antifouling and photothermal bactericidal properties for treating an infected hernia. *ACS nano* **2020,** *14* (2), 2265-2275.

(238) Zhang, G.; Wu, Z.; Yang, Y.; Shi, J.; Lv, J.; Fang, Y.; Shen, Z.; Lv, Z.; Li, P.; Yao, X. A multifunctional antibacterial coating on bone implants for osteosarcoma therapy and enhanced osteointegration. *Chemical Engineering Journal* **2022,** *428*, 131155.

(239) He, X.; Sathishkumar, G.; Gopinath, K.; Zhang, K.; Lu, Z.; Li, C.; Kang, E.-T.; Xu, L. One-step self-assembly of biogenic Au NPs/PEG-based universal coatings for antifouling and photothermal killing of bacterial pathogens. *Chemical Engineering Journal* **2021,** *421*, 130005.

(240) Swartjes, J. J.; Sharma, P. K.; Kooten, T.; van der Mei, H. C.; Mahmoudi, M.; Busscher, H. J.; Rochford, E. T. Current developments in antimicrobial surface coatings for biomedical applications. *Current Medicinal Chemistry* **2015,** *22* (18), 2116-2129.

(241) Samantaray, P. K.; Madras, G.; Bose, S. The key role of modifications in biointerfaces toward rendering antibacterial and antifouling properties in polymeric membranes for water remediation: A critical assessment. *Advanced Sustainable Systems* **2019,** *3* (10), 1900017.

(242) Ahonen, M.; Kahru, A.; Ivask, A.; Kasemets, K.; Kõljalg, S.; Mantecca, P.; Vinković Vrček, I.; Keinänen-Toivola, M. M.; Crijns, F. Proactive approach for safe use of antimicrobial coatings in healthcare settings: opinion of the COST action network AMiCI. *International journal of environmental research and public health* **2017,** *14* (4), 366.

(243) Adlhart, C.; Verran, J.; Azevedo, N. F.; Olmez, H.; Keinänen-Toivola, M. M.; Gouveia, I.; Melo, L. F.; Crijns, F. Surface modifications for antimicrobial effects in the healthcare setting: A critical overview. *Journal of Hospital Infection* **2018,** *99* (3), 239-249.

(244) Alvarez-Ordóñez, A.; Coughlan, L. M.; Briandet, R.; Cotter, P. D. Biofilms in food processing environments: challenges and opportunities. *Annual review of food science and technology* **2019,** *10*, 173-195.

(245) Wei, T.; Qu, Y.; Zou, Y.; Zhang, Y.; Yu, Q. Exploration of smart antibacterial coatings for practical applications. *Current Opinion in Chemical Engineering* **2021,** *34*, 100727.

(246) Hu, D.; Li, H.; Wang, B.; Ye, Z.; Lei, W.; Jia, F.; Jin, Q.; Ren, K.-F.; Ji, J. Surface-adaptive gold nanoparticles with effective adherence and enhanced photothermal ablation of methicillin-resistant Staphylococcus aureus biofilm. *ACS nano* **2017,** *11* (9), 9330-9339.

(247) Merkl, P.; Zhou, S.; Zaganiaris, A.; Shahata, M.; Eleftheraki, A.; Thersleff, T.; Sotiriou, G. A. Plasmonic Coupling in Silver Nanoparticle Aggregates and Their Polymer Composite Films for Near-Infrared Photothermal Biofilm Eradication. *ACS applied nano materials* **2021,** *4* (5), 5330-5339.

(248) de Kraker, M. E.; Wolkewitz, M.; Davey, P. G.; Koller, W.; Berger, J.; Nagler, J.; Icket, C.; Kalenic, S.; Horvatic, J.; Seifert, H.; Kaasch, A. J.; Paniara, O.; Argyropoulou, A.; Bompola, M.; Smyth, E.; Skally, M.; Raglio, A.; Dumpis, U.; Kelmere, A. M.; Borg, M.; Xuereb, D.; Ghita, M. C.; Noble, M.; Kolman, J.; Grabljevec, S.; Turner, D.; Lansbury, L.; Grundmann, H. Clinical impact of antimicrobial resistance in European hospitals: excess mortality and length of hospital stay related to methicillin-resistant Staphylococcus aureus bloodstream infections. *Antimicrobial agents and chemotherapy* **2011,** *55* (4), 1598-605.

(249) Liu, T.; Zhang, Y.; Wan, Q. Methicillin-resistant Staphylococcus aureus bacteremia among liver transplant recipients: epidemiology and associated risk factors for morbidity and mortality. *Infection and drug resistance* **2018,** *11*, 647-658.

(250) Bassetti, M.; Peghin, M.; Trecarichi, E. M.; Carnelutti, A.; Righi, E.; Del Giacomo, P.; Ansaldi, F.; Trucchi, C.; Alicino, C.; Cauda, R.; Sartor, A.; Spanu, T.; Scarparo, C.; Tumbarello, M. Characteristics of Staphylococcus aureus Bacteraemia and Predictors of Early and Late Mortality. *PloS one* **2017,** *12* (2), e0170236.

(251) Yilmaz, M.; Elaldi, N.; Balkan, II; Arslan, F.; Batirel, A. A.; Bakici, M. Z.; Gozel, M. G.; Alkan, S.; Celik, A. D.; Yetkin, M. A.; Bodur, H.; Sinirtas, M.; Akalin, H.; Altay, F. A.; Sencan, I.; Azak, E.; Gundes, S.; Ceylan, B.; Ozturk, R.; Leblebicioglu, H.; Vahaboglu, H.;

Mert, A. Mortality predictors of Staphylococcus aureus bacteremia: a prospective multicenter study. *Annals of clinical microbiology and antimicrobials* **2016,** *15*, 7.

(252) Zimlichman, E.; Henderson, D.; Tamir, O.; Franz, C.; Song, P.; Yamin, C. K.; Keohane, C.; Denham, C. R.; Bates, D. W. Health care-associated infections: a meta-analysis of costs and financial impact on the US health care system. *JAMA internal medicine* **2013,** *173* (22), 2039-46.

(253) Gould, I. M.; Reilly, J.; Bunyan, D.; Walker, A. Costs of healthcare-associated methicillin-resistant Staphylococcus aureus and its control. *Clinical microbiology and infection : the official publication of the European Society of Clinical Microbiology and Infectious Diseases* **2010,** *16* (12), 1721-8.

(254) Donlan, R. M.; Costerton, J. W. Biofilms: survival mechanisms of clinically relevant microorganisms. *Clinical microbiology reviews* **2002,** *15* (2), 167-93.

(255) Cloutier, M.; Mantovani, D.; Rosei, F. Antibacterial Coatings: Challenges, Perspectives, and Opportunities. *Trends in Biotechnology* **2015,** *33* (11), 637-652.

(256) Kaur, R.; Liu, S. Antibacterial surface design–Contact kill. *Progress in Surface Science* **2016,** *91* (3), 136-153.

(257) Gao, J.; Huddleston, N. E.; White, E. M.; Pant, J.; Handa, H.; Locklin, J. Surface Grafted Antimicrobial Polymer Networks with High Abrasion Resistance. *ACS Biomaterials Science & Engineering* **2016,** *2* (7), 1169-1179.

(258) Zanini, S.; Polissi, A.; Maccagni, E. A.; Dell'Orto, E. C.; Liberatore, C.; Riccardi, C. Development of antibacterial quaternary ammonium silane coatings on polyurethane catheters. *J Colloid Interface Sci* **2015,** *451*, 78-84.

(259) Li, H.; Bao, H.; Bok, K. X.; Lee, C. Y.; Li, B.; Zin, M. T.; Kang, L. High durability and low toxicity antimicrobial coatings fabricated by quaternary ammonium silane copolymers. *Biomaterials science* **2016,** *4* (2), 299-309.

(260) Hoque, J.; Akkapeddi, P.; Ghosh, C.; Uppu, D. S. S. M.; Haldar, J. A Biodegradable Polycationic Paint that Kills Bacteria in Vitro and in Vivo. *ACS Applied Materials & Interfaces* **2016,** *8* (43), 29298-29309.

(261) Chai, D.; Liu, W.; Hao, X.; Wang, H.; Wang, H.; Hao, Y.; Gao, Y.; Qu, H.; Wang, L.; Dong, A.; Gao, G. Mussel-inspired synthesis of magnetic N-Halamine nanoparticles for antibacterial recycling. *Colloid and Interface Science Communications* **2020,** *39*, 100320.

(262) Hui, F.; Debiemme-Chouvy, C. Antimicrobial N-Halamine Polymers and Coatings: A Review of Their Synthesis, Characterization, and Applications. *Biomacromolecules* **2013,** *14* (3), 585-601.

(263) Townsend, L.; Williams, R. L.; Anuforom, O.; Berwick, M. R.; Halstead, F.; Hughes, E.; Stamboulis, A.; Oppenheim, B.; Gough, J.; Grover, L.; Scott, R. A.; Webber, M.; Peacock, A. F.; Belli, A.; Logan, A.; de Cogan, F. Antimicrobial peptide coatings for hydroxyapatite: electrostatic and covalent attachment of antimicrobial peptides to surfaces. *Journal of the Royal Society, Interface* **2017,** *14* (126).

(264) Yu, K.; Lo, J. C.; Yan, M.; Yang, X.; Brooks, D. E.; Hancock, R. E.; Lange, D.; Kizhakkedathu, J. N. Anti-adhesive antimicrobial peptide coating prevents catheter associated infection in a mouse urinary infection model. *Biomaterials* **2017,** *116*, 69-81.

(265) Yazici, H.; O'Neill, M. B.; Kacar, T.; Wilson, B. R.; Oren, E. E.; Sarikaya, M.; Tamerler, C. Engineered Chimeric Peptides as Antimicrobial Surface Coating Agents toward Infection-Free Implants. *ACS Applied Materials & Interfaces* **2016,** *8* (8), 5070-5081.

(266) Melo, L. D. R.; Veiga, P.; Cerca, N.; Kropinski, A. M.; Almeida, C.; Azeredo, J.; Sillankorva, S. Development of a Phage Cocktail to Control Proteus mirabilis Catheter-associated Urinary Tract Infections. *Frontiers in microbiology* **2016,** *7*, 1024-1024.

(267) Hosseinidoust, Z.; Olsson, A. L. J.; Tufenkji, N. Going viral: Designing bioactive surfaces with bacteriophage. *Colloids and Surfaces B: Biointerfaces* **2014,** *124*, 2-16.

(268) Hosseinidoust, Z.; Van de Ven, T. G.; Tufenkji, N. Bacterial capture efficiency and antimicrobial activity of phage-functionalized model surfaces. *Langmuir* **2011,** *27* (9), 5472-80.

(269) Bayazidi, P.; Almasi, H.; Asl, A. K. Immobilization of lysozyme on bacterial cellulose nanofibers: Characteristics, antimicrobial activity and morphological properties. *International Journal of Biological Macromolecules* **2018,** *107*, 2544-2551.

(270) Lopes, N. A.; Barreto Pinilla, C. M.; Brandelli, A. Antimicrobial activity of lysozyme-nisin co-encapsulated in liposomes coated with polysaccharides. *Food Hydrocolloids* **2019,** *93*, 1-9.

(271) Drozdov, A. S.; Shapovalova, O. E.; Ivanovski, V.; Avnir, D.; Vinogradov, V. V. Entrapment of Enzymes within Sol–Gel-Derived Magnetite. *Chemistry of Materials* **2016,** *28* (7), 2248-2253.

(272) Regina, V. R.; Søhoel, H.; Lokanathan, A. R.; Bischoff, C.; Kingshott, P.; Revsbech, N. P.; Meyer, R. L. Entrapment of Subtilisin in Ceramic Sol–Gel Coating for Antifouling Applications. *ACS Applied Materials & Interfaces* **2012,** *4* (11), 5915-5921.

(273) Liu, Y.; Vincent Edwards, J.; Prevost, N.; Huang, Y.; Chen, J. Y. Physico- and bio-activities of nanoscale regenerated cellulose nonwoven immobilized with lysozyme. *Materials Science and Engineering: C* **2018,** *91*, 389-394.

(274) Yuan, S.; Wan, D.; Liang, B.; Pehkonen, S. O.; Ting, Y. P.; Neoh, K. G.; Kang, E. T. Lysozyme-Coupled Poly(poly(ethylene glycol) methacrylate)−Stainless Steel Hybrids and Their Antifouling and Antibacterial Surfaces. *Langmuir* **2011,** *27* (6), 2761-2774.

(275) Tegl, G.; Thallinger, B.; Beer, B.; Sygmund, C.; Ludwig, R.; Rollett, A.; Nyanhongo, G. S.; Guebitz, G. M. Antimicrobial Cellobiose Dehydrogenase-Chitosan Particles. *ACS Applied Materials & Interfaces* **2016,** *8* (1), 967-973.

(276) Tavakolian, M.; Okshevsky, M.; van de Ven, T. G. M.; Tufenkji, N. Developing Antibacterial Nanocrystalline Cellulose Using Natural Antibacterial Agents. *ACS Applied Materials & Interfaces* **2018,** *10* (40), 33827-33838.

(277) Mohamad, N. R.; Marzuki, N. H. C.; Buang, N. A.; Huyop, F.; Wahab, R. A. An overview of technologies for immobilization of enzymes and surface analysis techniques for immobilized enzymes. *Biotechnology & Biotechnological Equipment* **2015,** *29* (2), 205-220.

(278) Kumar, J. K. Lysostaphin: an antistaphylococcal agent. *Applied Microbiology and Biotechnology* **2008,** *80* (4), 555-561.

(279) Francius, G.; Domenech, O.; Mingeot-Leclercq, M. P.; Dufrêne, Y. F. Direct observation of Staphylococcus aureus cell wall digestion by lysostaphin. *Journal of bacteriology* **2008,** *190* (24), 7904-7909.

(280) Kokai-Kun, J. F.; Chanturiya, T.; Mond, J. J. Lysostaphin eradicates established Staphylococcus aureus biofilms in jugular vein catheterized mice. *The Journal of antimicrobial chemotherapy* **2009,** *64* (1), 94-100.

(281) Johnson, C. T.; Wroe, J. A.; Agarwal, R.; Martin, K. E.; Guldberg, R. E.; Donlan, R. M.; Westblade, L. F.; García, A. J. Hydrogel delivery of lysostaphin eliminates orthopedic implant infection by Staphylococcus aureus and supports fracture healing. *Proceedings of the National Academy of Sciences* **2018,** *115* (22), E4960-E4969.

(282) Belyansky, I.; Tsirline, V. B.; Martin, T. R.; Klima, D. A.; Heath, J.; Lincourt, A. E.; Satishkumar, R.; Vertegel, A.; Heniford, B. T. The Addition of Lysostaphin Dramatically Improves Survival, Protects Porcine Biomesh from Infection, and Improves Graft Tensile Shear Strength. *Journal of Surgical Research* **2011,** *171* (2), 409-415.

(283) Satishkumar, R.; Vertegel, A. A. Antibody-directed targeting of lysostaphin adsorbed onto polylactide nanoparticles increases its antimicrobial activity againstS. aureusin vitro. *Nanotechnology* **2011,** *22* (50), 505103.

(284) Satishkumar, R.; Sankar, S.; Yurko, Y.; Lincourt, A.; Shipp, J.; Heniford, B. T.; Vertegel, A. Evaluation of the Antimicrobial Activity of Lysostaphin-Coated Hernia Repair Meshes. *Antimicrobial agents and chemotherapy* **2011,** *55* (9), 4379-4385.

(285) Shah, A.; Mond, J.; Walsh, S. Lysostaphin-coated catheters eradicate Staphylococccus aureus challenge and block surface colonization. *Antimicrobial agents and chemotherapy* **2004,** *48* (7), 2704-2707.

(286) Duman, Z. E.; Ünlü, A.; Çakar, M. M.; Ünal, H.; Binay, B. Enhanced production of recombinant Staphylococcus simulans lysostaphin using medium engineering. *Preparative Biochemistry and Biotechnology* **2019,** *49* (5), 521-528.

(287) Bradford, M. M. A rapid and sensitive method for the quantitation of microgram quantities of protein utilizing the principle of protein-dye binding. *Analytical Biochemistry* **1976,** *72* (1), 248-254.

(288) *ISO 22196 : Plastics - Measurement of antibacterial activity on plastics surfaces* **2007**.

(289) Chao, C.; Liu, J.; Wang, J.; Zhang, Y.; Zhang, B.; Zhang, Y.; Xiang, X.; Chen, R. Surface modification of halloysite nanotubes with dopamine for enzyme immobilization. *ACS applied materials & interfaces* **2013,** *5* (21), 10559-10564.

(290) Kang, H.; Liu, X.; Zhang, S.; Li, J. Functionalization of halloysite nanotubes (HNTs) via mussel-inspired surface modification and silane grafting for HNTs/soy protein isolate nanocomposite film preparation. *Rsc Advances* **2017,** *7* (39), 24140-24148.

(291) He, S.; Dai, W.; Yang, W.; Liu, S.; Bian, X.; Zhang, C.; Lin, J. Nanocomposite proton exchange membranes based on phosphotungstic acid immobilized by polydopamine-coated halloysite nanotubes. *Polymer Testing* **2019,** *73*, 242-249.

(292) Hong, M.-S.; Park, Y.; Kim, T.; Kim, K.; Kim, J.-G. Polydopamine/carbon nanotube nanocomposite coating for corrosion resistance. *Journal of Materiomics* **2020,** *6* (1), 158-166.

(293) Lee, H.; Rho, J.; Messersmith, P. B. Facile Conjugation of Biomolecules onto Surfaces via Mussel Adhesive Protein Inspired Coatings. *Advanced Materials* **2009,** *21* (4), 431-434.

(294) Barth, A. Infrared spectroscopy of proteins. *Biochimica et Biophysica Acta (BBA) - Bioenergetics* **2007,** *1767* (9), 1073-1101.

(295) Talbert, J. N.; Goddard, J. M. Enzymes on material surfaces. *Colloids and Surfaces B: Biointerfaces* **2012,** *93*, 8-19.

(296) Liu, Y.; Ogorzalek, T. L.; Yang, P.; Schroeder, M. M.; Marsh, E. N. G.; Chen, Z. Molecular Orientation of Enzymes Attached to Surfaces through Defined Chemical Linkages at the Solid–Liquid Interface. *Journal of the American Chemical Society* **2013,** *135* (34), 12660-12669.

(297) Liu, Y.; Zeng, Z.; Zeng, G.; Tang, L.; Pang, Y.; Li, Z.; Liu, C.; Lei, X.; Wu, M.; Ren, P.; Liu, Z.; Chen, M.; Xie, G. Immobilization of laccase on magnetic bimodal mesoporous carbon and the application in the removal of phenolic compounds. *Bioresource Technology* **2012,** *115*, 21-26.

(298) George, R.; Sugunan, S. Kinetics of adsorption of lipase onto different mesoporous materials: Evaluation of Avrami model and leaching studies. *Journal of Molecular Catalysis B: Enzymatic* **2014,** *105*, 26-32.

(299) Dang, H.; Lovell, C. R. Microbial Surface Colonization and Biofilm Development in Marine Environments. *Microbiology and Molecular Biology Reviews* **2016,** *80* (1), 91-138.

(300) Galie, S.; García-Gutiérrez, C.; Miguélez, E. M.; Villar, C. J.; Lombó, F. Biofilms in the food industry: health aspects and control methods. *Frontiers in microbiology* **2018,** *9*, 898.

(301) Percival, S. L.; Suleman, L.; Vuotto, C.; Donelli, G. Healthcare-associated infections, medical devices and biofilms: risk, tolerance and control. *Journal of Medical Microbiology* **2015,** *64* (4), 323-334.

(302) Ledwoch, K.; Dancer, S. J.; Otter, J. A.; Kerr, K.; Roposte, D.; Rushton, L.; Weiser, R.; Mahenthiralingam, E.; Muir, D. D.; Maillard, J. Y. Beware biofilm! Dry biofilms containing bacterial pathogens on multiple healthcare surfaces; a multi-centre study. *Journal of Hospital Infection* **2018,** *100* (3), e47-e56.

(303) Kavanagh, R. K.; Mitra, A.; Basu, P. Biofilms in Healthcare. In *Practical Handbook of Microbiology*; CRC Press: 2021; pp 873-878.

(304) Achinas, S.; Charalampogiannis, N.; Euverink, G. J. W. A brief recap of microbial adhesion and biofilms. *Applied Sciences* **2019,** *9* (14), 2801.

(305) Maayan, M.; Mani, K. A.; Yaakov, N.; Natan, M.; Jacobi, G.; Atkins, A.; Zelinger, E.; Fallik, E.; Banin, E.; Mechrez, G. Fluorine-Free Superhydrophobic Coating with Antibiofilm Properties Based on Pickering Emulsion Templating. *ACS Applied Materials & Interfaces* **2021,** *13* (31), 37693-37703.

(306) Woo, J.; Seo, H.; Na, Y.; Choi, S.; Kim, S.; Choi, W. I.; Park, M. H.; Sung, D. Facile synthesis and coating of aqueous antifouling polymers for inhibiting pathogenic bacterial adhesion on medical devices. *Progress in Organic Coatings* **2020**, *147*, 105772.

(307) Su, Y.; Feng, T.; Feng, W.; Pei, Y.; Li, Z.; Huo, J.; Xie, C.; Qu, X.; Li, P.; Huang, W. Mussel-Inspired, Surface-Attachable Initiator for Grafting of Antimicrobial and Antifouling Hydrogels. *Macromolecular rapid communications* **2019**, *40* (17), 1900268.

(308) Guo, L. L.; Cheng, Y. F.; Ren, X.; Gopinath, K.; Lu, Z. S.; Li, C. M.; Xu, L. Q. Simultaneous deposition of tannic acid and poly (ethylene glycol) to construct the antifouling polymeric coating on Titanium surface. *Colloids and Surfaces B: Biointerfaces* **2021,** *200*, 111592.

(309) Francesko, A.; Fernandes, M. M.; Ivanova, K.; Amorim, S.; Reis, R. L.; Pashkuleva, I.; Mendoza, E.; Pfeifer, A.; Heinze, T.; Tzanov, T. Bacteria-responsive multilayer coatings comprising polycationic nanospheres for bacteria biofilm prevention on urinary catheters. *Acta biomaterialia* **2016**, *33*, 203-212.

(310) Atar-Froyman, L.; Sharon, A.; Weiss, E. I.; Houri-Haddad, Y.; Kesler-Shvero, D.; Domb, A. J.; Pilo, R.; Beyth, N. Anti-biofilm properties of wound dressing incorporating nonrelease polycationic antimicrobials. *Biomaterials* **2015**, *46*, 141-148.

(311) Azevedo, M.; Ramalho, P.; Silva, A.; Teixeira-Santos, R.; Pina-Vaz, C.; Rodrigues, A. Polyethyleneimine and polyethyleneimine-based nanoparticles: novel bacterial and yeast biofilm inhibitors. *Journal of medical microbiology* **2014**, *63* (9), 1167-1173.

(312) De Breij, A.; Riool, M.; Kwakman, P.; De Boer, L.; Cordfunke, R.; Drijfhout, J.; Cohen, O.; Emanuel, N.; Zaat, S.; Nibbering, P. Prevention of Staphylococcus aureus biomaterial-associated infections using a polymer-lipid coating containing the antimicrobial peptide OP-145. *Journal of Controlled Release* **2016**, *222*, 1-8.

(313) Raman, N.; Lee, M.-R.; López, A. d. L. R.; Palecek, S. P.; Lynn, D. M. Antifungal activity of a β-peptide in synthetic urine media: Toward materials-based approaches to reducing catheter-associated urinary tract fungal infections. *Acta biomaterialia* **2016,** *43*, 240-250.

(314) Ivanova, K.; Fernandes, M. M.; Francesko, A.; Mendoza, E.; Guezguez, J.; Burnet, M.; Tzanov, T. Quorum-quenching and matrix-degrading enzymes in multilayer coatings synergistically prevent bacterial biofilm formation on urinary catheters. *ACS applied materials & interfaces* **2015,** *7* (49), 27066-27077.

(315) Donelli, G.; Francolini, I.; Romoli, D.; Guaglianone, E.; Piozzi, A.; Ragunath, C.; Kaplan, J. Synergistic activity of dispersin B and cefamandole nafate in inhibition of staphylococcal biofilm growth on polyurethanes. *Antimicrobial agents and chemotherapy* **2007**, *51* (8), 2733-2740.

(316) Thallinger, B.; Brandauer, M.; Burger, P.; Sygmund, C.; Ludwig, R.; Ivanova, K.; Kun, J.; Scaini, D.; Burnet, M.; Tzanov, T. Cellobiose dehydrogenase functionalized urinary catheter as novel antibiofilm system. *Journal of Biomedical Materials Research Part B: Applied Biomaterials* **2016,** *104* (7), 1448-1456.

(317) Yuan, S.; Zhao, J.; Luan, S.; Yan, S.; Zheng, W.; Yin, J. Nuclease-functionalized poly (styrene-b-isobutylene-b-styrene) surface with anti-infection and tissue integration bifunctions. *ACS applied materials & interfaces* **2014,** *6* (20), 18078-18086.

(318) Grover, N.; Plaks, J. G.; Summers, S. R.; Chado, G. R.; Schurr, M. J.; Kaar, J. L. Acylase-containing polyurethane coatings with anti-biofilm activity. *Biotechnology and bioengineering* **2016,** *113* (12), 2535-2543.

(319) Asker, D.; Awad, T. S.; Baker, P.; Howell, P. L.; Hatton, B. D. Non-eluting, surface-bound enzymes disrupt surface attachment of bacteria by continuous biofilm polysaccharide degradation. *Biomaterials* **2018,** *167*, 168-176.

(320) Wu, J. A.; Kusuma, C.; Mond, J. J.; Kokai-Kun, J. F. Lysostaphin disrupts Staphylococcus aureus and Staphylococcus epidermidis biofilms on artificial surfaces. *Antimicrobial agents and chemotherapy* **2003,** *47* (11), 3407-3414.

(321) Tas, C. E.; Berksun, E.; Koken, D.; Unal, S.; Unal, H. Photothermal Waterborne Polydopamine/Polyurethanes with Light-to-Heat Conversion Properties. *ACS Applied Polymer Materials* **2021,** *3* (8), 3929-3940.

(322) Tas, C. E.; Berksun, E.; Koken, D.; Kolgesiz, S.; Unal, S.; Unal, H. Waterborne Polydopamine-Polyurethane/Polyethylene Glycol-Based Phase Change Films for Solar-to-Thermal Energy Conversion and Storage. *Industrial & Engineering Chemistry Research* **2021,** *60* (41), 14788-14800.

(323) Xiong, Y.-B.; Lu, Z.-H.; Wang, D.-D.; Yang, M.-N. O.; Guo, H.-M.; Yang, Z.-H. Application of polydopamine functionalized magnetic graphene in triazole fungicides residue analysis. *Journal of Chromatography A* **2020,** *1614*, 460725.

VITA of Buket ALKAN TAŞ

Buket Alkan Taş was born on February 15, 1987, in Zonguldak, Turkey. She graduated from İstanbul Technical University with a B.Sc. degree in Chemistry Department in June 2012 and graduated from Istanbul Technical University with an M.Sc. degree in June 2014. Before begining Ph.D. education in Materials Science and Engineering Program at Sabanci University in Istanbul, she worked as a R&D Specialist at Organik Kimya Inc. Co. between September 2014 and June 2015. During her Ph.D. studies, she served as a teaching assistant in Polymer Synthesis (MAT302, five semesters) and Organic Chemistry (NS207, four semesters) courses.